

Ute Daschiel

# Photochemical modulation of the refractive index and the surface properties of selected polymers

DISSERTATION

Zur Erlangung des akademischen Titels einer Doktorin der technischen  
Wissenschaften

eingereicht an der  
Technischen Universität Graz

Betreuer: Univ. Prof. Wolfgang Kern  
Institut für Chemie der Kunststoffe, Montanuniversität Leoben

Diese Dissertation wurde am Institut für Chemische Technologie von Materialien (TU  
Graz) und am Institut für Chemie der Kunststoffe (MUL) von Oktober 2006 bis  
Dezember 2009 erarbeitet.

## STATUTORY DECLARATION

I declare that I have authored this thesis independently, that I have not used other than the declared sources / resources, and that I have explicitly marked all material which has been quoted either literally or by content from the used sources.

.....  
date

.....  
(signature)

## Acknowledgement

First of all I want to thank Prof. Wolfgang Kern for supervising and his group for a really good working atmosphere, especially Sabine Bichler, Thomas Griesser, Barbara Rupp, Sandra Schlögl, and Thomas Höfler.

Thanks to Evelyn Zottler, Birgit Ungerböck, Thomas Bauer, Julia Spanring and Roman Führer who participated in experimental works of the present study. Roman Führer performed his diploma thesis at the University of Leoben within the present project.

Thanks to the ICTM and its employee who played an important role to make my work so comfortable. My thank goes especially to Gerhard Seyfriedsberger and Martin Weinberger for encouraging and supporting me. Thomas Rath and Eugen Mayer thanks for their kind help with several problems. Thanks to Josefine Hobisch for SEC measurements, Petra Kaschnitz for NMR measurements and Anna Track for XPS measurements.

Thanks to Julian Wagner and Hartmuth Schröttner (Felmi, TU Graz) for electron microscopic measurements.

Further thanks to Valentin Satzinger, Volker Schmidt, Georg Jacopic and Heinz Pichler (Joanneum Research, NMP Weiz) for operating the laser, ellipsometric and profile measurements.

Special thanks go to Harald Kren and my family for supporting me and keeping me grounded.

Part of the research work of this PhD thesis was performed within the  $K_{\text{plus}}$ -projects „*Functionalized Polymer Surfaces*” (project-no.: II-S8) and “*Functional and Reactive Polymer Surfaces and Interfaces*” (project no.: III-S1.02) project at the Polymer Competence Center Leoben GmbH (PCCL, Austria) within the framework of the  $K_{\text{plus}}$ -and COMET program of the Austrian Ministry of Traffic, Innovation and Technology with contributions by the *Institute of Chemical Technology of Materials* (TU Graz) and the *Institute of chemistry of Polymeric Materials* (University of Leoben). The PCCL is funded by the Austrian Government and the State Governments of Styria and Upper Austria.

Another part of the research work was performed within the project cluster ISOTEC *Integrated Organic Sensor and Optoelectronic Technologies* of the Austrian Nanoinitiative, which is funded by Austrian Research Promotion Agency (FFG).

## Abstract

In this work new methods to create patterns by changing selected properties of polymers were developed. Surfaces of polymers such as low density polyethylene (LDPE) and polystyrene (PS) were successfully modified by special irradiation techniques in a reactive gas atmosphere. Patterns were produced in the micrometer range by using a contact mask technique. For LDPE, a xenon excimer lamp with an emission wavelength of 172 nm was used as radiation source, while a KrF excimer-laser (248 nm) coupled with a UV projection system was used for PS. A reaction chamber containing the target polymer was filled with a mixture of oxygen and trimethylsilane at different ratios before illumination. Fourier-Transform Infrared (FT-IR) and X-ray photoelectron spectroscopy (XPS) measurements proved the introduction of alkylsilyl groups via a photo-induced reaction. Further characterisations were carried out by means of optical and electron microscopy.

To produce three-dimensional structures, special polymers bearing different derivatives of aryl esters were synthesised. FT-IR and UV/VIS spectroscopy were used to identify the occurring photoreactions as photodecarboxylation and photo-Fries reaction. The photo-induced refractive index change of the polymers was measured via ellipsometry and showed changes of up to +0.07. Furthermore, two photon processes were investigated by irradiation with a fs-pulsed Ti:sapphire laser. The refractive index change accompanying the photoreaction induced by two photon absorption allows the creation of 3D patterns in a single step.

## Kurzfassung

Ziel dieser Arbeit war die Entwicklung neuer Methoden zur strukturierten Modifizierung von ausgewählten Polymeren. Oberflächen von Polymeren wie LDPE oder Polystyrol konnten mittels speziellen Belichtungsmethoden in Reaktivgasatmosphäre erfolgreich modifiziert und strukturiert werden. Mit Hilfe von Maskenverfahren konnten Strukturen im Mikrometermaßstab erzielt werden. Zur Belichtung von LDPE wurde eine Xe-Excimer Lampe (172 nm) und für PS ein KrF-Excimer Laser (248 nm) gekoppelt mit einem UV-Projektionssystem verwendet. Die Polymerprobe wurde in einer Belichtungskammer platziert, die vor der Belichtung mit einer Gasmischung aus Trimethylsilan und Sauerstoff in verschiedenen Verhältnissen gespült wurde. Mittels Fourier-Transform Infrarot (FT-IR) und Röntgen Photoelektronen Spektroskopie (XPS) konnte die photo-induzierte Einführung von Alkylsilyl-Gruppen nachgewiesen werden. Weiters wurden Licht- und Elektronenmikroskopie als Charakterisierungsmethoden verwendet.

Um drei-dimensionale Strukturen zu erhalten wurden spezielle Polymere, die über verschiedene Arylesterderivate in den Seitenketten verfügen, synthetisiert. FT-IR und UV/VIS Spektroskopie wurden zur Identifizierung der eintretenden Photoreaktionen als Photodecarboxylierung und Photo-Fries Reaktion verwendet. Der photo-induzierte Brechungsindexhub wurde mittels Ellipsometrie bestimmt und beträgt bis zu +0.07. Weiters wurden Zwei-Photonen Prozesse durch Belichtungen mit einem fs-gepulsten Ti:Sa Laser untersucht. Die durch Zwei-Photonenabsorption bewirkte Photoreaktion erzeugt einen Brechungsindexunterschied, der die Herstellung von 3D Strukturen in nur einem Schritt erlaubt.

## Table of contents

1	General Introduction .....	1
2	PART A: Synthesis, photochemistry, and optical patterning of selected polymers .....	4
2.1	Introduction to Part A.....	4
2.2	Photoreactive styrene and silicone polymers bearing 4-(N,N-diphenylamino)phenyl benzoate units: one-photon and two-photon reactions.....	6
2.2.1	Summary.....	6
2.2.2	Introduction .....	7
2.2.3	Experimental Part.....	9
2.2.3.1	Starting Compounds.....	9
2.2.3.2	Synthesis of aryl esters.....	10
2.2.3.3	Free radical polymerisations.....	12
2.2.3.4	Characterisation of monomers and polymers.....	14
2.2.3.5	Determination of absorbance coefficients .....	14
2.2.3.6	UV Irradiation procedures.....	15
2.2.4	Results and discussion.....	16
2.2.4.1	Synthesis of monomers, model compounds and polymers .....	16
2.2.4.2	UV irradiation of polymer films.....	18
2.2.4.3	Photoreactions in polymers P1, P2 and in model compounds .....	18
2.2.4.4	Photoreactions in polymer P3 and model compound L3 .....	23
2.2.4.5	Photoinduced refractive index changes in polymers P1-P3 .....	24
2.2.4.6	Laser irradiation under two-photon conditions .....	27
2.2.5	Conclusion .....	28
2.2.6	References.....	29
2.3	Photoreactive styrene and silicone polymers bearing 4-(N,N-diphenylamino)phenyl benzoate units: one-photon and two-photon reactions.....	30
2.3.1	Summary.....	30
2.3.2	Introduction .....	30
2.3.3	Experimental Part.....	32
2.3.3.1	Starting Compounds.....	32
2.3.3.2	Polystyrene derivative P1 .....	32
2.3.3.3	Modified polysiloxane P2 .....	33
2.3.3.4	UV illumination process .....	33
2.3.4	Results and discussion.....	34
2.3.4.1	Polystyrene based system.....	34
2.3.4.2	Polysiloxane based system P2 .....	40
2.3.5	Conclusion .....	46
2.3.6	Acknowledgement.....	46
2.3.7	References.....	46
2.4	Refractive index patterning and waveguide patterning of polynorbornene copolymers bearing 4-(N,N-diphenylamino)phenyl benzoate units .....	48
2.4.1	Summary.....	48

2.4.2	Introduction .....	48
2.4.3	Experimental Part.....	50
2.4.3.1	Starting Compounds.....	50
2.4.3.2	Monomers .....	50
2.4.3.3	Statistic polymerization procedure of norbornene derivatives to give the copolymers P1a, P2a, P1b and P2b .....	54
2.4.3.4	UV illumination process .....	56
2.4.4	Results and Discussion .....	56
2.4.4.1	Synthesis.....	56
2.4.4.2	UV absorption of polymers .....	56
2.4.4.3	UV irradiation of polymers .....	57
2.4.5	Conclusion .....	62
2.4.6	References.....	63
2.5	Conclusion of part A and outlook .....	64
<b>3</b>	<b>Part B: UV and VUV Assisted Patterned Surface Modification of PS and LDPE in a Reactive Gas Atmosphere .68</b>	
3.1	Introduction to Part B.....	68
3.2	Modification of Polyethylene by VUV Irradiation in the Presence of Trimethylsilane and Oxygen.....	70
3.2.1	Summary.....	70
3.2.2	Introduction .....	70
3.2.3	Experimental Part.....	72
3.2.3.1	Materials.....	72
3.2.3.2	Characterisation Methods.....	72
3.2.3.3	VUV Irradiation Experiments.....	73
3.2.4	Results and Discussion .....	74
3.2.4.1	General Aspects .....	74
3.2.4.2	Spectroscopic Measurements.....	75
3.2.4.3	Scanning Electron Microscopy, AFM and Contact Angle Measurements.. .....	80
3.2.4.4	Surface Patterning .....	81
3.2.5	Conclusion .....	82
3.2.6	References.....	83
3.3	Patterned Surface Modification of Polystyrene by UV Irradiation in the Presence of Trimethylsilane.....	85
3.3.1	Summary.....	85
3.3.2	Introduction .....	85
3.3.3	Experimental Part.....	86
3.3.3.1	Materials.....	86
3.3.3.2	Characterisation methods.....	87
3.3.3.3	Irradiation Experiments.....	87
3.3.4	Results and Discussion .....	88
3.3.4.1	Irradaiton of PS under neat oxygen.....	90
3.3.4.2	Irradaiton of PS under TMS/O <sub>2</sub> .....	91
3.3.5	Conclusion .....	97
3.3.6	References.....	98

3.4	Conclusion of Part B and outlook .....	99
4	General Summary .....	102
5	Appendix 1 .....	104
6	Appendix 2: List of publications .....	105



# 1 General Introduction

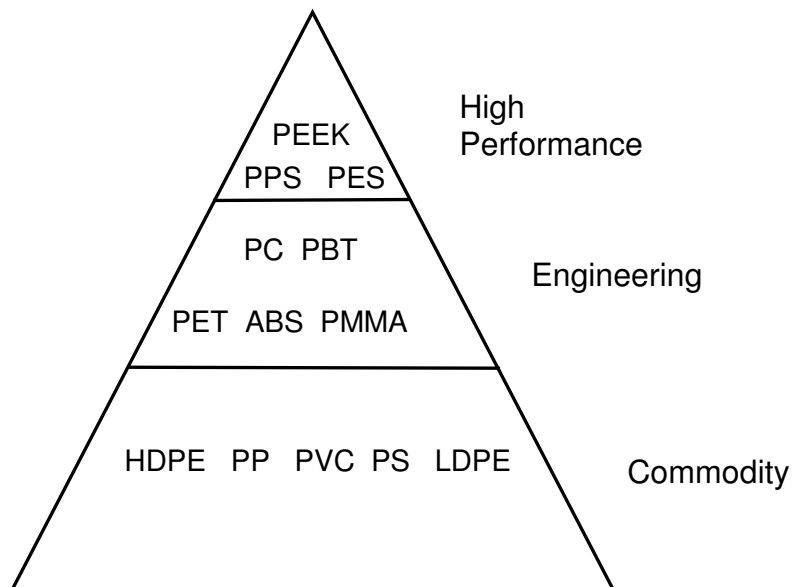


Figure 1: polymer pyramid

Polymers have been used by mankind since time began. To give some examples, polysaccharides or proteins of meat are important parts of our food, whereas wool or silk, both proteins, are used for clothes and amber used for jewel. Synthetic polymers were discovered in the 19<sup>th</sup> century, when E. Simon polymerised styrene by heating up the liquid up, resulting in a translucent solid and Wurtz successfully synthesised polyethylenoxide.<sup>[1,2]</sup> The first chemical modification of a natural polymer was carried out by Henri Braconnot when he produced a derivatization of cellulose.<sup>[3]</sup> The first thermoplastic was celluloid, which was used as an ivory replacement in the production of dolls. Nowadays it is still in use for table tennis balls or plectra.

In the course of time polymers have gained more and more importance. They are currently in use in all possible domains such as automotive and electronics as well as medicine and aircraft engineering. In everyday life polymers cannot be dismissed, since they are utilised for food technology, packaging and clothes.

Classifying polymers on the basis of their stable working temperature, a pyramid is built (compare Figure 1). In the bottom row commodity polymers like HDPE, PP and PS are listed, in the middle row PET, PC and PMMA are mainly used for engineering polymers whereas the high performance polymers PPS and PEEK are displayed in the top row. With increasing working temperature the costs of the polymers also rise. It becomes clear that a cost-benefit analysis is needed to evaluate the correct polymer for every application.<sup>[4]</sup>

Since the production of commodity polymers is cheaper than that of special polymers, numerous investigations to modify properties of standard polymers have been carried out. The two most common industrial applications are corona<sup>[5]</sup> and plasma treatment of polymer surfaces.<sup>[6]</sup> These methods result in a change of hydrophobicity to hydrophilicity, the crosslinking of polymers or the addition of functional groups. These treatments need specific equipment, other methods such as chemical etching or chemical vapour deposition are used to modify surfaces.<sup>[7,8]</sup> UV methods present a very easy and also cheap method. Different types of lamps and lasers are in use, for example mercury lamps or excimer lasers. An essential advantage of UV techniques is the possibility of producing structures by modifying polymer surfaces.

For some applications, surface modification of polymers is not sufficient to achieve the desired properties. Mainly in the field of electronics, special polymers have found application for OLEDs or organic solar cells in the past few years. Polymers also play a very important role in optoelectronics industry. In these fields, modification of commodity polymers cannot meet the requirements; hence synthesis of new monomers is necessary. For electronic technology, the possibility to structure the polymers is especially important. For example, photo resist techniques are essential for microelectronics and the production of integrated circuit boards respectively.

The main goal of this work is the photochemical structuring of two different polymer types, special polymers (part A) and commodity polymers (part B).

For the first topic (part A), polymers need to be synthesised in order to obtain photosensitive materials. The photoreaction is investigated under normal irradiation with a mercury medium pressure lamp and with a fs-pulsed Ti:sapphire laser for two photon absorption. Analyses are done by FT-IR spectroscopy and microscopy, UV/VIS spectroscopy, ellipsometry and phase contrast microscopy. The photochemical modification of special polymers should create a refractive index pattern within the material. Therefore the photoreactions of aryl esters are under investigation. The photo-Fries reaction is one of them and is expected to create a high refractive index change.<sup>[9]</sup> New monomers and polymers are developed to give high refractive index changes upon normal irradiations and under two-photon conditions. "Two photon absorption" (TPA) is the simultaneous absorption of two photons. The energy of these photons is only the half of the energy for one photon absorption. TPA gets probable only for high intensities. Pulsed lasers and a large amount of equipment are necessary for these processes. Nevertheless, TPA enables three dimensional structuring of polymers in only one step and presents a promising technology for the future. To increase the probability of TPA, special monomers are designed, polymerised and

investigated. These materials can find their application in optical memories, waveguide technology or holography.

In part B, surfaces of polystyrene (PS) and polyethylene (LDPE) are modified in the presence of trimethylsilane and a trimethylsilane/oxygen mixture. A Xe-excimer lamp and a KrF-excimer laser, coupled with a UV projection system, are available as irradiation equipment. Analytical studies are carried out by means of Fourier-Transform-Infrared (FTIR) spectroscopy, X-ray induced photoelectron spectroscopy (XPS), FTIR and electron microscopy, and contact angle measurements. The desired result of the surface modification of PS and LDPE is the covalent binding of organosilyl and organosilicon groups to the surface. The new layer should function as a barrier and act as a scratch- and shock-proofed protection layer. Improved properties of surfaces of metal or paper could be achieved by plasma deposition of siloxane layers.<sup>[10,11]</sup> The used commodity polymers should attain advanced properties by surface modification which extends their field of application.

---

[1] E. Simon, *Ann.Chem.Pharm.*, 31, **1839**, 265

[2] A. Wurtz, *C.R. Hebd. Seances Acad. Sci.* 49, **1859**, 813; 50, **1860**, 1195

[3] Tess R.W., Poehlein G.W., „*Applied Polymer Science*“, 2<sup>nd</sup> edition, American Chemical Society, 1985

[4] H. Harig, C.J. Langenbach, „*Wissenschaftsethik und Technikfolgenbeurteilung*“, Band 3, Springer, **1999**, 83-86

[5] Y. Zhu, M. Otsubo, C. Honda, *Polymer Testing* 25, **2006**, 313–317

[6] X. Wang, M.G. McCord, *J. Appl. Polym. Sci.* 104, **2007**, 3614

[7] S. Guruvenket, G. Mohan Rao, Manoj Komath, Ashok M. Raichur, *Applied Surface Science* 236, **2004**, 278–284

[8] B. Feddes, J.G.C. Wolke, W.P. Weinhold, A.M. Vredenberg, J.A. Jansen, *J. Adhes. Sci. Technol.* 18, **2004**, 655

[9] T. Höfler, T. Grießer, X. Gstrein, G. Trimmel, G. Jakopic, W. Kern, *Polymer* 48, **2007**, 1930

[10] Grünwald H, Adam R, Bartella J, Jung M, Dicken W, Kundel S, Nauenberg K, Gebele T, Mitzlaff S, Ickes G, Patz U, Snyder J, *Surf Coat Technol* 111, **1999**, 278-296

[11] Benitez F, Martinez E, Galan M, Serrat J, Esteve J. *Surf Coat Technol* 125, **2000**, 383-378

## **2 PART A: Synthesis, photochemistry, and optical patterning of selected polymers**

### **2.1 Introduction to Part A**

The main goal of part A is the investigation of new synthesised polymers which are patternable under two photon conditions. An optical property, more precisely the refractive index of the polymer should be modified by short pulsed laser illumination. For “two photon absorption” (TPA) of the material, the irradiation source needs to fulfill some requirements. Only at high light intensities TPA becomes probable, therefore short-pulsed lasers are necessary. The wavelength of the light must be in the range of the doubled wavelength of normal absorption, since two photons of the half energy are absorbed simultaneously to excite the molecule. The laser beam has to be focused within the material, which enables 3D patterning. In the surrounding material, the light is not absorbed. Only in the vicinity of the laser focus, the intensity is high enough to excite the molecule and cause potentially a photoreaction. Since the probability of TPA is proportional to the laser pulse intensity squared, the resolution of this process is much higher than under normal conditions.

New Polymers bearing aryl ester units are developed for this work. Different ester groups and different polymer backbones are synthesised and analysed by means of FT-IR, UV-VIS and NMR. The photoreactions of these polymers are investigated under normal irradiation with a mercury medium pressure lamp and analysed via FT-IR and UV/VIS spectroscopy. The refractive index change upon irradiation of the used polymers is analysed by means of ellipsometric spectroscopy. This change is essential for the optical pattern of the polymer in this work, regardless of which illumination condition.

To observe the refractive index change upon two photon conditions, phase contrast microscopy is used to distinguish between areas with different indices. For the irradiation, an optically pumped fs-pulsed Ti:sapphire laser is used. The normal emission wavelength of the amplified laser lies at 800 nm. Additionally, an OPA (optical parametric amplifier) can be pumped with the emission at 800 nm and creates a tunable emission wavelength between 600 and 800 nm. A picture of the laser is shown in Figure 2.



**Figure 2: fs-pulsed Ti:sapphire laser at the institute of Nanostructured Materials and Photonics, Joanneum Research GmbH (Weiz, A)**

The new polymers are developed to show high refractive index changes upon normal irradiations and under two-photon conditions. A big advantage of the TPA process is the 3D patterning that can be created in one step. For producing a waveguide, a channel is illuminated with the laser beam in the depth of the polymer. In case of an increase of the refractive index, light can now be guided through this channel because of total reflexion. Total reflexion occurs when light is reflected in a medium with a higher refractive index to the boarder of a material with a lower refractive index. The polymers can find their application not only for waveguide technology but also for other optical technologies such as optical memories, or holography.

Chapter 2.2 deals with the development of new aryl ester groups, which are also promising chromophores for TPA structuring at 600 nm. Small model compounds and polymers are investigated and compared with respect to their photoreactions. First TPA experiments are shown. Subsequently, synthesis to incorporate the ester with the highest yield of photoreaction into two different matrices was performed, which is presented in Chapter 2.3. The photoreactivity under one and two photon conditions is compared. Finally, Chapter 2.4 deals with a new polymer backbone. Via ring-opening-metathesis-polymerisation (ROMP) polynorbornenes were synthesised bearing aryl esters, to create refractive index pattern under two photon conditions.

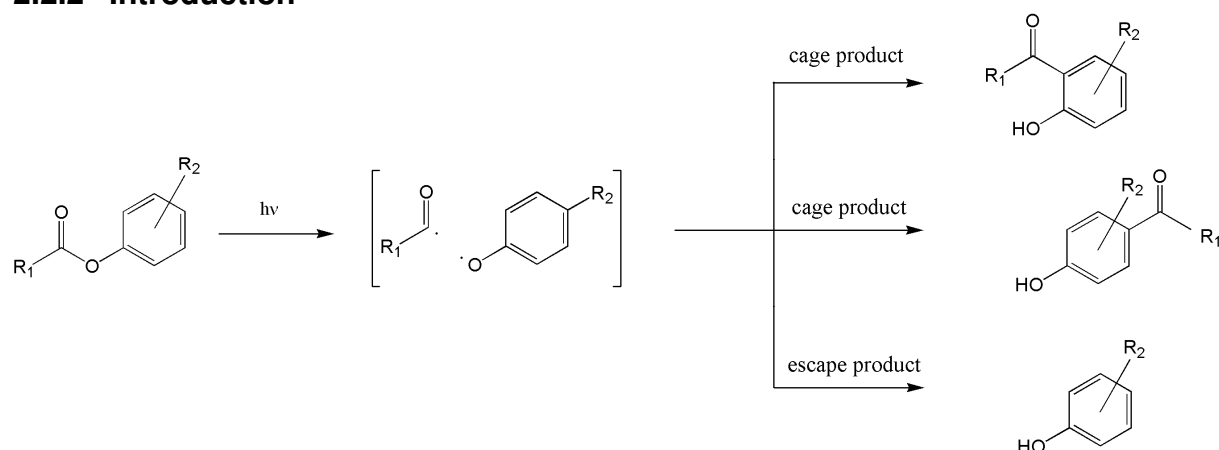
## 2.2 Photoreactive styrene and silicone polymers bearing 4-(N,N-diphenylamino)phenyl benzoate units: one-photon and two-photon reactions

### 2.2.1 Summary

Part of the work described in this chapter was done during the diploma thesis. Since the work and results of this chapter are essential for the further chapters it is presented as well.

Photoreactive polymers bearing aliphatic and aromatic esters of 4-(N,N-diphenylamino)phenol in the side chain were prepared from their monomers by free radical polymerization. These polymers were poly[acrylic acid, 4-(N,N-diphenylamino)phenyl ester] (**P1**) and poly[4-vinylbenzoic acid, 4-(N,N-diphenylamino)phenyl ester] (**P2**). In addition, poly[4-vinylbenzoic acid, naphthalene-1-yl ester] was synthesized (**P3**). These materials absorb UV light up to  $\lambda = 350$  nm. The polymers **P1-P3** as well as low-molecular-weight model compounds were investigated with respect to their photoreactions under UV illumination. It was found that decarboxylation is the dominant reaction and that the photo-Fries rearrangement occurs as a minor reaction. The fully aromatic ester units in **P2** were more reactive than the ester units in **P1**. In the polymers, decarboxylation proceeded more efficiently than in the low-molecular-weight model compounds. Upon UV illumination of the polymers, large increases of the refractive index were observed ( $\Delta n_{450}$  up to +0.07). This is in agreement with the structural changes in the polymers after irradiation as calculated from group contributions to molar refraction. A preliminary investigation under 610 nm fs laser irradiation indicated that refractive index patterns can be produced by two-photon effects (TPA). The polymers are of potential interest for applications in the field of optical waveguides.

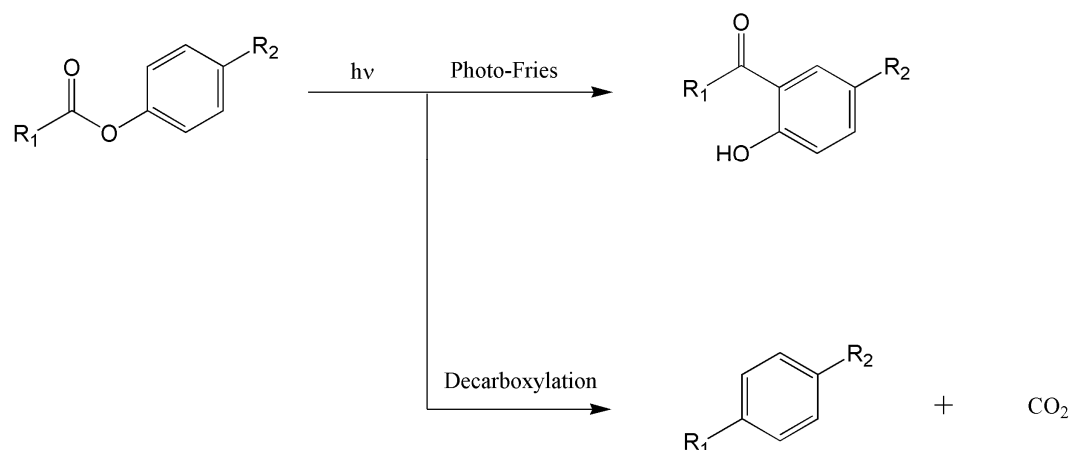
## 2.2.2 Introduction



**Scheme 1. General mechanism and products of the Photo-Fries reaction.**

Materials with tunable refractive index are of interest for numerous applications, among them optical elements and holographic recording materials. Due to the increasing demand for such materials we continued our investigations to identify new polymers which give a large increase in their refractive index upon UV irradiation. Materials which can be index patterned by lithographic techniques are especially useful for the production of optical waveguides.

In a previous contribution <sup>[1]</sup> we reported on the synthesis and characterization of polynorbornenes bearing phenyl ester units. Upon UV illumination, the photo-Fries reaction is observed in these polymers. The photo-Fries rearrangement has been known since the 1960s, when Anderson and Reese reported that aryl esters undergo a rearrangement under UV irradiation.<sup>[2]</sup> The main products are the corresponding ortho- and para-hydroxyketones. Mechanistic investigations by Lochbrunner et al.<sup>[3]</sup> showed that as a first step the molecule is excited to the S<sub>1</sub> state ( $\pi$ - $\pi^*$  transition). This optically excited state then crosses with a  $\pi$ - $\sigma^*$  state, from which an elongation of the C-O bond in the ester group occurs. At this point either the C-O bond is cleaved or the molecule relaxes to the ground state. If bond fragmentation occurs, two radicals are formed in a solvent cage (cf. Scheme 1). The photogenerated radicals can recombine to a derivative of cyclohexadienone as the “cage product” (ortho- and para-isomers). Tautomerism then gives hydroxyketones, which can be described as acyl migration products. The “escape product” of the geminate radical pair is mainly phenol which is formed by H abstraction from the solvent (Scheme 1). Indeed, the photo-Fries rearrangement has also been studied for solid polymers such as poly(phenyl acrylate).<sup>[4]</sup>



**Scheme 2. Two major routes for the reaction of aromatic esters upon UV irradiation: Photo-Fries reaction and photoextrusion of CO<sub>2</sub> (decarboxylation).**

It is less well-known that UV illumination of aryl esters also yields decarboxylation products, cf. Scheme 2. Decarboxylation was first observed by Finnegan and Knudsen.<sup>[5]</sup> Also this reaction proceeds from the excited S<sub>1</sub> state and transforms the aromatic ester R-COO-R' into a hydrocarbon R-R'. For this photoextrusion of CO<sub>2</sub> a concerted mechanism has been proposed. It is known that sterical hindrance of the ester and solvent effects can enhance the yield of the decarboxylation product. Templating effects have been observed by Weiss et al.<sup>[6]</sup> The limited mobility of aromatic esters dissolved in a polymeric matrix leads to an enhanced yield of the photo-decarboxylation product and at the same time the yield of the Fries rearrangement product is lowered.<sup>[6]</sup> A review on topic of photo-Fries rearrangements has recently been published by Miranda et Galindo<sup>[7]</sup>.

Our previous contribution<sup>[1]</sup> on photo-Fries reactions in polymeric media has focused on polymers bearing phenyl esters of aliphatic carboxylic acids in the side chain. These materials absorb UV light up to  $\lambda \sim 270$  nm. In the present investigation, we wished to see if the UV absorbance of photoreactive polymers bearing aromatic ester groups can be shifted to higher wavelengths (up to 350 nm) which would facilitate optical patterning processes. To achieve this, the 4-(N,N-diphenylamino)phenyl of acrylic acid and 4-vinylbenzoic acid, respectively, were prepared and polymerized. These new polymers were investigated with respect to their photoproducts and UV induced changes in their refractive index. Until now, polymers and low-molecular-weight derivatives of triphenylamine have attracted interest for organic light emitting devices (OLEDs),<sup>[8,9]</sup> and *bis*-(N,N-diphenylamino) stilbenes have been found to be excellent initiators in two-photon photopolymerizations<sup>[10,11]</sup>. Moreover, the present study describes the preparation and photochemistry of a polymer bearing benzoic acid 1-naphthyl ester units.



Another aim of the present study was to investigate these polymers under two-photon conditions. Over the last few decades, two photon absorption (TPA) has been studied intensively for laser induced initiation of polymerization reactions and 3D microfabrication, fluorescence imaging and photodynamic therapy. However, specific photocleavages and rearrangements based on two photon absorption are rarely studied. To test the photo-Fries reaction as possible TPA photoreaction, polymers containing 4-(N,N-diphenylamino)phenyl and 1-naphthyl ester units were tentatively investigated under 610 nm laser irradiation.

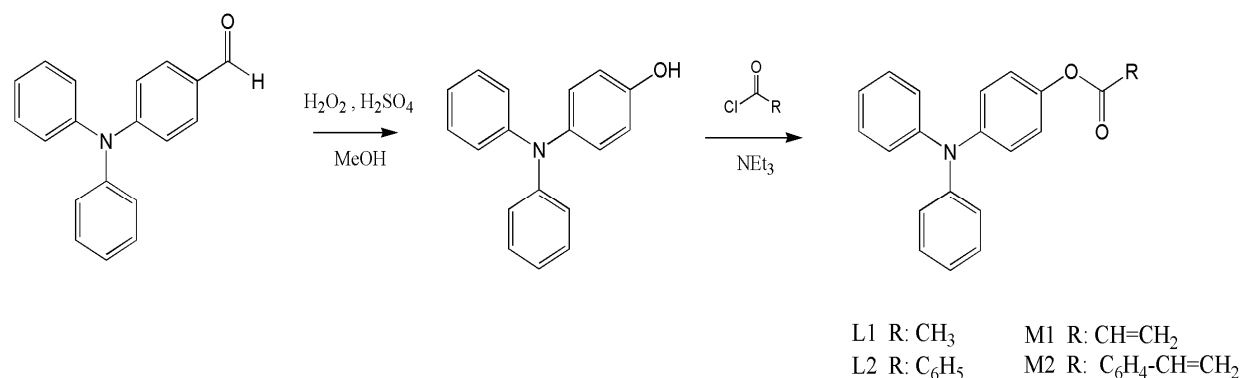
## 2.2.3 Experimental Part

### 2.2.3.1 Starting Compounds

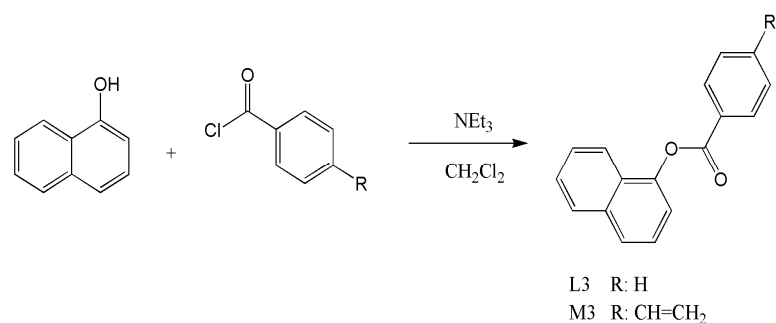
The following materials were obtained from commercial sources and used as received: 4-(N,N-diphenylamino)benzaldehyde, 4-vinyl benzoic acid, benzoyl chloride and acetyl chloride from Fluka; acryloyl chloride from Lancaster. Toluene (Fluka) was dried by distillation over Na/K, methylene chloride (Fluka) was distilled over P<sub>2</sub>O<sub>5</sub> prior to use. The synthetic routes to obtain the desired compounds are shown in Scheme 3 and Scheme 4. 4-(N,N-Diphenylamino)phenol was prepared as following: under argon, 10 g (37 mmol) of 4-(N,N-diphenylamino)benzaldehyde, 7.5 mL of H<sub>2</sub>O<sub>2</sub> (30 %) and 1 mL of H<sub>2</sub>SO<sub>4</sub> (conc.) were added to 100 mL of methanol. The suspension was stirred and cooled down in an ice bath for 15 minutes and then remained at 20 °C for another three hours. 400 mL of distilled water and 300 mL of ethyl acetate were added. Then the aqueous phase was extracted for three times with 300 mL of ethyl acetate. In the next step the combined organic phases were dried with Na<sub>2</sub>SO<sub>4</sub> and concentrated under reduced pressure. The residue was purified on a silica gel column with cyclohexane : ethyl acetate = 2 : 1 as eluent. 6.8 g (26 mmol) of a yellow solid were obtained (68 % yield). <sup>1</sup>H (500MHz, 20 °C, CDCl<sub>3</sub>): δ = 4.79 (1H, s), 6.77-7.26 (14 H, bm) <sup>13</sup>C (CDCl<sub>3</sub>, 20 °C, 125 MHz): δ = 151.9, 148.1, 140.9, 129.0, 127.5, 122.9, 121.9, 116.2 FTIR (CaF<sub>2</sub>): 3351 (s, OH), 1586, 1506, 1491, 1277 cm<sup>-1</sup>

The synthesis of 4-vinylbenzoyl chloride was performed as following: 3.0 g (20 mmol) of 4-vinyl benzoic acid were dissolved in 20 mL of toluene. 4.0 mL of thionyl chloride were added dropwise to this solution, then the temperature was raised to 90 °C. After three hours of stirring, the reaction solution was distilled *in vacuo*. The product was received as a yellowish oil (purity 95%). The yield was 2.5 g (75 %). <sup>1</sup>H (500MHz, 20 °C, CDCl<sub>3</sub>): δ = 5.50 (1H, d, <sup>3</sup>J = 11 Hz), 5.95 (1 H, d, <sup>3</sup>J = 17.5 Hz), 6.78 (1H, dd, <sup>3</sup>J = 11, 17.5 Hz), 7.5 (5 H; m), FTIR (CaF<sub>2</sub>): 1773 (C=O in acid chlorides), 2934, 1602 (aromatic vib.) 1630 cm<sup>-1</sup> (C=C double bond)

### 2.2.3.2 Synthesis of aryl esters



Scheme 3. Synthesis of the model compounds L1, L2 and of the monomers M1 and M2



Scheme 4. Synthesis of the model compound L3 and of the monomer M3

Photoreactive aryl esters were prepared from the chlorides of acetic acid, acrylic acid, benzoic acid and 4-vinylbenzoic acid with 1-naphthol and 4-(N,N-diphenylamino)phenol, respectively. The general procedure for the synthesis of the low-molecular-weight model compounds acetic acid, 4-(N,N-diphenylamino)phenyl ester (**L1**), benzoic acid, 4-(N,N-diphenylamino)phenyl ester (**L2**) and benzoic acid, naphthalene-1-yl ester (**L3**) (see Scheme 3 and Scheme 4) and the photoreactive monomers acrylic acid, 4-(N,N-diphenylamino)phenyl ester (**M1**), 4-vinylbenzoic acid, 4-(N,N-diphenylamino)phenyl ester (**M2**) and 4-vinyl benzoic acid, naphthalene-1-yl ester (**M3**) (see Scheme 3 and Scheme 4) is described in the following. Under argon, 1 equivalent of alcohol was dissolved in dry methylene chloride to obtain a 5 wt.-% solution. After cooling down to 0°C, 1.1 equivalents of triethylamine and 1.1 equivalents of acid chloride were added dropwise. Then the reaction solution was stirred for 30 minutes, after removal of the ice bath the reaction mixture was stirred for another 60 min. To this reaction solution equal volumina of water and dichloromethane were added. After separation of the organic phase, the aqueous phase was extracted with methylene chloride

(six times). The combined organic phases were concentrated *in vacuo*, washed with diluted hydrochloric acid, distilled water, aqueous sodium bicarbonate and distilled water again. The organic phase was dried over Na<sub>2</sub>SO<sub>4</sub> and concentrated under reduced pressure. The crude product was purified on a silica gel column with cyclohexane : ethyl acetate = 50 : 1 as eluent. Yields ranged between 30 and 88 %. The characteristic data are given in the following.

*Data for acetic acid, 4-(N,N-diphenylamino)phenyl ester (L1):*

Yellowish solid, 52 % yield. <sup>1</sup>H (500MHz, 20°C, CDCl<sub>3</sub>): δ = 2.22 (3 H, s), 6.89 (2 H, d, <sup>3</sup>J = 9 Hz), 6.93 (2 H, t, <sup>3</sup>J = 7, 7, 15 Hz), 7.00 (6 H, m, <sup>3</sup>J = 5, 8, 9 Hz), 7.17 (4 H, t <sup>3</sup>J = 15, 8 Hz) <sup>13</sup>C(CDCl<sub>3</sub>, 20°C, 125 MHz): δ = 169.9, 147.9, 146.0, 129.5, 125.0, 124.3, 123.0, 122.4, 21.4, IR (CaF<sub>2</sub>): 1761 (C=O stretch. vib.), 1589,1501 (aromatic vib.), 1195, 1214 cm<sup>-1</sup> (C-O-Ar ester vib.)

*Data for benzoic acid, 4-(N,N-diphenylamino)phenyl ester (L2):*

Yellowish solid, 30 % yield. <sup>1</sup>H (500MHz, 20°C, CDCl<sub>3</sub>): δ = 6.94 (2 H, t, <sup>3</sup>J = 7.5, 15 Hz), 7.01-7.07 (8 H, bm), 7.18 (4 H, t, <sup>3</sup>J = 8, 15,5 Hz), 7.44 (2 H, t, <sup>3</sup>J = 8, 15 Hz), 7.56 (1 H, t, <sup>3</sup>J = 7.5, 15 Hz) <sup>13</sup>C(CDCl<sub>3</sub>, 20°C, 125 MHz): δ = 165.1, 147.5, 145.7, 145.3, 133.3, 129.3, 129.0, 128.3, 124.7, 123.8, 122.5, 122.1, IR (CaF<sub>2</sub>): 1741 (C=O stretch. vib.), 1588, 1501 (aromatic vib.),1200 cm<sup>-1</sup> (C-O-Ar ester vib.)

*Data for benzoic acid, naphthalene-1-yl ester (L3):*

White solid, 85 % yield. <sup>1</sup>H (500MHz, 20°C, CDCl<sub>3</sub>): δ = 8.21 (2H, d, <sup>3</sup>J = 8.0), 7.81 (1H, d, <sup>3</sup>J = 8.0), 7.77 (1H, d, <sup>3</sup>J = 7.5), 7.66 (1H, d, <sup>3</sup>J = 8.5), 7.55 (1H, dd, <sup>3</sup>J = 7.5, 15) 7.45- 7.36 (5H, m), 7.25 (1H, d, <sup>3</sup>J = 7.5), IR (CaF<sub>2</sub>): 2966 (m, aromatic CH), 1735 (s, ester C=O), 1597 (w, aromatic C=C), 1510 (w, aromatic C=C), 1261, 1254 (s, C-O-Ar), 1223 (s, C-O-C)

*Data for acrylic acid, 4-(N,N-diphenylamino)phenyl ester (M1)*

Yellow solid, 73 % yield. <sup>1</sup>H (500MHz, 20°C, CDCl<sub>3</sub>): δ = 5.93 (1 H, d, <sup>3</sup>J = 10.5 Hz), 6.24 (1 H, dd, <sup>3</sup>J = 10.5, 17.5 Hz); 1 H (d): 6.53 (1 H, d, <sup>3</sup>J = 17.5 Hz), 6.94 (4 H, m); 7.01 (6 H, m), 7.17 (4 H, m) <sup>13</sup>C(CDCl<sub>3</sub>, 20°C, 125 MHz): δ = 165.0, 147.9, 145.8, 145.7, 132.8, 129.5, 128.2,125.0, 124.3, 123.1, 122.4, IR (CaF<sub>2</sub>): 1756 (C=O),1636 (C=C), 1587, 1276, 1315 cm<sup>-1</sup>

*Data for 4-vinylbenzoic acid, 4-(N,N-diphenylamino)phenyl ester (M2)*

Yellow solid, 72 % yield.  $^1\text{H}$  (500MHz, 20°C,  $\text{CDCl}_3$ ):  $\delta$  = 5.53 (1 H, d,  $^3\text{J}$  = 11 Hz), 5.84 (1 H, d,  $^3\text{J}$  = 17.5 Hz), 6.71 (1 H, dd,  $^3\text{J}$  = 11, 17.5 Hz), 6.95 (2 H, m), 7.05 (6 H, m), 7.18 (6 H, m), 7.45 (2 H, d,  $^3\text{J}$  = 8 Hz), 8.07 (2 H, d,  $^3\text{J}$  = 8 Hz);  $^{13}\text{C}$ ( $\text{CDCl}_3$ , 20°C, 125 MHz):  $\delta$  = 165.3, 148.0, 146.3, 145.8, 142.8, 136.2, 130.7, 129.6, 129.5, 128.9, 126.5, 125.2, 124.6, 124.3, 123.0, 122.6, 117.2; IR ( $\text{CaF}_2$ ): 1738 (C=O), 1629 (C=C), 1500, 1263, 1313  $\text{cm}^{-1}$

*Data for 4-vinyl benzoic acid, naphthalene-1-yl ester (M3)*

Yellow solid, 88 % yield.  $^1\text{H}$  (500MHz, 20°C,  $\text{CDCl}_3$ ):  $\delta$  = 8.32 (2 H, d,  $^3\text{J}$  = 8.5 Hz), 7.94 (2 H, dd,  $^3\text{J}$  = 8.5, 18.5 Hz), 7.81 (1 H, d,  $^3\text{J}$  = 8.5 Hz), 7.61 (2 H, d,  $^3\text{J}$  = 8.5 Hz), 7.53 (3 H, d,  $^3\text{J}$  = 7.5, 15.5 Hz), 7.41 (1 H, d,  $^3\text{J}$  = 7.5 Hz), 6.84 (1 H, dd,  $^3\text{J}$  = 10.5, 17.5 Hz), 5.96 (1 H, d,  $^3\text{J}$  = 17.5 Hz), 5.47 (1 H, d,  $^3\text{J}$  = 10.5 Hz);  $^{13}\text{C}$ ( $\text{CDCl}_3$ , 20°C, 125 MHz):  $\delta$  = 165.2, 147.1, 143.0, 136.2, 135.0, 130.9, 128.7, 128.3, 127.2, 126.8, 126.7, 126.3, 125.7, 121.5, 118.5, 117.4; IR ( $\text{CaF}_2$ ): 1733 (C=O), 1629 (C=O), 1508, 1253, 1268  $\text{cm}^{-1}$

### 2.2.3.3 Free radical polymerisations

The monomers acrylic acid, 4-(N,N-diphenylamino)phenyl ester (**M1**), 4-vinylbenzoic acid, 4-(N,N-diphenylamino)phenyl ester (**M2**) and 4-vinyl benzoic acid, naphthalene-1-yl ester (**M3**) were homopolymerised to obtain the corresponding polymers poly[acrylic acid, 4-(N,N-diphenylamino)phenyl ester] (**P1**), poly[4-vinylbenzoic acid, 4-(N,N-diphenylamino)phenyl ester] (**P2**) and poly[4-vinyl benzoic acid, naphthalene-1-yl ester] (**P3**). The structures of the polymers are shown in Scheme 6. Free radical polymerisations were carried out as follows: under argon atmosphere 1.0 equivalent of monomer and 0.01 equivalents of AIBN were dissolved in dry toluene to obtain a 5 wt.-% solution. To remove oxygen, a stream of argon was passed through the solution. The reaction solution was then heated to 80°C and stirred for 21 hours at this temperature. After cooling to 20°C, the polymer was precipitated with a fivefold excess of methanol. The polymer was re-dissolved in toluene, filtered, and reprecipitated from methanol. After thorough washing with methanol, the polymer was dried *in vacuo* at 20°C. The yields ranged between 25 and 80 %. All polymers were characterized with NMR, FTIR and UV/VIS spectroscopy and by size exclusion chromatography (SEC).

*Data for poly[acrylic acid, 4-(N,N-diphenylamino)phenyl ester] (P1)*

White solid, yield = 80 %.  $^1\text{H}$  ( $\text{CDCl}_3$ , 500MHz, 20 °C, ):  $\delta$  = 6.93 – 7.21 (14 H, bm), 2.02-2.92 (3 H, bm),  $^{13}\text{C}$  ( $\text{CDCl}_3$ , 20 °C, 125 MHz):  $\delta$  =147.4 , 145.4, 145.7, 129.1, 123.9, 122.7, 122.1, 53.3; SEC ( $\text{CHCl}_3$ ):  $M_n$  = 3400 g mol $^{-1}$ ;  $M_w$  = 5300 g mol $^{-1}$  ; PDI=1.6; IR ( $\text{CaF}_2$ ): 1756 (C=O), 1587, 1502, 1315, 1276, 1197 cm $^{-1}$

*Data for poly[4-vinylbenzoic acid, 4-(N,N-diphenylamino)phenyl ester] (P2)*

Yellow solid, yield 25 %.  $^1\text{H}$  ( $\text{CDCl}_3$ , 500MHz, 20 °C, ):  $\delta$  = 2 H (b):  $\delta$  = 7.8 ppm, 14 H (bm):  $\delta$  = 7.00 -7.26 ppm, 2 H (b):  $\delta$  = 6.34 - 6.68 ppm, 3 H:  $\delta$  = 0.86 – 1.87 ppm;  $^{13}\text{C}$  ( $\text{CDCl}_3$ , 20 °C, 125 MHz):  $\delta$  =165.1, 149.8, 147.6, 145.5, 130.5, 127.8, 124.5, 124.1, 122.8, 122.3, 40.9; SEC (THF):  $M_n$  = 8200 g mol $^{-1}$ ;  $M_w$ =18800 g mol $^{-1}$  ; PDI=2.3; IR ( $\text{CaF}_2$ ): 1738 (C=O), 1500, 1313, 1263, 1200 cm $^{-1}$

*Data for poly[4-vinyl benzoic acid, naphthalene-1-yl ester] (P3)*

White solid, yield = 40 %.  $^1\text{H}$  ( $\text{CDCl}_3$ , 500MHz, 20 °C, ):  $\delta$  = 8.25 (2 H, b), 7.81-7.71 (2 H. bm), 7.60 (1 H. d), 7.22 (4 H, bm), 6.85 (2 H, b), 2.31 - 1.70 (3 H, b)  
 $^{13}\text{C}$  ( $\text{CDCl}_3$ , 20 °C, 125 MHz):  $\delta$  =165.2, 147.1, 143.0, 136.2, 135.0, 130.9, 128.7, 128.3, 127.2, 126.8, 126.7, 126.3, 125.7, 121.5, 118.5, 117.4  
SEC (THF):  $M_n$  = 12700 g mol $^{-1}$  ;  $M_w$  = 24000 g mol $^{-1}$ ; PDI=1.9  
IR ( $\text{CaF}_2$ ): 1733 (C=O), 1508, 1390, 1253, 1268 cm $^{-1}$

#### 2.2.3.4 Characterisation of monomers and polymers

For spectroscopic and optical measurements, polymer films were prepared on CaF<sub>2</sub> plates by spin-casting from chloroform solutions (**P1** and **P2**) and from anisole solution (**P3**). FT-IR spectra were recorded with a Perkin-Elmer Spectrum One instrument (spectral range between 4000 and 450 cm<sup>-1</sup>). All FT-IR spectra of the samples were taken in transmission. For quantitative analysis, the peak areas were calculated from absorbance spectra. UV/VIS spectra were recorded with a JASCO V-530 UV/VIS spectrophotometer. <sup>1</sup>H and <sup>13</sup>C NMR spectra were taken with a Varian INOVA 500 MHz spectrometer operating at 499.803 MHz and 125.687 MHz, respectively. The peaks from non-deuterated residual solvents were used for referencing the NMR spectra.<sup>[12]</sup>

Weight and number average molecular weights ( $M_w$  and  $M_n$ ) and the polydispersity index

$PDI = M_w M_n^{-1}$  were determined with size exclusion chromatography (SEC). The setup was as follows: Merck Hitachi L6000 pump, separation columns from Polymer Standards Service (8 mm x 300 mm, STV 5 μm grade size; 10<sup>6</sup>, 10<sup>4</sup>, and 10<sup>3</sup> Å pore size), refractive index detector (model Optilab DSP Interferometric Refractometer) from Wyatt Technology. Polystyrene standards from Polymer Standard Service were used for calibration. The eluent was THF or chloroform.

Optical micrographs of Ti:sapphire-laser illuminated samples were taken with a microscope (Olympus, BX 51) equipped with a phase-contrast condenser and phase-contrast objective. The refractive index of the polymer layers was measured by spectroscopic ellipsometry. A Woollam VASE spectroscopic ellipsometer was employed (Xenon short arc lamp, wavelength range 240 nm-1100 nm, spectral bandwidth 4 nm). The implemented software uses the Levenberg-Marquardt fit algorithm. From ellipsometric data both the film thickness and the dispersion of the refractive index (Cauchy fit) were obtained.

#### 2.2.3.5 Determination of absorbance coefficients

For quantitative analysis of the photo-Fries reaction, the infrared absorbance coefficients of model compounds, phenyl acetate (educt) and 2-hydroxyacetophenone (product) were determined. Solutions containing equimolar amounts of educt and product in acetonitrile (between 1.0 and 10.0 mmol L<sup>-1</sup>) were measured in a liquid cell with KBr windows (optical pathlength = 117 μm). Both the peak areas and the signal heights of the ester carbonyl band of phenyl acetate (1750 cm<sup>-1</sup>) and the ketone carbonyl band of 2-hydroxyacetophenone (1641 cm<sup>-1</sup>) were evaluated. The absorbance values showed a linear dependence on the

concentration. From these FT-IR spectra the ratios between the areas of the ester band of phenyl acetate ( $1750\text{ cm}^{-1}$ ) and the ketone band of 2-hydroxyacetophenone ( $1641\text{ cm}^{-1}$ ) were calculated and plotted versus the concentration (range  $1.0 - 10.0\text{ mmol L}^{-1}$ ). From linear regression, an intensity ratio  $1.6 : 1$  was found for the signals of the ester carbonyl peak and the ketone carbonyl peak. With this ratio a quantitative evaluation of the progress of the photo-Fries reaction was performed.

### 2.2.3.6 UV Irradiation procedures

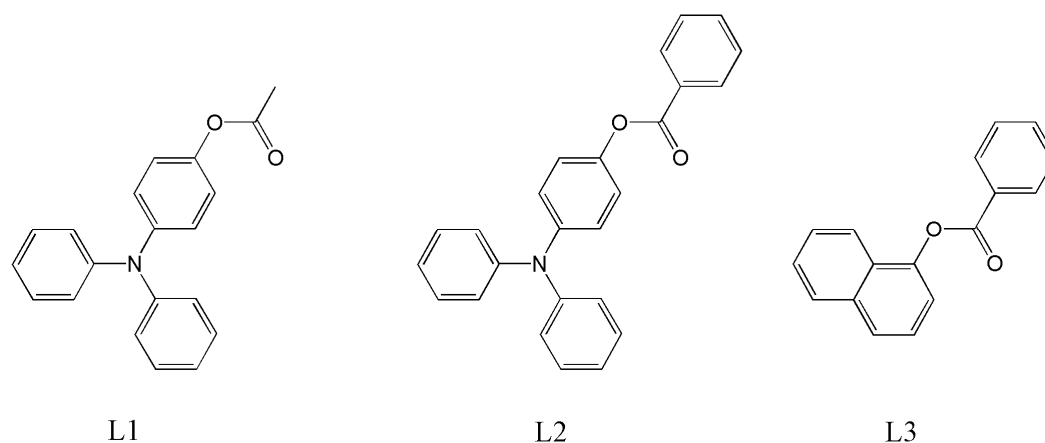
Samples to be irradiated were spin-cast onto  $\text{CaF}_2$  discs at 2000 rpm. Polymer films were spin-cast from  $\text{CHCl}_3$  solutions (**P1**, **P2**;  $5\text{ g L}^{-1}$ ) and from anisole solution (**P3**;  $5\text{ g L}^{-1}$ ). Films of the low-molecular-weight compounds were cast from solution onto  $\text{CaF}_2$  discs in a similar fashion. Film thicknesses (both of the polymers **P1-P3** and of the low-molecular-weight compounds **L1-L3**) were in the range of  $0.5\text{ }\mu\text{m}$ . Films of the model compounds **L1-L3** did not crystallize after spin casting from solution. After drying, the samples were UV irradiated under nitrogen atmosphere ( $\text{N}_2 > 99,999\%$ ). Due to the different photoreactivity of the polymers, two different irradiation setups were used. For some samples the polychromatic light of a mercury medium pressure lamp was used. For the unfiltered light, a power density of  $45\text{ mW cm}^{-2}$  was measured in the spectral range between 230 and 400 nm. In most cases, the mercury lamp was equipped with an interference filter (313 nm). The power density of the filtered light was evaluated to be  $0.6\text{ mW cm}^{-2}$  at  $\lambda = 313\text{ nm}$ . Measurements of the power density (i.e. the light power impinging on the sample surface) was measured with a spectroradiometer (Solatell, Sola Scope 2000TM, measuring range from 230 to 470 nm). The samples were illuminated for periods between 300 s and 1800 s. This corresponds to an energy density  $E$  between 14 and  $81\text{ J cm}^{-2}$  for the polychromatic process (spectral range: 230 - 400 nm). For the monochromatic irradiations at  $\lambda = 313\text{ nm}$ , the energy density  $E$  ranged between  $0.2$  and  $1.1\text{ J cm}^{-2}$ .

For two-photon-absorption (TPA) experiments, an optically pumped titan-sapphire laser system (Mai Tai, pulse duration: 120 fs, repetition rate: 1 kHz, 610 nm) was used. Polymer samples to be irradiated were prepared by casting a solution of the polymer onto glass substrates. Prior to use, the samples were carefully dried *in vacuo*. The polymer films had a thickness of approx.  $3\text{ }\mu\text{m}$ . Laser irradiation in the  $xy$  plane was done by focusing the beam (focal width of the laser beam approx.  $1\text{ }\mu\text{m}$ ) onto the polymer surface and moving the beam along the  $x$ -axis with constant speed. Inscripting of lines along the  $x$ -axis was performed with different laser powers (average pulse power between 0.1 and 0.7 mW). The line patterns inscribed were inspected by optical phase contrast microscopy.

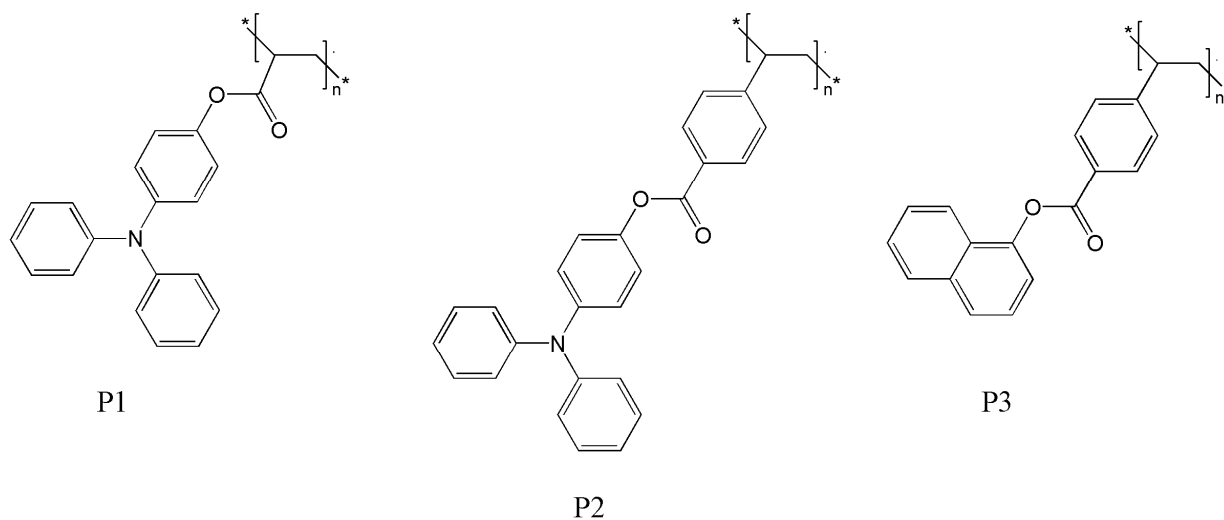
## 2.2.4 Results and discussion

### 2.2.4.1 Synthesis of monomers, model compounds and polymers

All aryl esters (**L1**, **L2**, **L3**, **M1**, **M2** and **M3**) were synthesized from the acid chlorides and aromatic alcohols in good yields (approx. 80%). The structures of the model compounds **L1**, **L2** and **L3** are represented in Scheme 5, for the structures of **M1**, **M2** and **M3**, see Scheme 3 and Scheme 4.



Scheme 5. Structures of the low-molecular-weight model compounds **L1**, **L2** and **L3**



Scheme 6. Structures of the polymers **P1**, **P2** and **P3**



The polymerisations of **M1**, **M2** and **M3** to their homopolymers **P1**, **P2** and **P3** (see Scheme 6 for the structures) were carried out as free radical reactions with azo-*bis*-isobutyronitrile (AIBN). In the case of the two 4-(*N,N*-diphenylamino)phenyl esters (**M1** and **M2**) polymers with a comparably low weight-average molar mass ( $M_w = 5300$  and  $18800 \text{ g mol}^{-1}$ , respectively) were obtained. A possible explanation of this low  $M_w$  values may be a steric hindrance of the vinylic double bonds caused by the bulky triphenylamine group. A similar situation has been found for polymers of 4-(*N,N*-diphenylamino)styrene.<sup>[13]</sup> Also trace amounts of impurities may have acted as chain transfer agents. For monomer **M3** (1-naphthylester) the polymerisation proceeded smoothly and homopolymer **P3** was obtained with  $M_w = 24000 \text{ g mol}^{-1}$ . All polymers **P1-P3** were readily soluble in organic solvents such as chloroform, toluene and tetrahydrofuran. The polymers were colourless and showed good film forming properties when spin-cast from chloroform solution (**P1**, **P2**) and from anisole solution (**P3**).

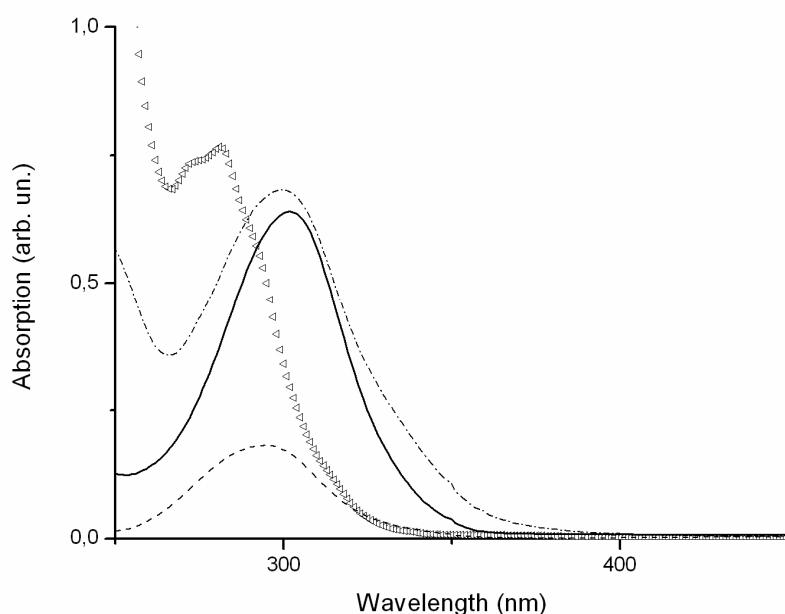


**Figure 3:** UV/Vis-spectra of **P1** (solid line;  $5 \cdot 10^{-6} \text{ mol L}^{-1}$ ), **P2** (dash-dotted line;  $5 \cdot 10^{-4} \text{ mol L}^{-1}$ ), **P3** (triangles;  $1 \cdot 10^{-3} \text{ mol L}^{-1}$ ) in chloroform solution and 4-(*N,N*-diphenylamino)phenol (dashed line,  $1 \cdot 10^{-5} \text{ mol L}^{-1}$ ) in acetonitrile solution

The UV absorbance spectra of these polymers in chloroform solution (spectral range 250 – 450 nm) are represented in Figure 3. For comparison, this figure also contains the absorbance spectrum of 4-(*N,N*-diphenylamino)phenol in acetonitrile solution. It can be seen that 4-(*N,N*-diphenylamino)phenol absorbs up to 360 nm with a peak at 300 nm. The polymers **P1** and **P2** both contain a D- $\pi$ -D chromophore with the *N,N*-diphenylamino and the  $-\text{O}(\text{C}=\text{O})\text{-R}$  groups as donors (D) attached to a benzene ring. The UV absorption of **P1** and

**P2** peaks at 300 nm and extends to approx. 370 nm. Polymer **P3**, which contains the 1-naphthyl ester unit, absorbs up to 320 nm. The UV spectrum of **P3** is comparable to that of 1-naphthol with its strong UV absorbance peaking at 300 nm and extending to approx. 330 nm (spectrum recorded in methanol solution).<sup>[14]</sup>

#### 2.2.4.2 UV irradiation of polymer films

We investigated which photoreactions occur in polymers bearing strongly UV absorbing esters of 4-(N,N-diphenylamino)phenol and 1-naphthol. The photoreactions of the polymers (**P1-P3**) and the low-molecular-weight model compounds (**L1-L3**) were followed by quantitative FT-IR-spectroscopy. FT-IR spectroscopy proved to be an appropriate tool because the functional group in the educt (i.e. the ester unit) and the functional group in the expected photo-Fries product (i.e. hydroxyketone) display well-resolved signals in the infrared spectrum. For the ester group  $R_1-(CO-O)-R_2$  the C=O signal is found at  $1740\text{ cm}^{-1}$  (in case that both the substituents  $R_1$  and  $R_2$  are aromatic) and at  $1760\text{ cm}^{-1}$  for  $R_1$  being an aliphatic and  $R_2$  an aromatic group. After a photo-Fries rearrangement the formation of hydroxyl groups can be detected from a broad signal at  $3400\text{ cm}^{-1}$  (O-H stretch vibr.), while an additional peak at  $1640\text{ cm}^{-1}$  (C=O stretch vib.) is typical of ortho-hydroxyketones.<sup>[15]</sup>

In order to get an insight into the reaction rate of the photo-Fries rearrangement, the FT-IR signals of the ester ( $1740\text{ cm}^{-1}$  and  $1760\text{ cm}^{-1}$ , resp.) and of the ketone product ( $1640\text{ cm}^{-1}$ ) were evaluated. Absorbance FT-IR spectra of liquid films of **L1-L3** and of polymer films **P1-P3** were recorded after different periods of UV irradiation and the carbonyl signals were integrated. Using the infrared absorbance coefficients of model compounds (phenyl acetate and 2-hydroxyacetophenone), both the depletion of the ester units (educt) as well as the yield of hydroxyketone (photo-Fries product) were assessed quantitatively.

#### 2.2.4.3 Photoreactions in polymers P1, P2 and in model compounds L1, L2

The low-molecular-weight compounds **L1** and **L2** correspond to the polymers **P1** and **P2**. We wished to see if the distribution of photoproducts differs when changing from a low-molecular-weight compound to the corresponding polymer. Moreover, the difference in reactivity between **L1** and **L2** (and **P1** and **P2**, respectively) should give evidence to which degree the photoreactivity varies when the structure is changed from an ester of an aliphatic carboxylic acid (**L1**, **P1**) to an ester of an aromatic carboxylic acid (**L2**, **P2**). The quantitative data of this investigation are summarized in Table 1 and Table 2.

**Table 1: UV irradiation of polymers P1, P2 and P3: conversion of the ester group and reaction yield of the photo-Fries product.**

Polymer	Irradiation time <i>min</i>	E <i>J cm<sup>-2</sup></i>	Ester remaining %	o-Hydroxyketone generated %
<b>P1</b> <sup>a)</sup>	0	0	100	0
	5	14	66	2
	30	81	19	6
<b>P2</b> <sup>b)</sup>	0	0	100	0
	10	0.4	55	5
	30	1.1	22	5
<b>P3</b> <sup>b)</sup>	0	0	100	0
	10	0.4	60	3
	30	1.1	21	8

<sup>a)</sup> Polychromatic irradiation. Energy density E measured for the wavelength range 230 – 400 nm

<sup>b)</sup> Monochromatic irradiation at  $\lambda = 313$  nm

**Table 2: UV irradiation of the model compounds L1, L2 and L3: conversion of the ester group and reaction yield of the photo-Fries product.**

Compound	Irradiation time <i>min</i>	E <i>J cm<sup>-2</sup></i>	Ester remaining %	o-Hydroxyketone generated %
<b>L1</b>	0	0	100	0
	5	14	95	4
<b>L2</b>	0	0	100	0
	90	3,2	18	20
<b>L3</b>	0	0	100	0
	90	3,2	40	10

<sup>a)</sup> Polychromatic irradiation. Energy density E measured for the wavelength range 230 – 400 nm

<sup>b)</sup> Monochromatic irradiation at  $\lambda = 313$  nm

The FT-IR spectrum of a film of **P1** (prior to irradiation) displays almost the same signals as the model compound **L1**, as shown in Figure 4. The carbonyl stretching vibration with an intense signal is at  $1756\text{ cm}^{-1}$  and the signals for the C-O-aryl deformation vibration arise at  $1197$  and  $1136\text{ cm}^{-1}$  (asymmetric and symmetric modes, respectively). The signals at  $1587$  and  $1502\text{ cm}^{-1}$  are attributed to the aromatic ring vibration, while the bands at  $1276$  and  $1315\text{ cm}^{-1}$  stem from the C-N stretching vibration of the N-aryl bond. The illumination of this polymer with unfiltered UV light (power density  $45\text{ mW cm}^{-2}$ ) leads to a disappearance of the ester signals at  $1756$  (C=O),  $1197$  (C-O-C) and at  $1136\text{ cm}^{-1}$  (C-O-C). In contrast, the peaks

typical of the aromatic system and of the N-aryl bond remain virtually unchanged. A very weak signal evolves at  $1637\text{ cm}^{-1}$ , which indicates the formation of the ortho-hydroxyketone (in 2-hydroxyacetophenone, the C=O signal appears at  $1641\text{ cm}^{-1}$ ). These results indicate the formation of the photo-Fries product in a low yield. When the UV irradiation experiment is carried out with a liquid film of compound **L1**, similar changes are observed in the FTIR spectrum.

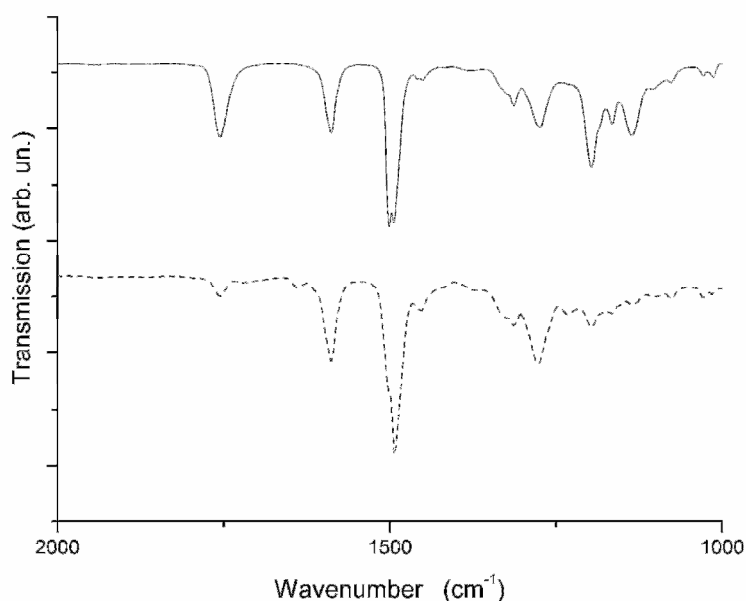


**Figure 4:** FT-IR spectra of **P1** prior to (solid line) and after polychromatic irradiation (dotted line) with an energy density of  $81\text{ J cm}^{-2}$  (measured between 230 and 400 nm). The illumination of the polymer leads to a depletion of the ester signals and at the same time a weak signal at  $1637\text{ cm}^{-1}$  (ketone) arises.

A quantitative evaluation based on the IR absorbance coefficients of phenyl acetate and 2-hydroxyacetophenone (*vide supra*) showed that after 5 min of polychromatic irradiation ( $14\text{ J cm}^{-2}$ ) approx. 34% of the ester groups in **P1** were converted. However, the yield of ortho-hydroxyketone amounted to only 2%, as listed in Table 1. Even after prolonged illumination (81% ester conversion) the yield of ketone is as low as 6%. It is interesting to compare these data to those obtained with the corresponding low-molecular weight compound **L1**, as listed in Table 2. After 5 min of polychromatic irradiation ( $14\text{ J cm}^{-2}$ ) only 5% of the ester units were converted, but the yield of ketone was approx. 4%. It turns out that the photoreactivity of polymer **P1** is far higher than that of the model compound **L1**, but the yield of ketone (i.e. the photo-Fries product) is very low for the polymer.

In a similar fashion polymer **P2** and its low-molecular-weight counterpart **L2**, both containing aromatic esters of aromatic carboxylic acids, were studied. In this case, monochromatic irradiation at  $\lambda = 313\text{ nm}$  was used throughout the experiments. Figure 5

shows the spectrum of pristine **P2** (solid line), where the peaks at  $1738\text{ cm}^{-1}$  (C=O stretching),  $1263$ ,  $1200$  and at  $1073\text{ cm}^{-1}$  indicate the fully aromatic esters. This band assignment is supported by a comparison with the FTIR spectrum of benzoic acid phenyl ester which displays strong bands at  $1266$ ,  $1200$  and  $1060\text{ cm}^{-1}$ .<sup>[16]</sup> Other bands in this FT-IR spectrum are typical of aromatic rings ( $1500\text{ cm}^{-1}$  and  $1588\text{ cm}^{-1}$ ) and of N-aryl stretching vibrations (e.g.  $1313\text{ cm}^{-1}$ ). An N-aryl signal expected around  $1260\text{ cm}^{-1}$  obviously overlaps with the ester C-O-C band. UV illumination of **P2** results in a conversion of the ester group (decreasing signals at  $1738$ ,  $1263$ ,  $1200$  and  $1073\text{ cm}^{-1}$ ) and the formation of ketones (evolution of a weak signal at  $1631\text{ cm}^{-1}$ ).

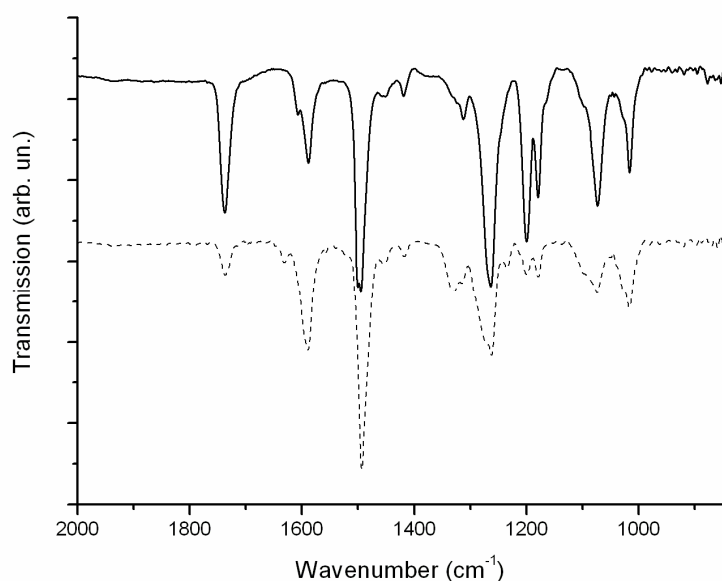
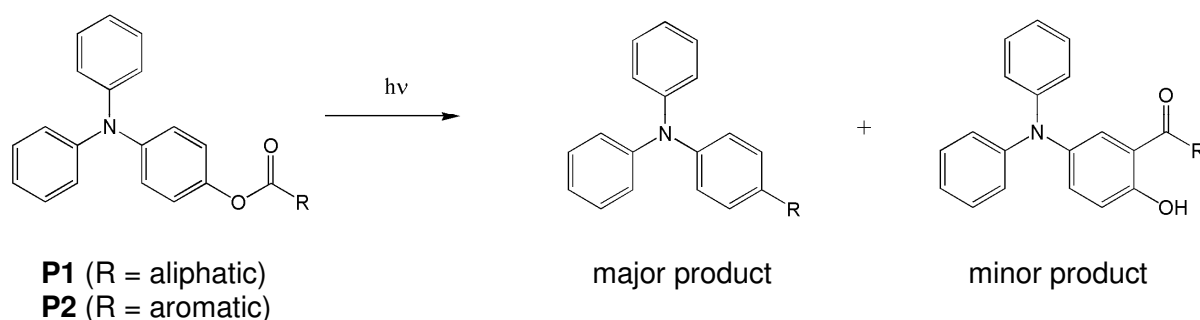


**Figure 5:** FT-IR spectra of **P2** prior to (solid line) and after irradiation (dotted line) with an energy density of  $1.1\text{ J cm}^{-2}$  (monochromatic at  $\lambda = 313\text{ nm}$ ). The illumination of the polymer leads to a depletion of the ester signals and at the same time a weak signal at  $1631\text{ cm}^{-1}$  (indicating the ketone) arises.

A quantitative evaluation (as listed in Table 1) shows that the reactivity of polymer **P2** is far higher than that of **P1**. For **P2**, monochromatic irradiation at  $\lambda = 313\text{ nm}$  with an energy density  $E = 1.1\text{ J cm}^{-2}$  is sufficient to convert 78% of the ester units. However, the yield of the photo-Fries product is as low as 5% which is similar to the situation found for **P1**. The low-molecular-weight compound **L2** gave similar changes in its FT-IR spectra after 313 nm irradiation: a decrease of the peak at  $1741\text{ cm}^{-1}$  (ester) accompanied by the evolution of a new signal  $1641\text{ cm}^{-1}$  (hydroxyketone). In this case, an energy density  $E = 3.2\text{ J cm}^{-2}$  was required to achieve 80% ester conversion but the yield of the photo-Fries product amounts to 20% (cf Table 2). The photoreactivity of the ester units in polymer **P2** is higher than in compound **L2**, but at the same time the yield of ketone is far lower for the polymer.

These results with polymers and model compounds containing 4-(N,N-diphenylamino)phenyl esters can be summarized as follows. UV illumination of the polymers **P1** and **P2** leads to a depletion of ester units. The degradation of esters proceeds at a faster rate for phenyl esters of aromatic carboxylic acids than for phenyl esters of aliphatic carboxylic acids. However, only low yields of the expected photo-Fries rearrangement product (ortho-hydroxyketone) are observed in the polymeric materials (aprox. 5% when 80% of the ester units have reacted). Considering the low-molecular-weight model compounds **L1** and **L2**, the decomposition of ester units is far less efficient than for their polymeric counterparts. Again, the fully aromatic compound **L2** reacts faster than **L1** which is an ester of an aliphatic carboxylic acid. Interestingly, the yield of photo-Fries rearrangement product is far higher for the low-molecular weight compounds.

From the spectral data we conclude that the decarboxylation of the ester groups (photoextrusion of CO<sub>2</sub>) is the main photoreaction in these materials, as shown in Scheme 7. Decarboxylation is more pronounced in polymers where limited mobility and perhaps also templating effects favour this reaction which is based on a concerted mechanism. This is in accordance with the literature (Weiss et al., ref.<sup>[6]</sup>).



**Scheme 7. Proposed photoproducts in polymers P1 and P2**

However, this effect was not expected, since most photoreactions proceed similarly in low-molecular weight compounds and in polymers. In this case it appears that the type of the reaction strongly depends on flexibility of the matrix. The photogenerated CO<sub>2</sub> is expected to dissolve in the polymer and then diffuse out (formation of bubbles was not observed). This is similar to photoresists containing azides and diazoquinones, which generate N<sub>2</sub> upon UV illumination.

#### 2.2.4.4 Photoreactions in polymer **P3** and model compound **L3**

The FT-IR spectrum of **P3**, which contains 1-naphthyl esters of an aromatic carboxylic acid, displays the signals typical of the ester units (1733 (C=O), 1268 (asym. C-O-C), and 1090  $\text{cm}^{-1}$  (sym. C-O-C)). The presence of the naphthyl group is indicated by bands at 1607, 1601, and 1390  $\text{cm}^{-1}$ , as shown in Figure 6. Irradiation of a film of **P3** with 313 nm UV light leads to the depletion of the ester signals and to the evolution of a band typical of ketones (1629  $\text{cm}^{-1}$ ), see the spectra in Figure 6. A quantitative evaluation shows that the yield of ketone is approx. 8% when 80% of the ester units have decomposed after irradiation with an energy density  $E = 1.1 \text{ J cm}^{-2}$ .

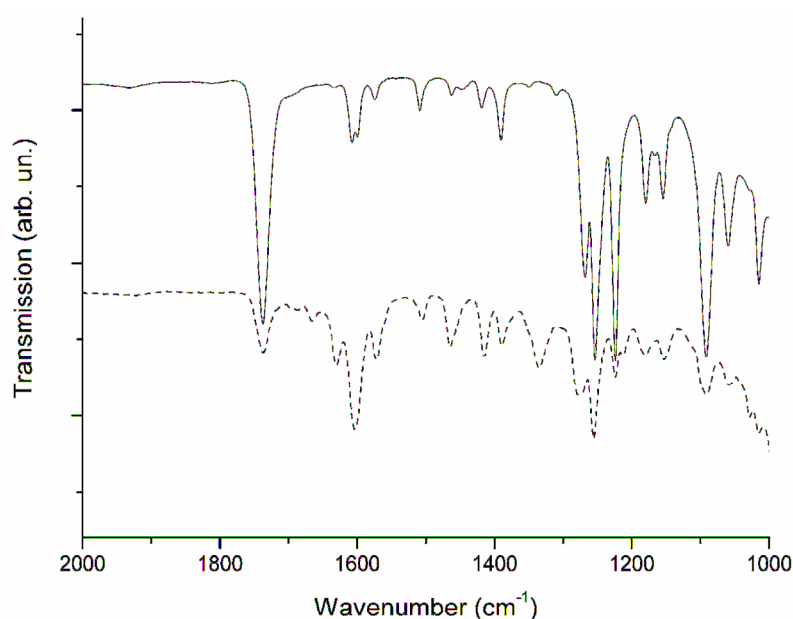
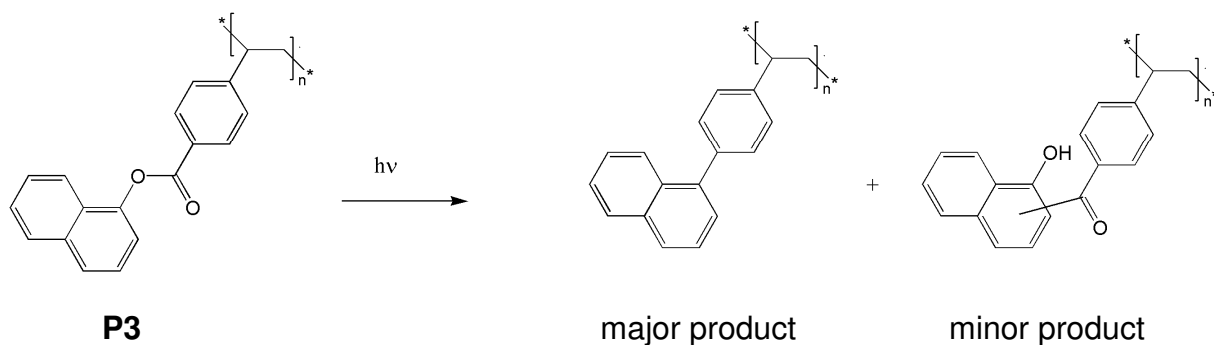


**Figure 6:** FT-IR spectra of **P3** prior to (solid line) and after irradiation (dotted line) with an energy density of  $1.1 \text{ J cm}^{-2}$  (monochromatic at  $\lambda = 313 \text{ nm}$ ). The illumination of the polymer leads to a depletion of the ester signals and the formation of ketone (band evolving at  $1631 \text{ cm}^{-1}$ ).

The low-molecular-weight model compound **L3** (benzoic acid 1-naphthyl ester) is less reactive with respect to the decomposition of the ester units: after irradiation with  $E = 3.2 \text{ J cm}^{-2}$  only 60% of the ester groups have reacted. At this stage of reaction the yield of ketone amounts to 10%. This indicates that the situation is similar to that found for **P2** and **L2**. Also for the naphthyl esters of benzoic acid the photoextrusion of  $\text{CO}_2$  is the main reaction. The proposed photoproducts of polymer **P3** are sketched in Scheme 8.



**Scheme 8. Proposed photoproducts in polymer P3**

### 2.2.4.5 Photoinduced refractive index changes in polymers P1-P3

One major goal of this investigation was to identify polymers which change in their refractive index upon UV irradiation. Spectroscopic ellipsometry was applied to determine the refractive index of polymer films prior to and after irradiation. Polymer **P1** was taken as an example for a polymer bearing 4-(N,N-diphenylamino)phenyl ester groups, and polymer **P3** was investigated as an example for bearing the 1-naphthyl ester chromophore.

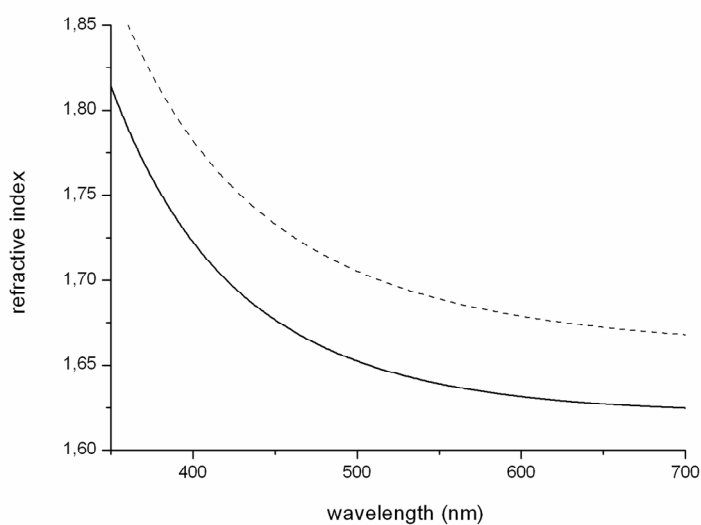


**Figure 7: Cauchy fit of the refractive index of a film of P1 (thickness 80 nm) on silicon. Solid line: before irradiation, dotted line: after irradiation (polychromatic; energy density  $E = 54 \text{ J cm}^{-2}$  measured between 230 and 400 nm).**



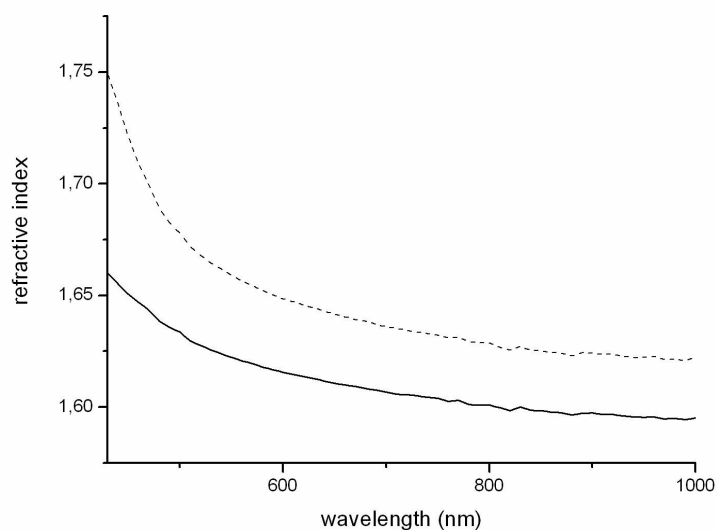


**Figure 8: Cauchy fit of the refractive index of a film of P2 (thickness 80 nm) on silicon. Solid line: before irradiation, dotted line: after UV irradiation (monochromatic at  $\lambda = 313$  nm) with an energy density of  $1.1 \text{ J cm}^{-2}$ .**

The Cauchy fits of the dispersion of the refractive indices of **P1** and **P3** are shown in Figure 7 and Figure 8, respectively. Illumination times were chosen such that a large fraction of the ester units, approx. 80%, had reacted. This was checked by recording FT-IR spectra. For both polymers, the refractive index showed a significant change after illumination. For **P1**, the refractive index  $n_{450}$  at the wavelength  $\lambda = 450$  nm was 1.676 prior to irradiation and 1.733 after polychromatic UV illumination with  $E = 54 \text{ J cm}^{-2}$ . This increase is equal to a refractive index change of  $\Delta n_{450} = 0.06$ , which is a result of the photoreactions depicted in Scheme 7. For the wavelength  $\lambda = 589$  nm ( $\text{Na}^{\text{D}}$  line),  $\Delta n_{589}$  amounts to 0.05.

Based on the concept of molar refraction, the refractive index of an organic compound (and also of a polymer) can be calculated from group contributions to the molar refraction (Lorentz-Lorenz equation, see ref. <sup>[17]</sup>). Using the data compiled by Van Krevelen,<sup>[18]</sup> for polymer **P1** an index of refraction  $n = 1.678$  (at  $\lambda = 589$  nm) is obtained, when the density of the polymer is assumed to be  $1.2 \text{ g cm}^{-3}$ . When **P1** undergoes complete photo-Fries rearrangement,  $n$  is expected to increase to 1.684. In contrast to this, a refractive index  $n = 1.752$  is calculated for the fully decarboxylated polymer. In both cases it has been assumed that the density of the polymer remains constant at  $1.2 \text{ g cm}^{-3}$ . Although it is questionable if the density of **P1** actually remains constant during the photoreactions, the theoretical prediction indicates that photodecarboxylation is the main reason for the experimentally observed increase of  $n$ .

For **P3**, a refractive index  $n_{450} = 1.651$  was measured prior to illumination. After monochromatic irradiation with  $\lambda = 313$  nm the refractive index  $n_{450}$  increased to 1.721, cf.

Figure 8. This corresponds to an increase of the refractive index by  $\Delta n_{450} = 0.07$ . At the wavelength  $\lambda = 589$  nm,  $\Delta n_{589}$  was 0.03. Again, these changes indicate large structural differences between the non-illuminated and the illuminated polymer films as predicted for the proposed decarboxylation reaction in the polymers **P1** and **P3**. The index changes measured for **P1** and **P3** exceed the index changes which have been reported for norbornene polymers containing phenyl esters of aliphatic carboxylic acids ( $\Delta n_{450} = 0.05$ ).<sup>[1]</sup> In comparison to this, the photoinduced isomerisation of R-SCN to R-NCS in poly(4-vinylbenzyl thiocyanate) results in a change of  $n$  by 0.03,<sup>[19]</sup> while the photoinduced [2+2] cycloaddition in copolymers of vinyl cinnamate results in a decrease of  $n$  by 0.02.<sup>[20]</sup> Summing up, the photoreactions in polymers containing aryl esters generally lead to a very large increase of the refractive index which makes these materials interesting for waveguide applications.

### 2.2.4.6 Laser irradiation under two-photon conditions

Changes in the refractive index caused by irradiation of polymer films with a Ti:sapphire-femtosecond laser ( $\lambda = 610 \text{ nm}$ ; two-photon conditions) were followed by optical microscopy. This investigation was limited to polymers **P2** and **P3** (the photoreactivity of **P1** appeared to be too low, *vide supra*). To visualize the change in the refractive index, a phase contrast setting was used. Areas with higher refractive indices appear dark, while areas with lower refractive index appear bright. Using this method, it can be detected if the laser irradiation leads to a change in the refractive index of the polymer film.

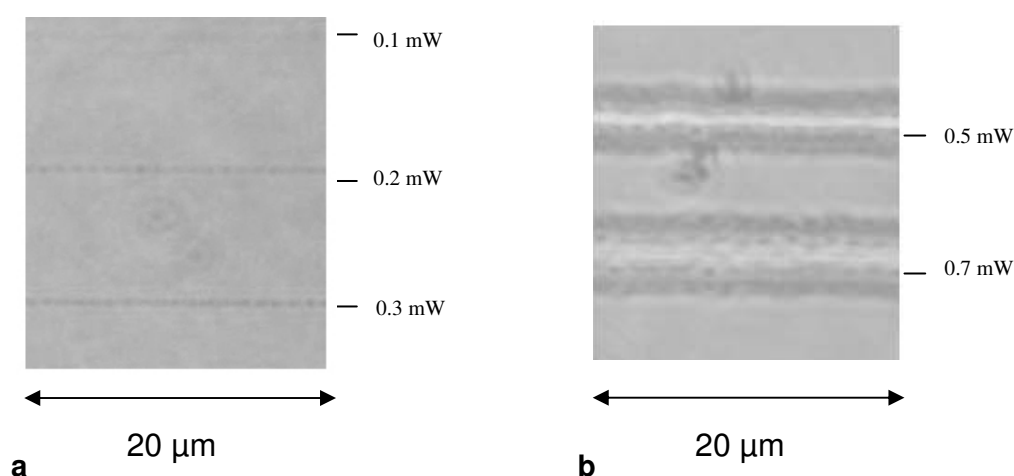


**Figure 9:** Phase contrast images of a film of **P3** after irradiation with a Ti:sapphire femtosecond laser ( $\lambda = 610 \text{ nm}$ ) with different pulse powers (0.1 mW, 0.2 mW, 0.3 mW, 0.5 mW and 0.7 mW). At low laser powers (0.1 mW, 0.2 mW, 0.3 mW) clearly resolved lines are discernible (a). These dark lines indicate an increase in refractive index. At higher laser power (0.5 mW and 0.7 mW) degradation of the polymer is observed (b).

For polymer **P2** it was found that irradiation with an average pulse power of 0.19 mW evoked a change in the refractive index (thin dark line in the microscope image). However, when the laser power is increased to 0.20 mW, laser ablation of the material was observed as indicated by a very broad, corrugated line in the microscope image. On the other hand, decreasing the laser power to values of 0.18 mW and less did not generate any detectable changes in the polymer. This indicates that the dynamic power range (i.e. the range for successful TPA laser patterning) of this material is very low.

For polymer **P3**, well-resolved line patterns were achieved with different laser powers (0.1, 0.2 and 0.3 mW). These lines were readily detectable under the optical microscope, as shown in Figure 9 a. The line width is approx.  $1 \mu\text{m}$  which matches with the focal width of the writing laser. The occurrence of dark lines indicates that the refractive index has increased in

the irradiated zones which suggests the occurrence of a two-photon effect. When the average pulse power is increased to 0.5 mW and higher values, destruction of the material was observed, cf. Figure 9 b.

These initial results suggest that the prepared polymers, especially **P3**, can be applied in two photon-induced photoreactions. A more detailed investigation of these photoprocesses under laser radiation is currently under progress. Ongoing work is also related to UV sensitive polymers equipped with D- $\pi$ -A chromophores, e.g. benzene rings bearing the N,N-diphenylamino (donor) and the  $-(C=O)-O-R$  (acceptor) group as substituents.

### 2.2.5 Conclusion

This study shows that polymers bearing (N,N-diphenylamino)phenyl and 1-naphthyl esters are highly reactive under UV illumination. Especially materials which contain aromatic esters of aromatic carboxylic acids (polymers **P2** and **P3**) react rapidly under 313 nm radiation. Photoinduced decarboxylation is the predominant reaction while the anticipated photo-Fries reaction is observed as a side reaction. The comparison with low-molecular-weight model compounds shows that the rate of ester degradation is higher in the polymers.

As a result of the photoreaction, the refractive index of the polymers (**P1**, **P3**) increases by  $\Delta n_{450}$  up to 0.07 (measured at  $\lambda = 450$  nm). This increase is large and matches the theoretical prediction based upon group contributions to molar refraction.

First results obtained from two-photon laser processing indicate that polymer **P3** may be a good candidate for the inscribing of 3D waveguide structures in polymeric media.

## 2.2.6 References

- [1] T. Höfler, T. Griesser, X. Gstrein, G. Trimmel, G. Jakopic, W. Kern, *Polymer* **48**, **2007**, 1930
- [2] J.C. Anderson, C.B. Reese, *Proc. Chem. Soc.* **1960**, 217
- [3] S. Lochbrunner, M. Zissler, J. Piel, E. Riedle, A. Spiegel, T. Bach, *J. Chem. Phys.* **2004**, *120*, 11634
- [4] S.-K. Li, J.E. Guillet, *Macromolecules* **10**, **1977**, 840
- [5] R.A. Finnegan, D. Knudsen, *Tetrahedron Lett.* **9**, **1968**, 3429
- [6] W. Gu, D.J. Abdallah, R.G. Weiss, *J. Photochem. Photobiol. A: Chem.* **139**, **2001**, 79
- [7] M.A. Miranda, F. Galindo, "Photo-Fries Reaction and Related Processes", in: *CRC Handbook of Organic Photochemistry and Photobiology*, W.M. Horspool, ed., 2<sup>nd</sup> edition, CRC Press, Boca Raton, USA, 2004
- [8] E. Bellmann, S.E. Shaheen, S. Thayumanavan, S. Barlow, R.H. Grubbs, S.R. Marder, B. Kippelen, M. Peyghambarian, *Chem. Mater.* **10**, **1998**, 1668
- [9] M. Behl, R. Zentel, D.J. Broer, *Macromol. Rapid. Comm.* **25**, **2004**, 1765
- [10] B.H. Cumpston, S.P. Ananthavel, S. Barlow, D.L. Dyer, J.E. Ehrlich, L.L. Erskine, A.A. Heikal, S.M. Kuebler, I.-Y. Lee, D. McCord-Maughon, J. Qin, H. Rockel, M. Rumi, X.-L. Wu, S.R. Marder, J.W. Perry, *Nature (London)* **398**, **1999**, 6722
- [11] S.M. Kuebler, M. Rumi, T. Watanabe, K. Braun, B.H. Cumpston, A.A. Heikal, L.L. Erskine, S. Thayumanavan, S. Barlow, S.R. Marder, J.W. Perry, *J. Photopolym. Sci. Technol.* **14**, **2001**, 657.
- [12] H.E. Gottlieb, V.Kotylar, A. Nudelman, *J. Org. Chem.* **62**, **1997**, 7512.
- [13] N. Tsutsumi, T. Murao, W. Sakai, *Macromolecules* **38**, **2005**, 7521.
- [14] "UV Atlas of Organic Compounds", Vol. 2, Verlag Chemie, Weinheim **1966**, p. E1/6.
- [15] G. Socrates, *Infrared Characteristic Group Frequencies*, 2<sup>nd</sup> edition, John Wiley & Sons, Chichester, **1998**.
- [16] *Spectral database of Organic Compounds*, National Institute of Advanced Industrial Science and Technology, SDBS No. 7164 (2007). Available under [www.aist.go.jp/RIODB/SDBS](http://www.aist.go.jp/RIODB/SDBS).
- [17] A.I. Vogel, *Practical Organic Chemistry*, Longmans, London **1956**, pp. 1034-1036
- [18] D.W. van Krevelen, *Properties of Polymers*, 3<sup>rd</sup> ed., Elsevier, Amsterdam **1990**, pp. 290-296.
- [19] G. Langer, T. Kavc, W. Kern, G. Kranzelbinder, E. Toussaere, *Macromol. Chem. Phys.* **202**, **2001**, 3457.
- [20] A. Nagata, T. Sakaguchi, T. Ichihashi, M. Miya, K. Ohta, *Macromol. Rapid Comm.* **18**, **1997**, 191.

## 2.3 Photoreactive styrene and silicone polymers bearing 4-(N,N-diphenylamino)phenyl benzoate units: one-photon and two-photon reactions

### 2.3.1 Summary

Novel polymers bearing 4-(N,N-diphenylamino)phenyl benzoate as two-photon chromophore were synthesised and investigated for two-photon absorption based photoreactions resulting in a high refractive index change of the polymer. Polysiloxanes as matrix offer a very easy way to attach the chromophore to an optically transparent and flexible matrix. Quantitative calculations on the yield of photoproducts have been carried out under one-photon (linear) and two photon (non linear) absorption conditions. It is shown that the aryl ester undergoes a photo-Fries reaction and a photodecarboxylation (extrusion of CO<sub>2</sub>). The ratio of both reactions depends on the polymeric matrix. Both photoproducts show a higher refractive index than the starting product (aryl ester), allowing an optical patterning of the polymers. The photoreactions were investigated by ellipsometry, UV-VIS and FT-IR spectroscopy, FT-IR microscopy and phase contrast microscopy.

### 2.3.2 Introduction

Two-photon absorption (TPA) has become more and more important because of its huge potential in various fields. Numerous investigations were carried out concerning two-photon induced photopolymerisation (TPP) and two-photon imaging. Compared to these methods photoconversions of organic compounds under TPA conditions have been studied less frequently. Examples are the two-photon induced cycloreversion reactions of 7-hydroxycoumarin for drug delivery <sup>[1]</sup>, the phototautomerisation of phthalocyanines <sup>[2]</sup> and the photocyclization of diarylethene derivatives<sup>[3,4]</sup>. These examples show the conversion of organic molecules dissolved in liquids or polymeric materials.

TPA absorption is known to occur in the presence of intense ultra-short laser pulses where molecules absorb two photons simultaneously reaching the same excited state as for one-photon absorption. A virtual excited state is created at half the energy of the one-photon energy. Therefore, the two-photon excitation is observed at the double wavelength compared to the one-photon process. The probability of this absorption process is proportional to the square of the laser pulse intensity, providing two important advantages of this method. On

the one hand, the material is not absorbing at the wavelength used, because the TPA process only occurs in the vicinity of the focused laser beam, where the intensity is sufficient, enabling three dimensional structuring in one step. On the other hand, the square dependency leads to high spatial resolution for the written structures. For TPA structuring or polymerisation in a solid; reactive molecules such as a photoinitiator and monomers need to be loaded into a matrix, where some disadvantages arise. Solid initiators or TPA chromophores can cause problems like aggregation. Liquid monomers reduce the thermal stability of the material before structuring. Often pre- or post treatments are necessary to stabilize the whole system. To circumvent these problems, the TPA chromophore can be attached covalently to a polymeric system. A TPA initiator was successfully covalently attached to a polysiloxane chain.<sup>[5]</sup> In a similar fashion, we wanted to synthesise polymeric systems, containing a TPA chromophore in the side chain for photoconversion, which means that no compounds other than the polymer are needed for the structuring process.

In this contribution we investigated the one- and two-photon reactions of aromatic esters, which are known to undergo a photo-Fries rearrangement upon UV irradiation. This photoreaction was first observed by Anderson and Reese, reporting the light induced conversion of aryl ester yielding the *ortho*- and *para*-hydroxyketones.<sup>[6]</sup> The reaction starts by excitation to the S<sub>1</sub> state. The photoproducts are formed after homolytic cleavage of the C-O bond.<sup>[7]</sup> We previously investigated polymers bearing phenyl ester units in the side chain, where we reported synthesis, characterisation and the observation of the occurring photo-Fries reaction.<sup>[8]</sup> Depending on many parameters, aryl esters show different yields on the photo-products and also different side reactions. One of those is the photo-decarboxylation reported by Finnegan and Knudsen in 1968.<sup>[9]</sup> This reaction also proceeds from the singlet state where an aromatic ester R-COO-R' is transformed into a hydrocarbon R-R' via a photoextrusion of CO<sub>2</sub>. For this reaction a concerted mechanism has been proposed. Sterical hindrance of the ester and solvent effects can influence the yield of decarboxylation product. Templating effects have been observed where the limited mobility of aromatic esters dissolved in a polymeric matrix leads to a higher yield of the photo-decarboxylation product whereas the yield of the Fries rearrangement is lowered.<sup>[10]</sup> Only recently we reported on polymers containing aryl esters in the side chain, where the photodecarboxylation is the main reaction upon UV irradiation.<sup>[11]</sup> All investigated polymers containing aryl esters showed high refractive index change upon irradiation, resulted from the high molecular change within the side chains. These index changes up to +0.07 enable the use for waveguides or optical data storage for these materials.

The main goal of the present work was to investigate the photoreaction of the chromophore 4-(diphenylamino)phenyl benzoate, contained in the side chain of a

polystyrene and a polysiloxane derivative, under one-photon and two-photon conditions. The polymers were studied with respect to their refractive index change upon illumination for applications in the field of waveguides or optical data storage.

### 2.3.3 Experimental Part

#### 2.3.3.1 Starting Compounds

Dichloromethane (from Fluka) was distilled over  $P_2O_5$ , Toluene (Fluka) was dried by distillation over Na/K. Styrene was received from Sigma-Aldrich and freshly distilled prior to use. The synthetic route to obtain 4-vinylbenzoic acid, 4-(N,N-diphenylamino)phenyl ester (**M1**) is described elsewhere<sup>[11]</sup>. All other chemicals were obtained from commercial sources (Fluka, Aldrich, Lanchester and ABCR) and used as received.

#### 2.3.3.2 Polystyrene derivative P1

Poly [4-vinylbenzoic acid, 4-N,N-diphenylaminophenyl ester - co- styrene] **P1** was prepared as follows (compare Figure 10): under argon, 200 mg of **M1** (0.5 mmol) and 4 mg of AIBN were placed in a Schlenk flask. Then 1 mL of toluene and 0.1 mL (0.86 mmol) of styrene were added. The solution was heated up to 70 °C and stirred over 16 h. The mixture was then dropped into 30 mL of methanol and stirred for 1 h. The yellowish precipitate was filtered off, dissolved in toluene, reprecipitated from methanol and dried *in vacuo* at 40 °C. The obtained polymer was characterised by NMR, size exclusion chromatography and FT-IR.  $M_n=32570$  g/mol; PDI = 4,08; Yellow solid, yield 80 %.  $^1H$ -NMR ( $\delta$ , 20 °C,  $CDCl_3$ , 500 MHz): 7.8 (br, 2H), 7.00–7.26 (br m, 17H), 6.34–6.68 (br, 4H), 0.86–2.20 (br, 6H); IR ( $CaF_2$ ): 1738 (C=O), 1500, 1313, 1263, 1200  $cm^{-1}$



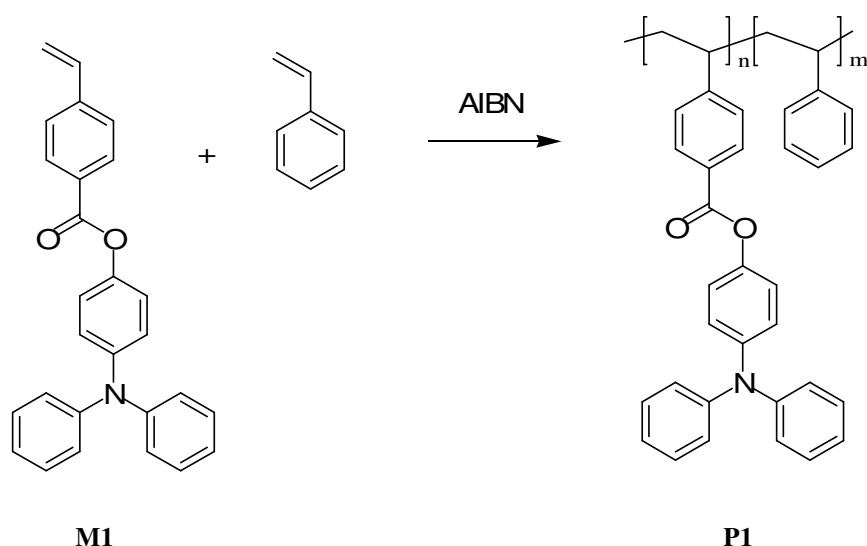


Figure 10: free radical polymerisation of M1 and styrene to give the copolymer P1

### 2.3.3.3 Modified polysiloxane P2

Hydrosilylation of a phenylsubstituted polysiloxane was carried out to covalently attach a chromophore to a polysiloxane chain, (as already shown from Oztemiz et al <sup>[5]</sup>) to obtain a flexible, optically transparent and photoreactive polysiloxane. Similar to a procedure of our group <sup>[12]</sup>, the phenylsubstituted silicone matrix is consisting of two different polysiloxane components: the vinyl terminated diphenylsiloxane - dimethylsiloxane copolymer (PDV 1635) and the hydride terminated methylhydrosiloxane – phenylmethylsiloxane copolymer (HPM 502). Therefore, a mixture of 100 mg HPM 502 and 1  $\mu\text{L}$  Pt-carbonyl catalyst (1.85-2.1% platinum concentration in vinylmethylcyclicsiloxanes) were added to 50 mg of **M1**. This mixture was heated in 0.5 mL 1,4-dioxane to 80  $^{\circ}\text{C}$  for 30 minutes to obtain **P2a** (compare Figure 17). After cooling down, 300 mg PDV 1635, 30 mg HPM 502, 3  $\mu\text{L}$  Pt-catalyst and 1.5 mL 1,4-dioxane were added. The solution was stirred for another 20 minutes at a temperature of 80  $^{\circ}\text{C}$ . The polymer obtained was characterized by FT-IR spectroscopy. IR ( $\text{CaF}_2$ ): 2962, 1738 (C=O), 1592, 1495, 1429, 1311, 1260, 1200, 1178, 1148-974 (br)  $\text{cm}^{-1}$

### 2.3.3.4 UV illumination process

The UV illumination was carried out with a medium pressure Hg lamp, equipped with a filter that is transmissive in the wavelength range between 260 nm and 350 nm. The power density amounts to 10  $\text{mW}/\text{cm}^2$ , measured with a spectroradiometer (Solatell, 2000TM). TPA experiments were performed with an optically pumped titan-sapphire laser system (Mai Tai, pulse duration: 120 fs, repetition rate: 1 kHz, 610 nm). Samples were coated on  $\text{CaF}_2$ -discs.

## 2.3.4 Results and discussion

### 2.3.4.1 Polystyrene based system

The synthesis of M1, which is a very easy three step synthesis with high yields, has been described in a previous contribution<sup>[11]</sup>. Poly [4-vinylbenzoic acid, 4-N,N-diphenylaminophenyl ester - co- styrene] (**P1**) was synthesized via a free radical polymerization with azo-*bis*-isobutyronitrile (AIBN) as thermal initiator. It is known, that triphenylamine groups inhibits such radical reactions leading to a very low molecular mass.<sup>[13]</sup> To get an acceptable high average molar mass, the monomer solution for the polymerisation reaction was set very concentrated, to result in a  $M_n$  of 33000  $\text{g mol}^{-1}$ . For higher masses a living radical polymerisation can be carried out.<sup>[13]</sup> In our case, the film forming properties of the polystyrene have been excellent also for thicker films up to 50  $\mu\text{m}$ , which met all our demands.

We investigated the photoreactions occurring in the different polymer systems, all of them bearing the strongly UV absorbing unit 4-(N,N-diphenylamino)phenyl benzoate. Illuminations carried out with a mercury medium pressure lamp allowed us to observe the reaction by FT-IR, UV-VIS spectroscopy and ellipsometry.

To identify the occurring photoreaction, illumination processes were followed by quantitative FT-IR-spectroscopy. For the ester group Ph-(CO-O)-Ph the C=O signal is found at 1740  $\text{cm}^{-1}$ . An ortho-hydroxyketone as the product of a photo-Fries rearrangement shows a broad signal at 3400  $\text{cm}^{-1}$  (O-H stretch vibr.) and a sharp peak at 1640  $\text{cm}^{-1}$  (C=O stretch vib.).<sup>[14]</sup>

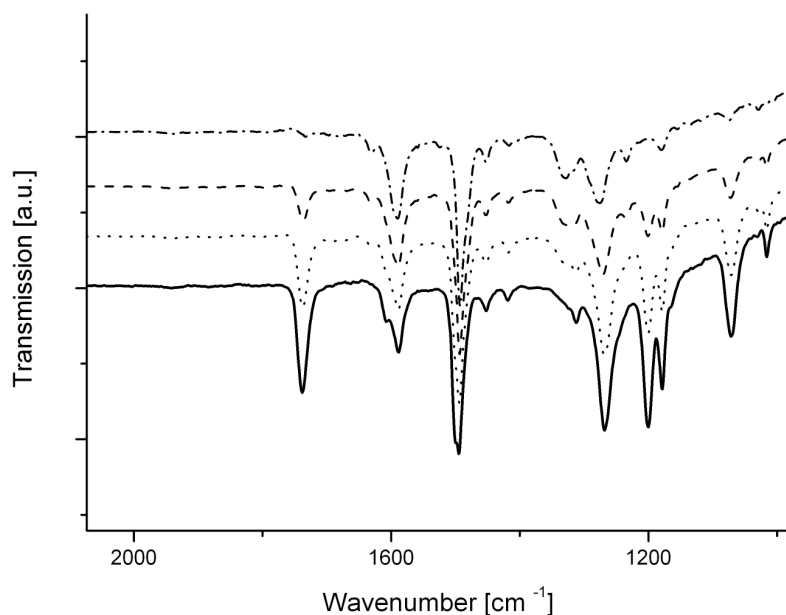


**Figure 11: FT-IR spectra of P1. Non irradiated (solid line), after 0,15 J/cm<sup>2</sup> of irradiation (dotted line), after 0,6 J/cm<sup>2</sup> of irradiation (dashed line) and after 6 J/cm<sup>2</sup> of irradiation (dash-dotted line)**

In Figure 11 the FT-IR spectra of **P1** is displayed, the non irradiated thin polymer film is shown as solid line, whereas the irradiated spectra are shown with interrupted lines. The original polymer shows peaks at 1738, 1263, 1200 and 1072 cm<sup>-1</sup> indicating the aromatic ester. Other bands can be found at 1590 and 1500 cm<sup>-1</sup>, typical of aromatic rings.

UV illumination of **P1** results in a conversion of the ester group, which can be seen by the decreasing signals at 1738, 1263, 1200 and 1072 cm<sup>-1</sup>. Only a weak ketone peak evolves at 1632 cm<sup>-1</sup>. Quantitative calculations of the photo-Fries product have been carried out using absorption coefficients of the carbonyl vibration signal of small model compounds: phenyl benzoate and 2-hydroxybenzophenone.<sup>[8]</sup> These calculations only represents estimations of the exact yield since the absorption coefficients of the 4-N,N-diphenylaminophenyl ester and the corresponding photo-Fries product might differ. Nevertheless, the following results show a good approximation. Illumination with 6 J/cm<sup>2</sup> yielded in a decrease of 95 % of the ester carbonyl vibration at 1738 cm<sup>-1</sup>. The new formed peak at 1632 cm<sup>-1</sup> evaluates a yield of 9 % of the ketone. These changes in the FT-IR spectra leads to the conclusion, that the aromatic ester has almost completely reacted, whilst less than 10 % of the reacted ester has built the corresponding photo-Fries product. As observed for similar molecules and polymers, we believe that the main reaction in this case is the photodecarboxylation, shown in Figure 12. The extrusion of CO<sub>2</sub> explains the decrease of the ester not observing any new carbonyl bonds in the spectra.

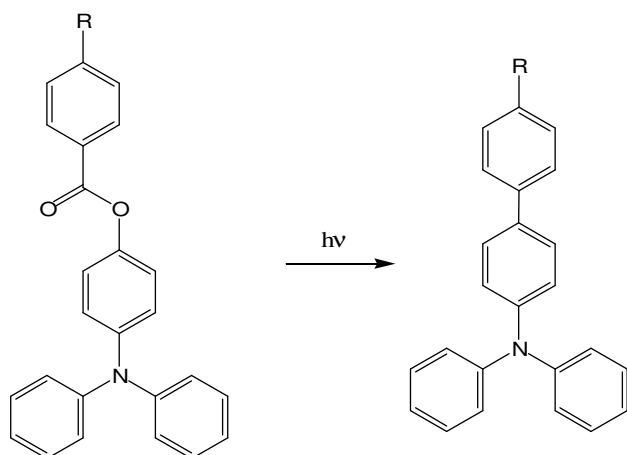


**Figure 12: Photodecarboxylation reaction in the chromophore 4-(N,N-diphenylamino)phenyl benzoate (R indicates a polymer backbone).**

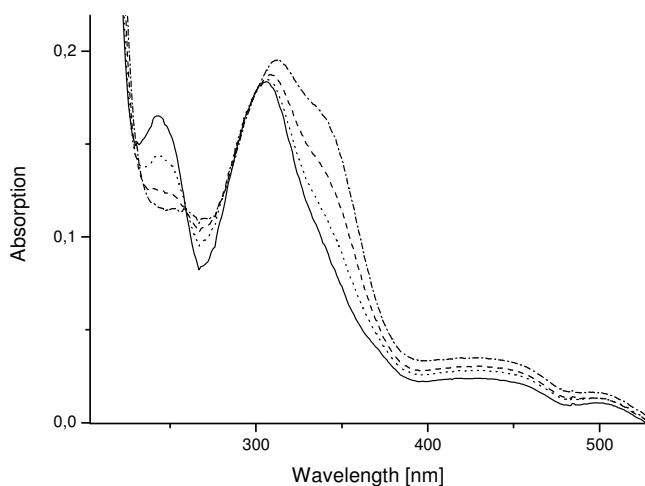


**Figure 13: UV-VIS spectrum of P1 non irradiated (solid line), after 15 seconds irradiation (dotted line), after 1 minute irradiation (dashed line) and after 10 minutes irradiation (dashed-dotted line)**

In Figure 13 the UV-VIS absorption spectra of **P1** (solid line) is depicted, where two maxima at 245 nm and at 305 nm can be observed. For the illumination process, a filter was used to cut off the wavelength under 260 nm, which ensures that the excitation of the chromophore is caused only by higher wavelengths. The illumination of **P1** was also followed by means of UV-VIS spectroscopy, shown with interrupted lines in Figure 13. Upon irradiation, we observe a decreasing absorption peak at 245 nm, while the second peak at 305 nm is building a shoulder at 342 nm, but still absorbing up to 390 nm and a little higher, respectively. Unfortunately, we found no literature data on the UV absorbance of the expected photoproduct, a biphenyl- N,N- diphenylamine. Therefore, we compared 9-phenylcarbazole (PC)<sup>[15]</sup> and 9-biphenylcarbazole (BPC).<sup>[16]</sup> The absorption of the PC

between 250 and 300 nm is higher than the absorption above 300 nm, whereas for BPC it is the other way round. The same can be observed in the spectra of **P1**, compare Figure 13. The illumination results in a dramatic decrease of the peak at 240 nm. The shoulder at 340 nm cannot be identified clearly. The spectrum of BPC shows no additional peak or shoulder at higher wavelength than PC. Possibly it stems from a built side product, a carbazole, which has an absorption maximum at 339 nm. Triphenylamines and diphenylamines are known to undergo cyclizations upon irradiation to build the corresponding carbazole. The photo-Fries product would show to absorption peaks around 260 and 440 nm. The minimum at 267 nm absorbs higher with longer illumination. Combined with the small increase of absorbance at 440 nm, these arising peaks can be attributed to the photo-Fries product<sup>[8]</sup>. According to the FT-IR spectra, the built ketone is less than 10 %, still agreeing with the UV-VIS spectra.

The main goal of this investigation was to create refractive index pattern upon laser irradiation under TPA conditions. For waveguide applications, an increase in refractive index has to be achieved by radiation processes. For the photoreactions of aryl esters an increase in refractive index occurs as a result of the changes in molecular structure. No further development or baking steps are required which constitutes a significant advantage of this procedure.

Spectroscopic ellipsometry was used to determine the refractive index change of thin polymer films upon illumination with a medium pressure Hg- lamp (polychromatic irradiation). The Cauchy fit of the dispersion of the refractive indices of **P1** prior to (solid line) and after illumination (dotted line) are shown in Figure 14. The refractive index at the wavelength 450 nm was 1.678 prior to irradiation and 1.718 after irradiation, which equals an increase of  $\Delta n_{450} = +0.040$ . For the wavelength  $\lambda = 589$  nm (Na<sup>D</sup> line),  $\Delta n_{589}$  amounts to +0.027. The changes of the refractive indices indicate large structural differences between the non-illuminated and the illuminated polymer films, as predicted for the proposed decarboxylation reaction in the chromophore as the main reaction. Comparable increases in the refractive index can be achieved by the classical photo-Fries rearrangement of phenyl esters<sup>[8]</sup> and the isomerisation of poly (4-vinylbenzyl thiocyanate).<sup>[17]</sup>

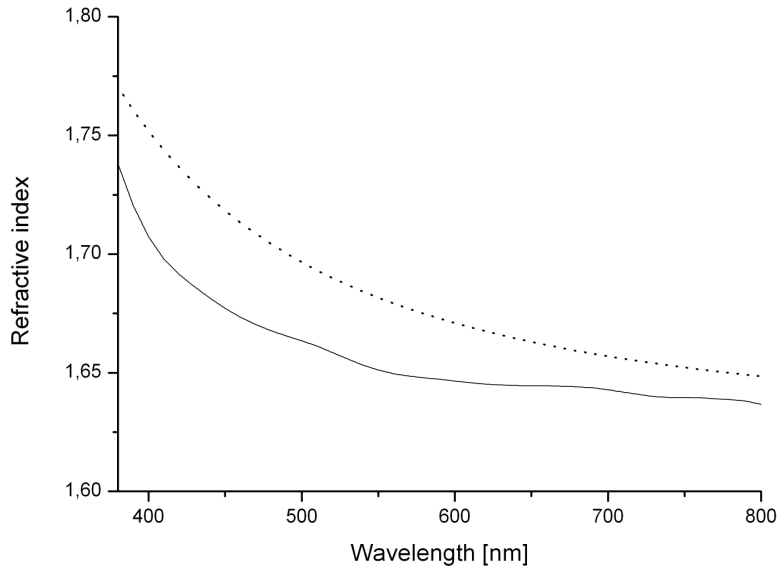


**Figure 14: Cauchy fit of the refractive index of a film of P1 on silicon. Solid line: prior to irradiation, dotted line: after UV irradiation**

### TPA experiments

Laser writing of optical waveguides in the polymeric materials was conducted to test the TPA characteristics. Phase contrast microscopy was used to distinguish between the higher refractive index in the illuminated areas and the lower refractive index in the non illuminated parts. Two photon experiments were carried out with a Ti:sapphire femtosecond laser with an emission wavelength of 610 nm. This wavelength is exactly twice the wavelength of the absorption maximum at 305 nm. Under one photon conditions, using a filter cutting off wavelengths beneath 260 nm enabled the same excitation. Lines were inscribed into the polymer films with different laser powers (compare Figure 15). High powers above 270  $\mu\text{W}$  caused material ablation of the polymer, visible in the microscope also without phase contrast mode. Only with powers of 260  $\mu\text{W}$  and 270  $\mu\text{W}$ , clearly defined lines with an diameter up to 20  $\mu\text{m}$  are visible in the phase contrast mode, but not without. This indicates a refractive index change of the material caused by the laser irradiation. To identify the reaction occurring within the material, a field was inscribed into the polymer (see Figure 16). On the left side, laser power of 270  $\mu\text{W}$  was used to inscribe 12 lines next to each other, creating a field with a higher refractive index as the surrounding material. Directly next to these lines another 12 lines were inscribed with higher laser powers causing destruction of the polymer, to locate the left part of the field in the FT-IR microscope without phase contrast mode. Both sides were measured with an FT-IR microscope using an aperture of 40 microns. As reference, the non irradiated material was measured. The spectra of the destroyed material showed a decrease of 40 % of the complete FT-IR spectra supporting the

assumption of material ablation in this part of the field. In the spectra of the left side indicated as black square in Figure 16, only the carbonyl peaks at  $1738\text{ cm}^{-1}$ ,  $1200\text{ cm}^{-1}$  and  $1070\text{ cm}^{-1}$  decreased of about 10 %, whilst other peaks at  $2920$  and  $1495\text{ cm}^{-1}$  stayed the same. Keeping in mind that not the complete cross section is illuminated, but only a layer within the polymer, and that destruction of the material happens in a larger diameter, an overall yield of about 40 % of the photoreaction in the left field is roughly estimated. An exact quantitative answer cannot be given, since it is not clear if the whole area of the left side is thoroughly structured. Nevertheless, these FT-IR microscope measurements allowed us to identify the reaction, occurred in the vicinity of the laser beam, which emerged to be the same reaction as under one photon condition, where the main reaction is the photo decarboxylation.

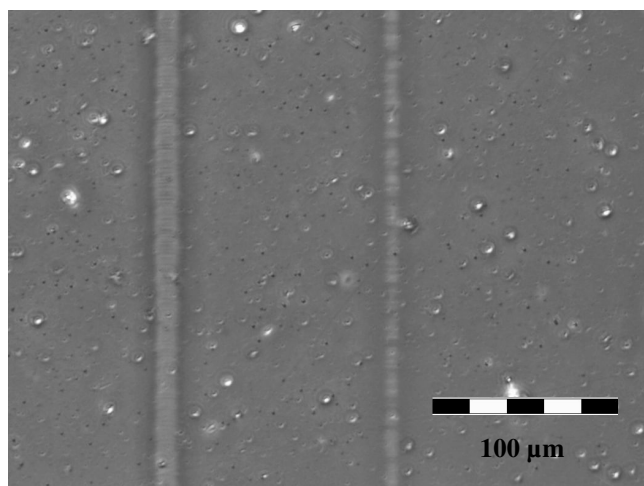


**Figure 15:** Phase contrast image of a film of P1 after irradiation with a Ti:sapphire femtosecond laser ( $\lambda = 610\text{ nm}$ ) with different pulse powers. For laser powers at  $270$  and  $260\text{ }\mu\text{W}$  clearly resolved lines are discernible, indicating an increase in refractive index.

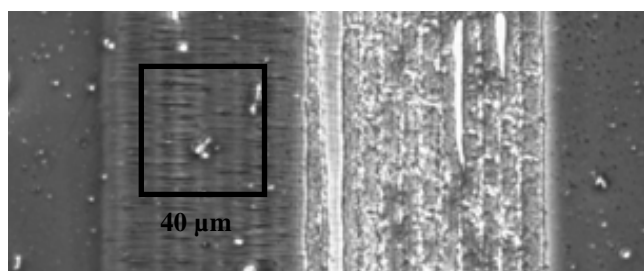


**Figure 16:** Phase contrast image of a film of P1 after irradiation with a Ti:sapphire femtosecond laser ( $\lambda = 610\text{ nm}$ ) with different pulse powers. On the left side: A field of clearly resolved lines inscribed with a power of  $270\text{ }\mu\text{W}$ , indicating an increase in refractive index. The black square indicates the FT-IR microscope aperture of  $40\text{ }\mu\text{m}$ . On the right side: higher power led to laser ablation.

### 2.3.4.2 Polysiloxane based system P2

For the synthesis of the polysiloxane based system **P2**, a completely different approach was done than for **P1**. The synthesis was carried out as an addition to a polysiloxane chain via a hydrosilylation reaction (see Figure 17) instead of a polymerisation reaction. This modified polysiloxane chain **P2a** can then be mixed into other polysiloxanes to be crosslinked, again via hydrosilylation reaction, resulting in an optical high transparent and flexible network (schematically depicted in Figure 18). Advantages of this procedure are the easy variance of photoactive component in the matrix and the possibility to simple attach chromophores covalently to a commercial available polysiloxane matrix. This could also be very useful when photoinitiators are used for two photon polymerisation reactions. Solid TPA chromophores often show bad solubility in the used matrix which causes problems for the irradiation experiments. Covalently attaching them to the matrix would exclude problems of this kind.



Figure 17: Pt catalyzed hydrosilylation reaction to obtain polymer **P3a**; R= 4-(diphenylamino)phenyl benzoate

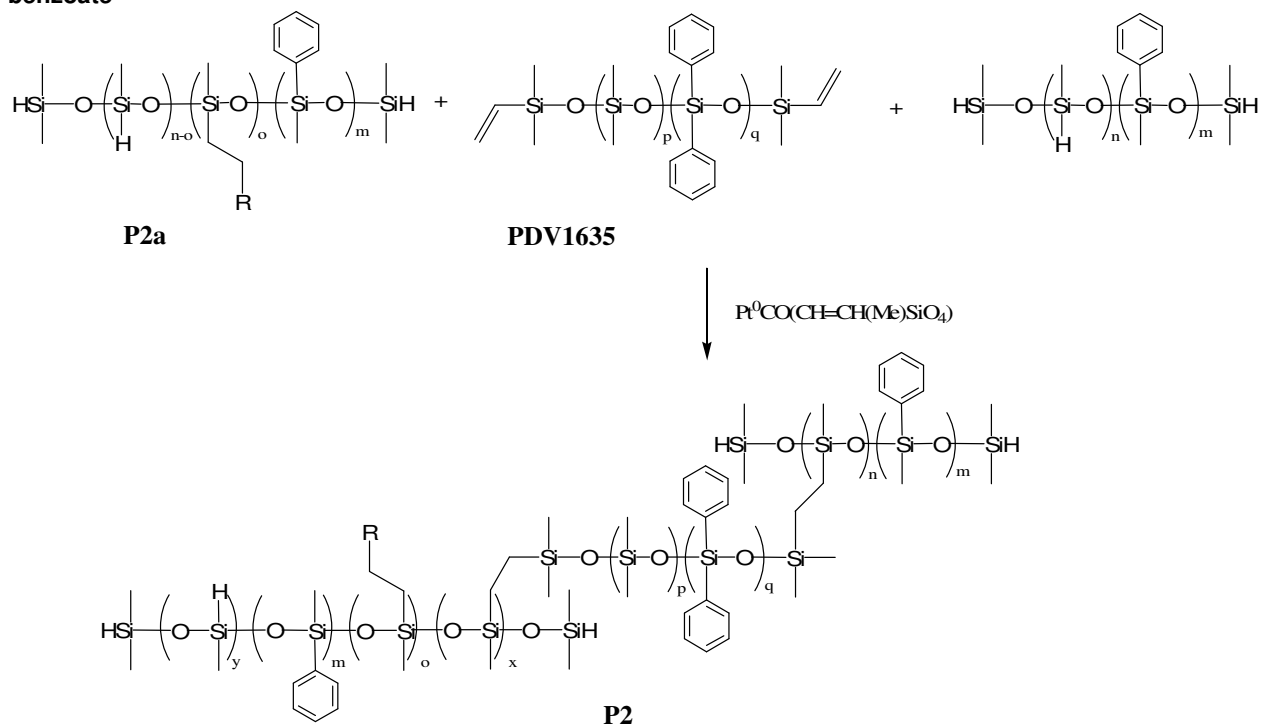
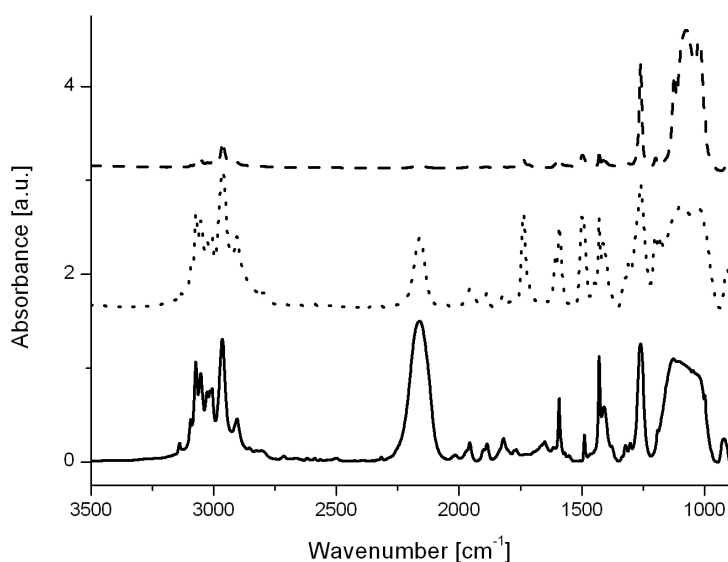


Figure 18: Synthesis of **P2** in a hydrosilylation reaction; R= 4-(diphenylamino)phenyl benzoate



The hydrosilylation reactions have been followed by FT-IR shown in Figure 19. The unmodified polysiloxane HPM 502 (solid line) show a big peak between 1200 and 1000  $\text{cm}^{-1}$ , characteristic for the Si-O vibration of polysiloxanes. The vibration peak at 1260  $\text{cm}^{-1}$  can be attributed to the silicon-carbon vibration. At 1593  $\text{cm}^{-1}$  the vibration peak of the aromatic rings can be found in the spectra. The Si-H groups show a strong characteristic absorbance at 2161  $\text{cm}^{-1}$ . During the addition of the chromophore, bearing a vinyl group, the Si-H group is converted due to a platin catalysed hydrosilylation reaction (cf. Figure 17). This group conversion can easily be followed in the FT-IR spectra where the Si-H peak at 2161  $\text{cm}^{-1}$  decreases drastically. A new peak at 1738  $\text{cm}^{-1}$  represents the aromatic ester of the chromophore. The remaining hydrosilylgroups still are available for the crosslinking of the chains. Adding now vinyl terminated polysiloxane chains and unmodified polysiloxane chains with hydrosilyl groups, the resulting product is a three dimensional network **P2**, simplified shown in Figure 18. In the FT-IR spectra of this siloxane matrix the Si-H peak at 2161  $\text{cm}^{-1}$  is comparable small, indicating a fully crosslinked matrix. Also the signals for the ester and for the aromatic systems are small, since only 10 % of the chromophore are contained. The most intensive signals are the Si-O and Si-C vibrations, showing the predominant compounds.



**Figure 19: FT-IR spectra of polysiloxane unmodified HPM 502 (solid line), attached to the chromophore P2a (dotted line) and crosslinked P2 (dashed line)**

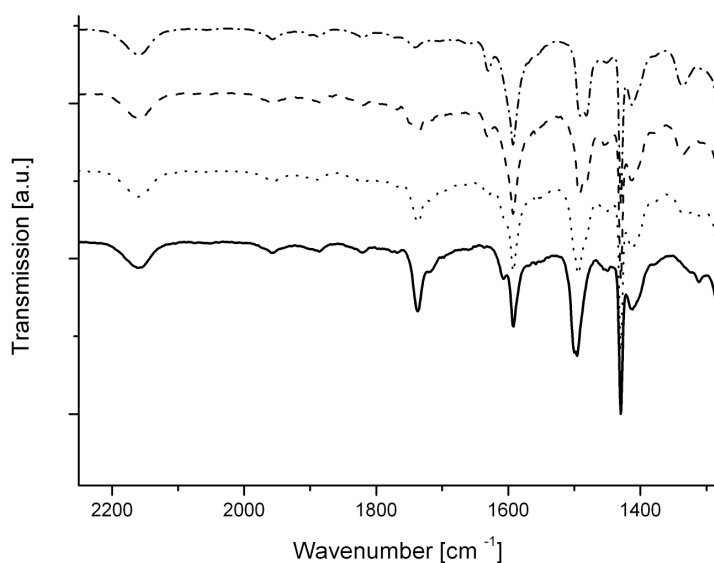


**Figure 20: FT-IR spectra of P2. Non irradiated (solid line), after 0,15 J/cm<sup>2</sup> of irradiation (dotted line), after 0,6 J/cm<sup>2</sup> of irradiation (dashed line) and after 6 J/cm<sup>2</sup> of irradiation (dash-dotted line)**

In Figure 20 FT-IR spectra of **P2** are displayed, the non irradiated thin polymer film is shown as solid line, whereas the irradiated spectra are shown with interrupted lines. The original polymer shows a signal of the aromatic ester at 1738 cm<sup>-1</sup>, signals at 1263, 1200 and 1072 cm<sup>-1</sup> cannot be found due to the overlapping strong Si-O vibrations. To focus on the conversion of the ester, the area between 2200 and 1300 cm<sup>-1</sup> is shown enlarged.

UV illumination of **P2** results in a conversion of the ester group, as already observed for **P1**. During irradiation, the signal at 1738 cm<sup>-1</sup> is decreasing while a ketone peak evolves at 1632 cm<sup>-1</sup>. Quantitative calculations out of the absorption spectra showed a conversion of about 85 % of the aromatic ester. Interestingly, the photo-Fries product amounts to about 20 % in this case. Still yielding very low the product seems to be doubled comparing to the polystyrene based system **P1**. Also for **P2** it is proposed that the main reaction is the photodecarboxylation and a photo-Fries rearrangement as a not negligible side reaction shown in Figure 21.

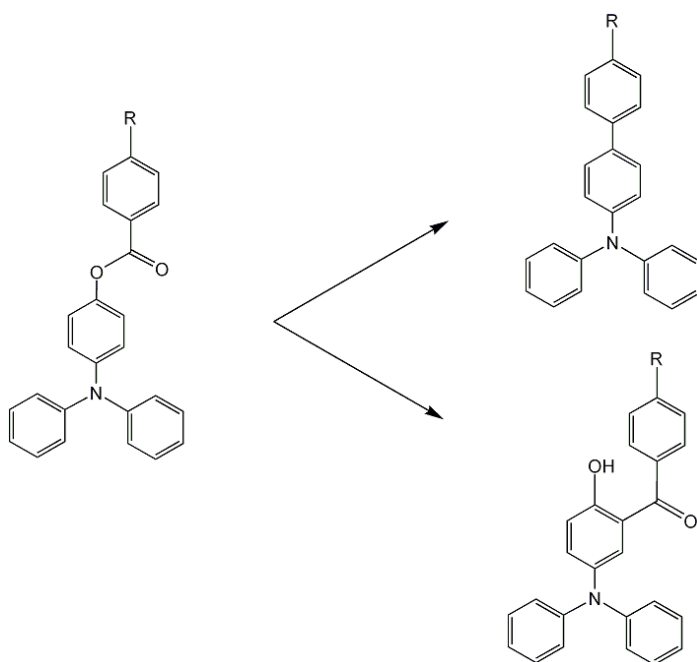


**Figure 21: Proposed photoreactions: photodecarboxylation (top) and photo-Fries reaction (bottom).**

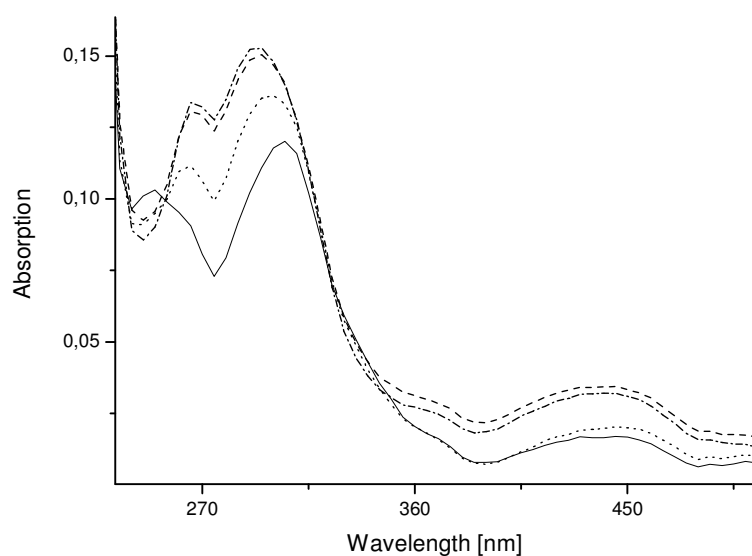


**Figure 22: UV/VIS- spectra of P2 non irradiated (solid line), after 15 seconds irradiation (dotted line), after 1 minute irradiation (dashed line) and after 10 minutes irradiation (dashed-dotted line)**

The UV/VIS- spectra of P2 are depicted in Figure 22, where the solid line shows the spectra of non irradiated P2, whereas interrupted lines are spectra after illumination. For P2 and P1, the UV/VIS absorption of the non illuminated samples is the same with two maxima at 245 nm and 305 nm. For P2, the peak at 245 nm decreases upon irradiation, but at the same time a new peak arises at 265 nm. This can be attributed to the built photo-Fries product.<sup>[8]</sup> It is well known that the hydroxyketone as the photo-Fries product is higher absorbing than the corresponding ester. This agrees with the FT-IR spectra, showing that for P2 the photo-Fries

rearrangement yielded 20 %. It seems that for **P2** the side product, absorbing at 340 nm, observed for the photoreaction of **P1**, is not built. For the identification of the photodecarboxylation, this spectrum offers no information, since the photo-Fries product is absorbing much stronger.

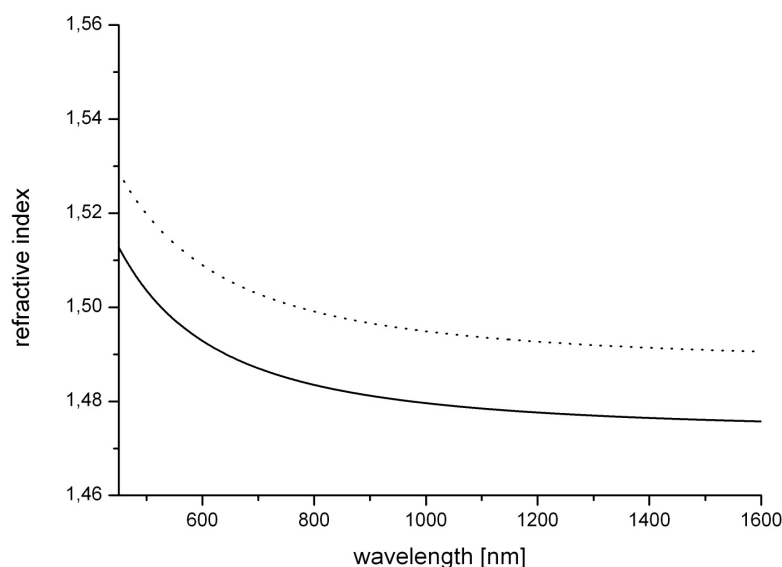


**Figure 23: Cauchy fit of the refractive index of a film of P2 on silicon. Solid line: before irradiation, dotted line: after UV irradiation**

The Cauchy fits of the dispersion of the refractive indices of **P2** prior to (solid line) and after illumination with a medium pressure Hg- lamp (dotted line) are shown in Figure 23. In the polysiloxane **P2** the refractive index change was +0.016 for the wavelengths  $\lambda = 450$  and 589 nm. The changes of the refractive indices indicate large structural differences between the non-illuminated and the illuminated polymer films, as predicted for the proposed photo reaction in the chromophore. Considering that in both polymeric systems the amount of the active chromophore is different (for **P1** 70 wt-% and for **P2** 10 wt-%) we expected the largest change for the polystyrene based system **P1**. Indeed, the change of **P1** upon irradiation is more than double compared to the change of **P2**. Keeping in mind, that for the two different polymer systems the photoreactions differ, as observed via UV/VIS and FT-IR spectroscopy, no linear dependence was predicted.

## TPA experiments

Laser writing of optical waveguides was also conducted to test the TPA characteristics of **P2**. A microscopic image in phase contrast mode of laser illuminated **P1** is shown in Figure 24. Areas with higher refractive index appear darker in this microscopic mode.

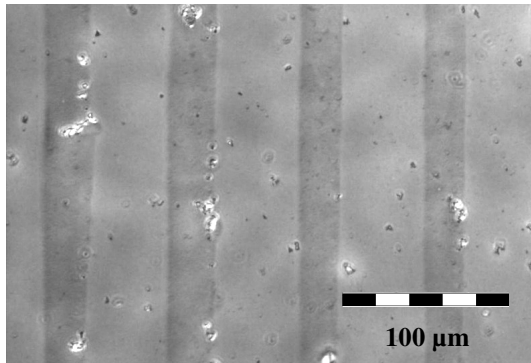


**Figure 24: Phase contrast images of a film of P2 after irradiation with a Ti:sapphire femtosecond laser ( $\lambda = 610$  nm) with different pulse powers (840  $\mu$ W, 850  $\mu$ W, 860  $\mu$ W and 870  $\mu$ W). The darker lines indicate a higher refractive index compared to the surrounding material.**

Lines were inscribed at laser powers of 840  $\mu$ W, 850  $\mu$ W, 860  $\mu$ W and 870  $\mu$ W. The material has a fabrication window between 700 and 800  $\mu$ W, where the refractive index can be increased without destroying the material. Although the polymer was filtered several times before casting it onto the substrate, there are still inclusions visible in the film. These inclusions might induce small destruction of the material when illuminated by the laser (light dots in the darker channels). To exclude this, a better filter system must be used. Summing up, in all synthesised polymers **P1** and **P2** an increase of the refractive index can be achieved by TPA. The fabrication windows vary and apparently depend on the polymeric matrix.

### 2.3.5 Conclusion

We have designed two new polymer based systems containing the chromophore 4-(N,N-diphenylamino)phenyl benzoate. Photoreactions of this TPA chromophore covalently attached to a polysiloxane and a polystyrene based system were followed under illumination with a mercury medium-pressure lamp by means of FT-IR and UV spectroscopy. The photodecarboxylation and the photo-Fries reaction both occur, although not in the same ratio for the two different systems. Both polymers showed high refractive index changes up to +0.04 upon irradiation, measured via ellipsometry. Furthermore we showed the successful inscription of a three dimensional refractive index pattern via two photon absorption and investigated the occurred photoreactions via FT-IR microscopy. We expect that this will lead to new photoreactive materials with possible applications in optics, optoelectronics and waveguide technology.

### 2.3.6 Acknowledgement

The authors thank J. Hobisch for carrying out the SEC analysis and P. Kaschnitz for NMR measurements. Financial support by the Austrian Science Fund (FWF, Vienna) within the project cluster ISOTEC of the Austrian Nanoinitiative is gratefully acknowledged. Part of this project was performed within the strategic project S8 of the Polymer Competence Center Leoben GmbH (PCCL) within the *Kplus* program.

### 2.3.7 References

- [1] Härtner S., Kim H.-C., Hampp N., *J. Photochem. Photobiol. A: Chem.* 187, **2007**, 242-246
- [2] Dobrizhev M., Makarov N.S., Rebane A., Wolleb H., Spahni H., *Journal of Luminescence* 128 (2), **2008**, 217-222
- [3] Sekkat Z., Ishitobi H., Kawata S., *Optics Communications* 222, **2003**, 269–276
- [4] Corredor C, Belfield K., Bondar M, Przhonska O., Hernandez F., Kachkovsky O., *Journal of Photochemistry and Photobiology A: Chemistry* 184, **2006**, 177–183
- [5] Oztemiz S., Jobanputra M.C., Clarson S.J., *Polymer Preprints*, 44 (1), **2003**, 1165
- [6] Anderson J.C., Reese C.B., *Proc. Chem. Soc.* **1960**, 217
- [7] S. Lochbrunner, M. Zissler, J. Piel, E. Riedle, A. Spiegel, T. Bach, *J. Chem. Phys.* 120, **2004**, 11634
- [8] Höfler T., Griesser T., Gstrein X., Trimmel G., Jakopic G., Kern W., *Polymer*, 48, **2007**, 1930
- [9] Finnegan R.A., Knudsen D., *Tetrahedron Lett.*, 9 (30), **1968**, 3429-3432

- [10] Gu W., Abdallah D.J., Weiss R.G., *J. Photochem. Photobiol. A: Chem.*, 139, **2001**, 79
- [11] Daschiel U., Hoefler T., Jacopic G., Schmidt V., Kern W., *Macromol. Chem. Phys.*, 208 (11), **2007**, 1190-1201
- [12] Langer G., Muehlbacher I., Pichler S., Stahr H., Stelzer F., Sassmannshausen J., PCT Int. Appl., **2009**, WO 2009021256 A1 20090219
- [13] Behl M., Hattemer E., Brehmer M., Zentel R., *Macromol. Chem. Phys.*, 203 (3), **2002**, 503-510
- [14] Socrates G., "*Infrared Characteristic Group Frequencies*", 2nd edition, John Wiley & Sons, Chichester, **1998**
- [15] "*UV Atlas of Organic Compounds*", Verlag Chemie, Weinheim **1966**
- [16] D. Y. Kondakov, W. C. Lenhart, and W. F. Nichols, *J. Appl. Phys.* 101, **2007**, 024512
- [17] G. Langer, T. Kavc, W. Kern, G. Kranzelbinder, E. Toussaere, *Macromol. Chem. Phys.*, 202, **2001**, 3459-3467

## 2.4 Refractive index and waveguide patterning of polynorbornene copolymers bearing 4-(N,N-diphenylamino)phenyl benzoate units

### 2.4.1 Summary

Functionalized polynorbornenes bearing aryl ester groups in the side chain were synthesised via ring-opening metathesis polymerization (ROMP). These new flexible and opaque polymers were investigated for photoreactions increasing the refractive index upon irradiation. Illumination experiments were conducted with a medium pressure mercury lamp and followed by ellipsometry, FT-IR and UV/VIS spectroscopy. The photoreactions of the aryl ester in the side chain were identified as photodecarboxylation and photo-Fries reaction leading to a higher refractive index. The materials were also tested for two-photon conditions, showing promising results for the use as waveguide materials or for optical data storage.

### 2.4.2 Introduction

The photo-Fries reaction has been intensively studied regarding the fundamentals and applications in different fields of technology. General aspects of the photo-Fries rearrangement are reviewed by Miranda et al.<sup>[1]</sup> and mechanistic studies have been carried out by Lochbrunner et al.<sup>[2]</sup> Polymers containing aryl ester groups have been investigated related to their photoreaction and their refractive index change, respectively for applications in optical technology.<sup>[3]</sup> The photo-Fries reaction was also exploited for thin modifiable photoreactive layers which can be applied for tuning inorganic surface properties and for modern immobilisation techniques.<sup>[4]</sup> Other postmodification techniques for aryl esters have been shown by Griesser et al.<sup>[5]</sup>

First investigated by Anderson and Reese in 1960, aryl ester were found to undergo a rearrangement upon irradiation to the corresponding *ortho*- and *para*- hydroxyketones.<sup>[6]</sup> Mechanistic studies showed that the photo-Fries rearrangement starts from an excited singlet state. In a second step this  $\pi-\pi^*$  state crosses a  $\pi-\sigma^*$  state followed by an elongation of the C-O-bond leading to the bond cleavage. The built radical pair can recombine in the solvent cage over a cyclohexadienone derivative to the hydroxyketone.<sup>[7]</sup> As side product phenol was observed most frequently. Another side reaction is the photo-decarboxylation, where a hydrocarbon is the product of a photoextrusion of CO<sub>2</sub>.<sup>[8]</sup> This reaction is preferred for sterical hindered molecules. Although the photoreactions of arylester were studied intensively for one photon conditions, the case is different for two-photon reactions. In this



field, two-photon induced polymerisation and two-photon fluorescence are topics researched extensively while two-photon induced photoreactions are studied rarely. Examples for photoconversions of organic molecules solved in liquids or polymeric materials are the two-photon induced cycloreversion reactions of 7-hydroxycoumarin for drug delivery<sup>[9]</sup>, the phototautomerisation of phthalocyanines<sup>[10]</sup> and the photocyclization of diarylethene derivatives<sup>[11,12]</sup>.

The rate of two photon process in general is dependent to the square of the incident light intensity. Ultra-short pulsed lasers exhibit high intensity at the focal spot, where the material absorbs two photons simultaneously. The quadratic dependence of the absorbance rate allows high spatial resolution. These features enable three dimensional structuring of materials in one single step. The refractive index change accompanying the photoreaction of the arylester under two photon conditions may be of use in optical and holographic recording.

In previous contributions we used norbornenes as backbone of a polymer and reactive arylesters in the side chain to obtain highly reactive materials for refractive index modulation. Irradiation caused a refractive index change of polynorbornenes containing naphthylester groups of about 0.04.<sup>[13]</sup> Polymers bearing phenylester of benzoic acid or acetic acid in the side chain showed an increase of up to 0.05<sup>[14]</sup>, whereas N-phenylamide groups in the side chain created a refractive index change of 0.1 upon illumination.<sup>[15]</sup> Polynorbornenes bearing a diphenylester were also used successfully for postmodification processes exploiting the hydroxyl group that is created by the photo-Fries rearrangement. Also a norbornene derivative containing a triphenylamine-moiety was successfully polymerized via ring opening metathesis polymerisation (ROMP).<sup>[16]</sup> This living polymerisation method leads to a narrow molecular-weight-distribution and enables polymerisation of various monomers due to the high acceptance of functional groups.<sup>[17]</sup>

Therefore we used norbornenes as polymerisable group exploiting all advantages of this method leading to sophisticated polymers. These photoreactive polymers bearing an aryl ester group in the side chain are expected to result in a high refractive index change upon irradiation. To enable TPA photoreactivity, triphenylamino-groups were incorporated into the absorbing unit of the aryl ester. Photoreactivity and refractive index change under one photon irradiation via a mercury medium pressure lamp were investigated. Furthermore, a fs-pulsed Ti:sapphire laser was used to study two photon activity of these new functional polymers. Via the two-photon based photo-process, structuring of these organic materials is possible in a single step. With this technique, 3D microstructures are accessible for optoelectronics and microelectronic components. Analytical studies were carried out by means of FT-IR and UV/VIS spectroscopy, ellipsometry and phase contrast microscopy.

## 2.4.3 Experimental Part

### 2.4.3.1 Starting Compounds

Dichloromethane (Fluka) was dried over  $P_2O_5$ , Toluene (Fluka) was dried over Na/K. *endo,exo*-Bicyclo[2.2.1]hept-5-ene-2,3-dicarboxylic acid dimethyl ester (**Mb**) was received from Orgentis Chemicals GmbH and further purified by distillation.. All other chemicals were obtained from commercial sources (Fluka, Aldrich, Lanchester and ABCR) and used as received.

### 2.4.3.2 Monomers

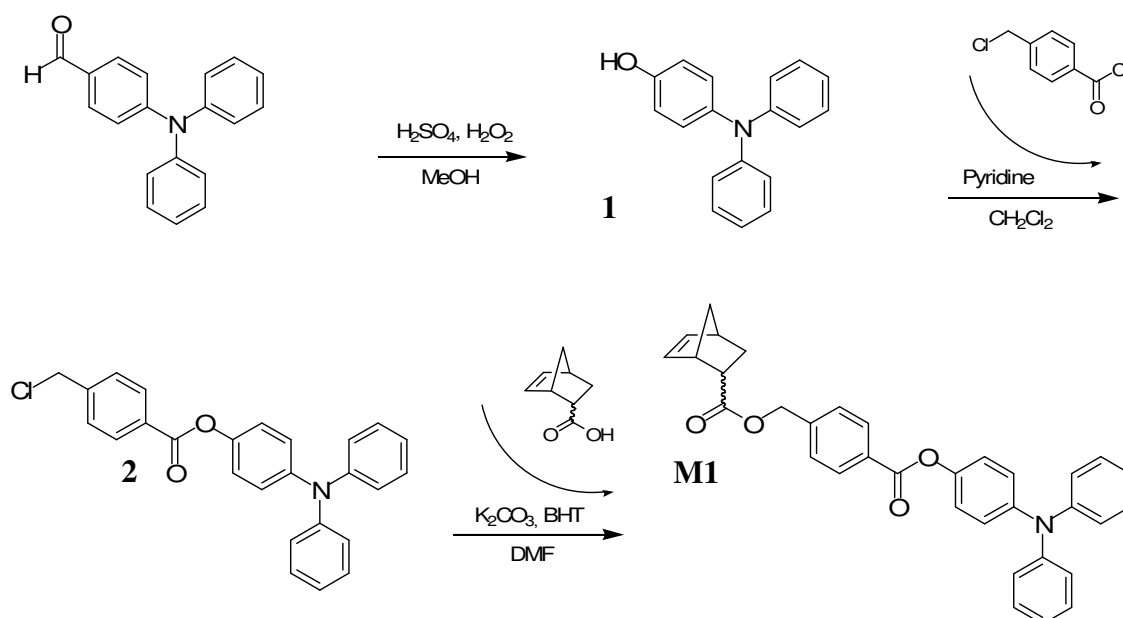


Figure 25: synthesis of **M1**

4-(N,N-Diphenylamino)phenol (**1**) was prepared as follows:

Under argon, 7.5 g (28 mmol) of 4-(N,N-diphenylamino)benzaldehyde and 5.9 mL of  $H_2O_2$  (30%) were added to 100 mL of methanol, followed by a dropwise addition of 0.75 mL of  $H_2SO_4$  (conc.) while the suspension was stirred and cooled in an ice bath for 15 min and then maintained at room temperature for another twelve hours. Distilled water (200 mL) and ethyl acetate (300 mL) were added. After addition of about 20 mL saturated  $NaHCO_3$ -solution, the aqueous phase was separated and extracted another two times with 300 mL of ethyl acetate. In the next step the combined organic phases were dried with  $Na_2SO_4$  and concentrated under reduced pressure. The residue (dark blue) was purified on a silica gel column with

cyclohexane/ethanol 80:1 as eluent. 4.4 g (17 mmol, 61% yield) of the product were obtained as a brown solid. <sup>1</sup>H NMR (δ, 400MHz, 20 °C, CDCl<sub>3</sub>): 4.64 (s, 1H), 6.78 (d, 2H), 6.95 (m, 2H), 7.04 (m, 6H), 7.21 (m, 4 H)

4-(N,N-Diphenylamino)phenyl 4-(chloromethyl) benzoate (**2**):

Under argon, 700 mg of 4-(N,N-diphenylamino)phenol (2,7 mmol, 1 eq), 557 mg of 4-chloromethylbenzoyl chloride (2,9 mmol, 1,1 eq) and 230 μL of pyridine (2,9 mmol, 1,1 eq) were solved in 10 mL of CH<sub>2</sub>Cl<sub>2</sub> and stirred for 5 hours. The dark brown solution was diluted with 30 mL CH<sub>2</sub>Cl<sub>2</sub>, and then extracted with water, diluted hydrochloric acid, aqueous sodium bicarbonate and water. The organic phase was dried over Na<sub>2</sub>SO<sub>4</sub> and concentrated under reduced pressure. The crude product was purified by column chromatography (cyclohexane : ethyl acetate = 50:1). <sup>1</sup>H-NMR (δ, 20 °C, CDCl<sub>3</sub>, 500 MHz): 8.19 (d, 2H), 7.53 (d, 2H), 7.26 (m, 4H), 7.14-7.08 (m, 8H), 7.02 (m, 2H), 4.65 (s, 2H)

4-((4-(Diphenylamino)phenoxy)carbonyl)benzyl bicyclo[2.2.1]hept-5-ene-2-carboxylate (mixture of the endo- and exo-form) (**M1**) :

By modifying a procedure of Lamberts et al. <sup>[18]</sup>, **2** (150 mg, 0.362 mmol, 1 eq) was solved in 10 mL of N,N-dimethylformamide (DMF) and bicyclo[2.2.1]hept-5-ene-2-carboxylic acid (50.1 mg, 0.362 mmol, 1 eq), K<sub>2</sub>CO<sub>3</sub> (100.2 mg, 0.725 mmol, 2 eq.) and butylhydroxytoluol (2 mg) were added. The mixture was heated to 80 °C and stirred for 48 h. After filtering the precipitate off, the solvent was removed under reduced pressure. Purification was done by column chromatography (silica gel, cyclohexane:ethyl acetate = 5:1). Yield: 100 mg (54%). Mixture of 17% exo- and 83% endo-derivative. <sup>1</sup>H-NMR (δ, 20 °C, CDCl<sub>3</sub>, 500 MHz): 8.18 (d, 2H), 7.47 (d, 2H), 7,27-7,24 (m, 6H), 7.14-7.08 (m, 6H), 7.02 (m, 2H), 6.21 (m, 1H), 5.89 (m, 1H), 5.16 (q, 2H), 3.28-2.91 (m, 3H), 1.95 (m, 1H), 1.49-1.42 (m). IR (CaF<sub>2</sub>): 1738 (C=O), 1500, 1313, 1263, 1200 cm<sup>-1</sup>

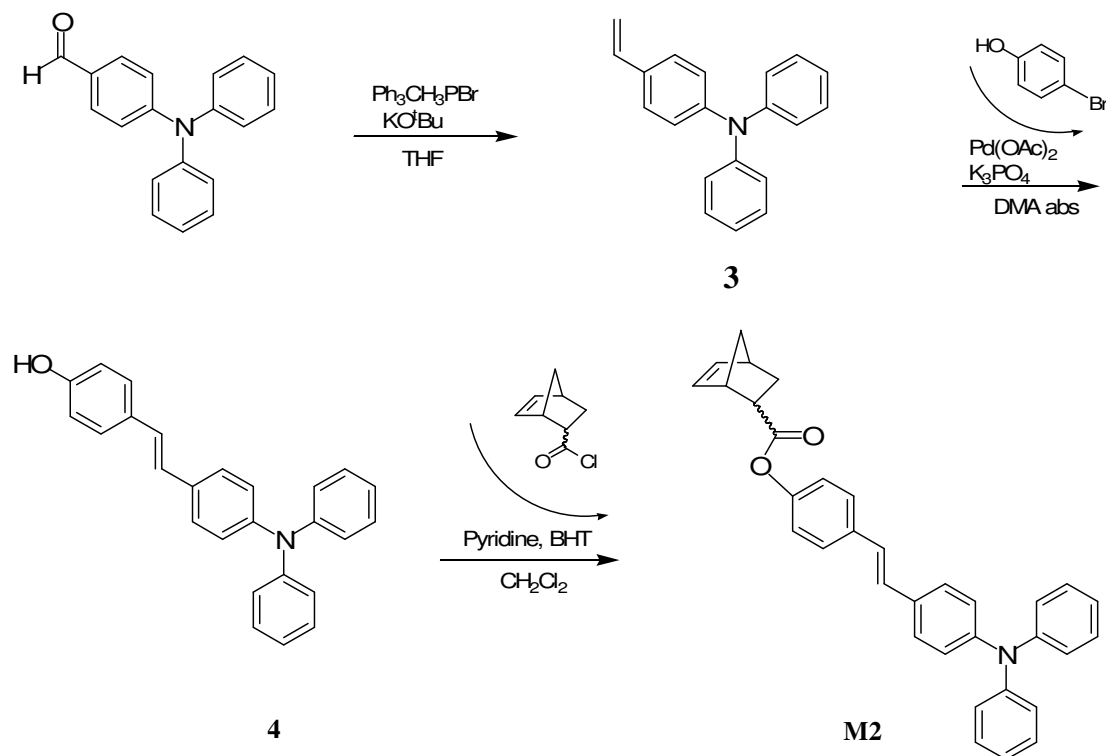


**Figure 26: synthesis of M2**

4-N,N-Diphenyl-4-vinylaniline<sup>[19]</sup> (**3**): 11.2 g (31.2 mmol, 1.1 eq) methyltriphosponium bromide were suspended in 35 mL THF abs. and cooled with an ice bath. The white suspension turned into yellow when 3.8 g (31.2 mmol, 1.1 eq) potassium tert-butyrate ( $\text{KO}^t\text{Bu}$ ) were added. After 5 minutes, the ice was removed and the suspension stirred for another 5 minutes. Then 7.6 g 4-(N,N-diphenylamino)benzaldehyde were added and the mixture was stirred for 18 hours before 50 mL water and 80 mL methylene chloride were added. The aqueous phase was extracted another time with 80 mL methylene chloride and the combined organic phases were dried over  $\text{Na}_2\text{SO}_4$  and the solvent was removed under reduced pressure. The brown oil was purified by column chromatography (silica gel, eluent = petrol ether). Yield (67 %),  $^1\text{H-NMR}$  ( $\delta$ , 20 °C,  $\text{CDCl}_3$ , 400 MHz): 7.31-7.01 (m, 14H), 6.68 (dd, 1H), 5.65 (d, 1H), 5.17 (d, 1 H)

4-(4-N,N-(Diphenylamino)styryl)phenol<sup>[20]</sup> (**4**):

900 mg **3** (3.3 mmol, 1.6 eq), 370 mg bromophenol (2.1 mmol, 1 eq), 420 mg  $\text{K}_3\text{PO}_4$  and 5 mL DMA were charged into a Schlenk flask (10 mL). 1 mL of a solution of  $\text{Pd}(\text{OAc})_2$  (0.006 mmol) were added. The mixture was heated up to 140 °C and stirred for 19 hours. After cooling down to room temperature, the solution was poured into 50 mL cold water and extracted with ethyl acetate (100 mL) twice. The combined organic phases were dried over

Na<sub>2</sub>SO<sub>4</sub> and the solvent removed under reduced pressure. The crude product was purified by column chromatography (silica gel, cyclohexane:ethyl acetate = 40:1) Yield: 40 %. <sup>1</sup>H-NMR (δ, 20 °C, CDCl<sub>3</sub>, 400 MHz): 7.37 (d, 2H), 7.26 (m, 6H), 7.11 (m, 4H), 7.04 (m, 4H), 6.93 (m, 2H), 6.81 (d, 2H), 4.76 (s, 1H)

4-(4-(Diphenylamino)styryl)phenyl bicyclo[2.2.1]hept-5-ene-2-carboxylate (**M2**):

Same procedure as for 2. Yield: 65 %. <sup>1</sup>H-NMR (δ, 20 °C, CDCl<sub>3</sub>, 500 MHz): 7.47 (m, 2H), 7.38 (m, 2H), 7.26 (m, 6H), 7.11 (m, 4H), 7.04 (m, 4H), 6.98 (m, 2H), 6.27 (m, 1H), 6.09 (m, 1H), 3.39-2.98 (m, 3H), 2.02 (m, 1H), 1.52 (m, 1H), 1.37 (d, 1H), 1.21 (m, 1H)

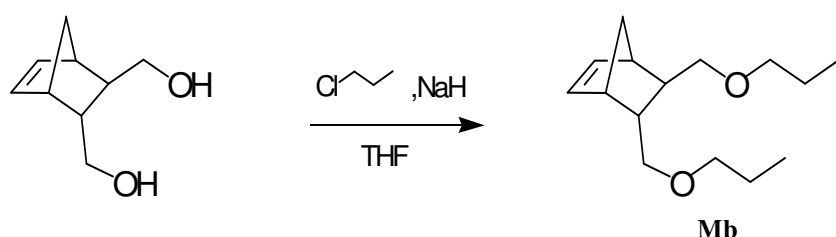


**Figure 27: synthesis of Mb**

5,6-Bis(propoxymethyl)bicyclo[2.2.1]hept-2-ene (**Mb**):

0.23 g NaH (9.7 mmol, 3 eq), 40 mL THF and 0.5 g bicyclo[2.2.1]hept-5-ene-2,3-diyldimethanol (3.2 mmol, 1 eq) were stirred for 1 h. The solution was cooled down with ice and a solution of 1-bromopropane (1.2g, 9.7 mmol, 3 eq) in 10 mL THF was added dropwise. The icebath was removed and the solution was heated to 65 °C and stirred for 48 h. After reaching room temperature, 10 mL NH<sub>4</sub>Cl solution (5%) was added. The aqueous phase was extracted with 30 mL diethylether. The combined organic phases were dried over Na<sub>2</sub>SO<sub>4</sub> and the solvent was removed under reduced pressure. The product was purified by column chromatography (silica gel, gradient of cyclohexane:ethyl acetate = 50:1 up to 5:1). Yield: 60 %. <sup>1</sup>H-NMR (δ, 20 °C, CDCl<sub>3</sub>, 400 MHz, ppm): 6.11 (m, 2H), 3.31 (m, 4H), 3.23 (m, 1H), 3.01 (m, 2H), 2.92 (m, 2H), 2.45 (m, 2H), 1.57 (m, 4H), 1.44 (m, 1H), 1.25 (m, 2H), 0.91 (t, 6H)

### 2.4.3.3 Statistic polymerization procedure of norbornene derivatives to give the copolymers P1a, P2a, P1b and P2b

For the ring opening metathesis polymerisation a modified Umicore pyridine initiator, shown in

Figure 28 was used to obtain the followed polymers: <sup>[21]</sup>

**P1a:** Poly-4-((4-(N,N-diphenylamino)phenoxy)carbonyl)benzyl bicyclo[2.2.1]hept-5-ene-2-carboxylate-co-bicyclo[2.2.1]hept-5-ene-2,3-dicarboxylic acid dimethyl ester

**P2a:** Poly-4-(4-(N,N-diphenylamino)styryl)phenyl bicyclo[2.2.1]hept-5-ene-2-carboxylate-co-bicyclo[2.2.1]hept-5-ene-2,3-dicarboxylic acid dimethyl ester

**P1b:** Poly-4-((4-(N,N-diphenylamino)phenoxy)carbonyl)benzyl bicyclo[2.2.1]hept-5-ene-2-carboxylate-co-5,6-bis(propoxymethyl)bicyclo[2.2.1]hept-2-ene

**P2b:** Poly-4-(4-(N,N-diphenylamino)styryl)phenyl bicyclo[2.2.1]hept-5-ene-2-carboxylate-co-5,6-Bis(propoxymethyl)bicyclo[2.2.1]hept-2-ene

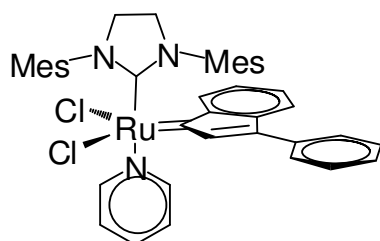


Figure 28: Modified Umicore type initiator

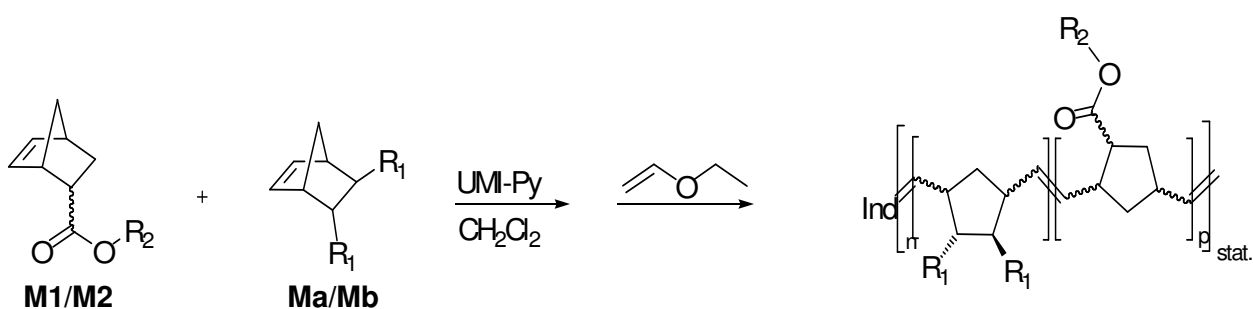


Figure 29: Copolymerization to give the norbornene copolymer

**Table 3: Copolymerization of P1a, P2a, P1b, and P2b**

Polymer	Monomer[eq]	Monomer[eq]
P1a	M1: 120	Mb: 240
P2a	M2: 180	Mb: 180
P1b	M1: 40	Ma: 300
P2b	M2: 40	Ma: 300

To a solution of Ma or Mb and M1 or M2 (compare Table 3) in dry CH<sub>2</sub>Cl<sub>2</sub> (about 4 wt %), a solution of the initiator (1 eq) in dry CH<sub>2</sub>Cl<sub>2</sub> (about 0.2 wt %) was added. The reaction was terminated with ethylvinyl ether (100 μL, excess) when no more monomer was monitored by TLC (cyclohexane/ethyl acetate 5:1, detection: 2% KMnO<sub>4</sub> solution, R<sub>f</sub>: 0.0) and stirred for at least 15 min at room temperature. The polymer was precipitated twice out of CH<sub>2</sub>Cl<sub>2</sub> solutions (1 mL) of the polymer into cold methanol (80 mL). After drying in the oven at 40 °C under reduced pressure the polymers were characterized by NMR, IR, UV/VIS and size exclusion chromatography (SEC).

**P1a:** Yield= 40 mg (66 %); M<sub>n</sub>= 23 420 g/mol; PDI=1.89; <sup>1</sup>H-NMR (δ, 20 °C, CDCl<sub>3</sub>, 400 MHz): 8,15 (d, 2H), 2,46 (s, 2H), 2,23 (d, 4H), 7,09 (d, 8H), 7,0 (d, 2H), 5,34 (m, 7H), 3,31 (m, 12H), 2,98 (s, 4H), 2,64 (s, 2H), 2,29 (s, 4H), 1,89 (m, 9H), 1,56 (m, 19H), 0,91 (s, 12H)

IR (CaF<sub>2</sub>): 2958, 2935, 2853, 1738 (C=O), 1589, 1496, 1266, 1200, 1170, 1076 cm<sup>-1</sup>

**P2a:** Yield= 155 mg (61%); M<sub>n</sub>= 72 670 g/mol; PDI=1.46; <sup>1</sup>H-NMR (δ, 20 °C, CDCl<sub>3</sub>, 400 MHz): 7,43 (s, 2H), 7,35 (s, 2H), 7,24 (m, 6H), 7,02 (m, 10H), 5,50 (bd, 4H), 3,31 (d, 8H), 3,16 (s, 1H), 2,98 (s, 3H), 2,66 (s, 1H), 2,29 (d, 3H), 1,9 (s, 3H), 1,55 (m, 10H), 1,26 (m, 2H), 0,91 (d, 6H); IR (CaF<sub>2</sub>): 2951, 1738 (C=O), 1588, 1500, 1436, 1313, 1265, 1200, 1170, 1070 cm<sup>-1</sup>

**P1b:** Yield= 119 mg (73%); M<sub>n</sub>= 107 220g/mol; PDI=1.14; <sup>1</sup>H-NMR (δ, 20 °C, CDCl<sub>3</sub>, 500 MHz): 8.18 (d, 2H), 7.47 (d, 2H), 7,27-7,24 (m, 6H), 7.14-7.08 (m, 6H), 7.02 (m, 2H), 5.50-5.19 (bm, 20 H), 3.64 (s, 48H), 3.24-2.72 (bm, 35 H), 1.98 (br, 10 H), 1.46 (br, 10 H). IR (CaF<sub>2</sub>): 2951, 1738 (C=O), 1589, 1500, 1436, 1313, 1265, 1200, 1170, 1070 cm<sup>-1</sup>

**P2b:** Yield= 161 mg (77%); M<sub>n</sub>= 100 280 g/mol; PDI=1.17; <sup>1</sup>H-NMR (δ, 20 °C, CDCl<sub>3</sub>, 500 MHz): 7,46 (d, 2H), 7,24(m, 8H), 5,19-5,50 (m, 14H), 3,65 (t, 36H), 2,98-3,25 (m, 25H), 1,975 (s, 8H), 1,48 (s, 6H); IR (CaF<sub>2</sub>): 2951, 1738 (C=O), 1588, 1500, 1436, 1313, 1265, 1200, 1170, 1070 cm<sup>-1</sup>

#### 2.4.3.4 UV illumination process

The UV illuminations were performed with a medium pressure Hg lamp. The power density was 100mW/cm<sup>2</sup>, measured with a spectroradiometer (Solatell, 2000TM). TPA experiments were carried out with an optically pumped titan-sapphire laser system (Mai Tai, pulse duration: 120 fs, repetition rate: 1 kHz, 610 nm). Polymers were coated on CaF<sub>2</sub>-discs.

### 2.4.4 Results and Discussion

#### 2.4.4.1 Synthesis

Ring opening metathesis polymerization (ROMP) provides a very efficient method to synthesize polymers with a narrow mass distribution. We achieved to synthesize 4 different polymers (**P1a**, **P2a**, **P1b** and **P2b**). The numbers 1 and 2 of the polymer represent two different photoreactive units, the letter a and b stand for the co-monomer. Co-monomer **Ma** contains a dipropyl ether instead of a dimethyl ester in **Mb**. **P1a** and **P2a** were synthesized to obtain more detailed information on the photoprocesses from FT-IR spectra, since the ester bands of **Mb** are overlapping with the esterbands of the photoreactive units.

#### 2.4.4.2 UV absorption of polymers P1a and P2a

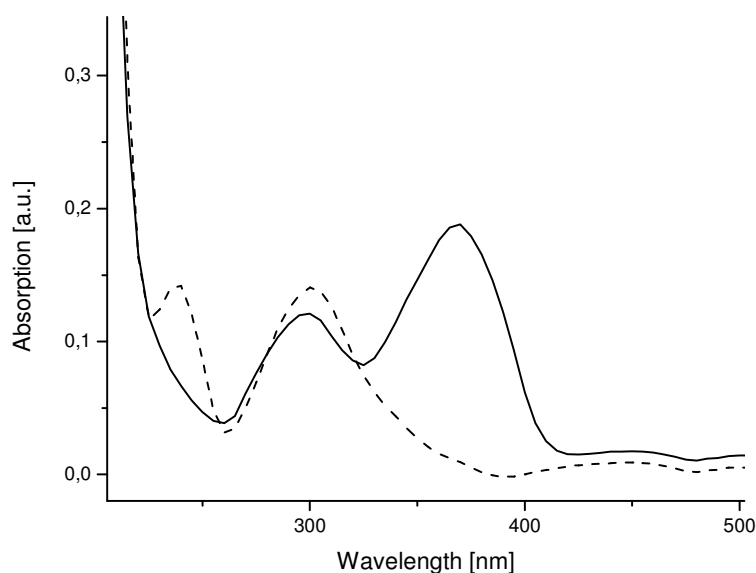


Figure 30: UV absorption of P1a (dashed line) and P2a (dashed line), measured as a thin solid film

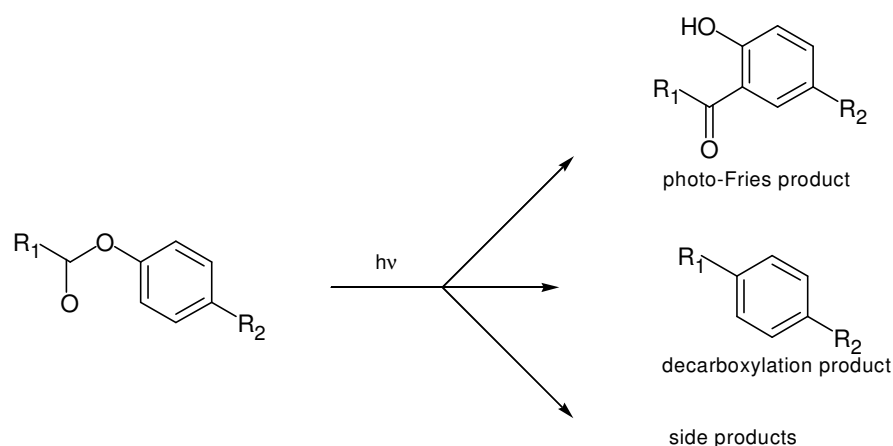


The main goal of this work was to achieve a refractive index change upon irradiation. To estimate an acceptable irradiation wavelength, absorption spectra of the polymers, shown in Figure 30, were taken. The absorption maxima of **P1a** are at 238 and 300 nm and of **P2a** at 300 and at 370 nm. Both spectra were taken from thin polymer films, where the film thicknesses and the amount of absorbent units are different.

#### 2.4.4.3 UV irradiation of polymers

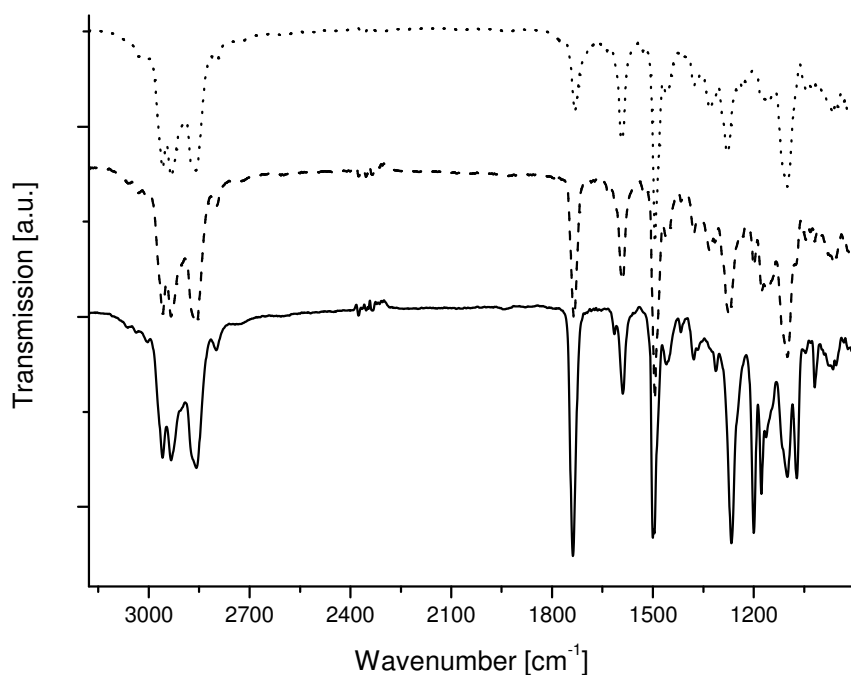
We investigated the photoreactions of **P1a** and **P2a** by FT-IR spectroscopy. Aromatic ester groups, present only in the monomers **M1** and **M2**, are expected to undergo a photoreaction. In general, two photoreactions have been observed for aromatic esters, the photo-Fries rearrangement leading to an ortho-hydroxyketone and a photodecarboxylation resulting in a hydrocarbon compound, compare

Figure 31.



**Figure 31: photoreactions of aromatic esters**

Functional groups such as esters, ketones and hydroxyl groups show intense vibrational signals in their FT-IR spectra. Aromatic esters show a carbonyl stretching vibration at a wavenumber of 1738 cm<sup>-1</sup>. The carbonyl vibration of the photo-Fries product, which is a ketone, would rise a signal at 1640 cm<sup>-1</sup> and the hydroxyl group of the product would rise a broad signal around 3500 cm<sup>-1</sup>.<sup>[22]</sup> Therefore FT-IR spectroscopy is a simple and effective method for the investigation of the photoreaction.



**Figure 32: FT-IR spectra of P1a non irradiated (solid line), irradiated with 30J/cm<sup>2</sup> (dashed line) and irradiated with 180J/cm<sup>2</sup> (dotted line)**

In Figure 32 the FT-IR spectra of **P1a** are shown: non irradiated (solid line), irradiated with 30 J/cm<sup>2</sup> (dashed line) and irradiated with 180 J/cm<sup>2</sup> (dotted line). The non irradiated polymer shows characteristic ester signals at 1738 cm<sup>-1</sup> (C=O vib.), 1266, 1200 and 1073 cm<sup>-1</sup>. The ether signal can be found at 1096 cm<sup>-1</sup>. Aromatic vibrations are located at 1587 and 1496 cm<sup>-1</sup>. The aliphatic groups of the polymer and the propyl groups show their signals at 2960, 2930 and 2857 cm<sup>-1</sup>.

Upon irradiation, no new signals arise. Only a decrease of the ester peaks at 1738, 1266, 1200 and 1073 cm<sup>-1</sup> can be observed. Other peaks for the aromatic units and the aliphatic groups remain the same. Calculations have been carried out quantitatively to estimate the amount of conversion of the ester out of the FT-IR absorbance spectra. The carbonyl vibration at 1738 cm<sup>-1</sup> decreased by about 40 %. No peaks of the photo-Fries product are detectable, which brings us to the conclusion, that the main photoreaction occurring in **P1a** is the decarboxylation reaction.

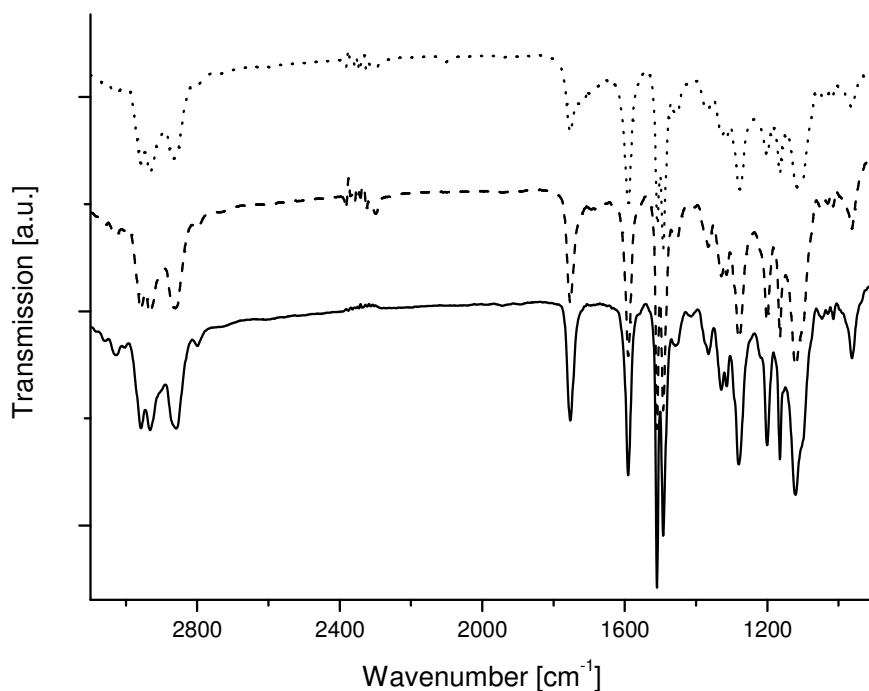


**Figure 33: FT-IR spectra of P2a non irradiated (solid line), irradiated with 30J/cm<sup>2</sup> (dashed line) and irradiated with 180J/cm<sup>2</sup> (dotted line)**

For **P2a**, the FT-IR spectra shown in Figure 33: non irradiated (solid line), irradiated with 30 J/cm<sup>2</sup> (dashed line) and irradiated with 180 J/cm<sup>2</sup> (dotted line). The non irradiated polymer film shows different characteristic ester signals, since the group next to the carbonyl bond is aliphatic in contrast to **P1a**, where this group is of aromatic nature. An intense characteristic carbonyl vibration signal of the ester arises at 1752 cm<sup>-1</sup>, C-O-Ar signals are at 1280, 1199, 1165 and 1121 cm<sup>-1</sup>. The ether signal can be found at 1096 cm<sup>-1</sup> as a shoulder of the ester peak at 1121 cm<sup>-1</sup>. Aromatic vibrations are located at 1589, 1510 and 1493 cm<sup>-1</sup>. The aliphatic groups of the polymer and the propyl groups show their signals at 2960, 2930 and 2857 cm<sup>-1</sup>, at the same wavenumbers as for **P1a**.

Upon irradiation, again no new signals arise. A depletion of the ester peaks at 1752, 1280, 1199, 1165 and 1121 cm<sup>-1</sup> can be observed. Quantitative calculations from the absorbance spectra indicate a decrease of about 25 % of the carbonyl stretching vibration at 1752 cm<sup>-1</sup>. As for **P1a**, we assume that the decarboxylation is the main photoreaction for **P2a**.

To investigate the photo-induced refractive index change of the polymer films, ellipsometric measurements have been carried out. An increase of the refractive index occurs as a result of the changes in molecular structure due to the photoreactions of aryl esters. The two polymers **P1b** and **P2b** both contain about 10 mol% photo reactive unit (monomer **M1** and **M2** respectively). The low fraction of the reactive ester is still assumed to achieve a sufficiently large change of the refractive index under illumination.

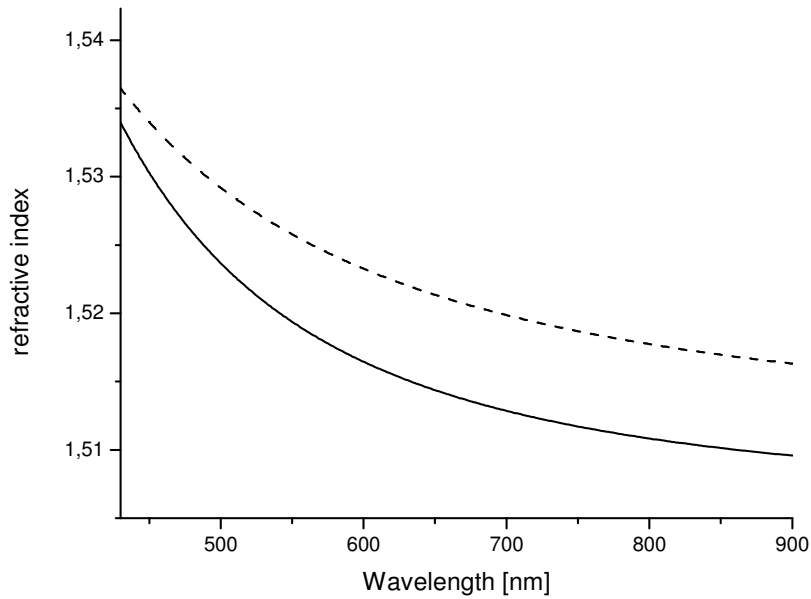


**Figure 34: Cauchy fit of the refractive index of a film of P1b on silicon. Solid line: before irradiation, dotted line: after irradiation**

The Cauchy fits of the refractive index of a **P1b**-film on silicon prior to irradiation (solid line) and after irradiation with a mercury medium pressure lamp (dotted line) are shown in Figure 34. The refractive index at the wavelength  $\lambda = 589 \text{ nm}$  ( $\text{Na}^{\text{D}}$  line) was 1.517 prior and 1.524 after irradiation,  $\Delta n_{589}$  amounts to +0.007 and is constant also for higher wavelength than 589 nm. Despite of the small amount of aryl ester in the polymer, the change of the refractive index is still above technical requirements.

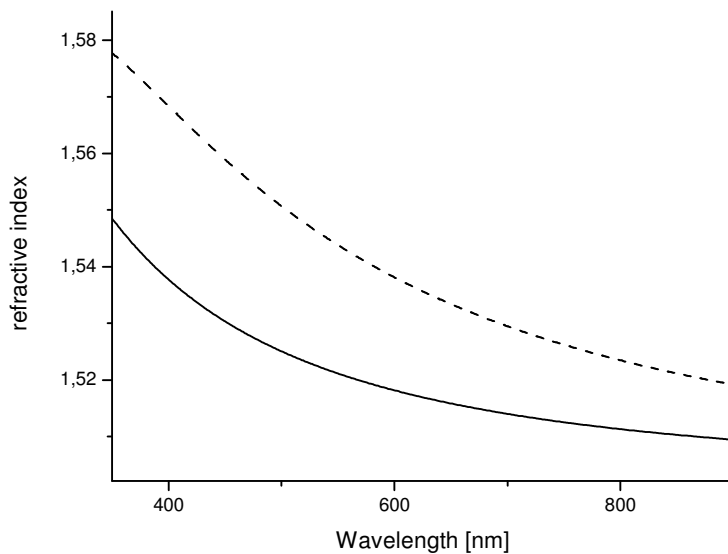


**Figure 35: Cauchy fit of the refractive index of a film of P2b on silicon. Solid line: before irradiation, dotted line: after irradiation**

The Cauchy fits of the refractive index of a **P2b**-film on silicon prior to irradiation (solid line) and after irradiation with a mercury medium pressure lamp (dotted line) are shown in Figure 35. The refractive index at the wavelength 450 nm was 1.530 prior to irradiation and 1.559 after irradiation, which equals an increase of  $\Delta n_{450} = +0.03$ . The refractive index at the wavelength  $\lambda = 589$  nm was 1.519 prior and 1.539 after irradiation, which equals an increase of  $\Delta n_{589} = +0.02$ . Above  $\lambda = 900$  nm the difference is 0.01 and for higher wavelengths than 900 nm even smaller. For both polymers, the refractive index changes are caused by the molecular change of the aryl ester upon irradiation and present the condition for the development of waveguides and optical data storages.

To obtain waveguide structures in one step, illuminations under two-photon conditions have been carried out. A femtosecond pulsed Ti:sapphire laser was used at a wavelength of 610 nm (coupled with an OPA) for **P1b** and at 800 nm for **P2b**.

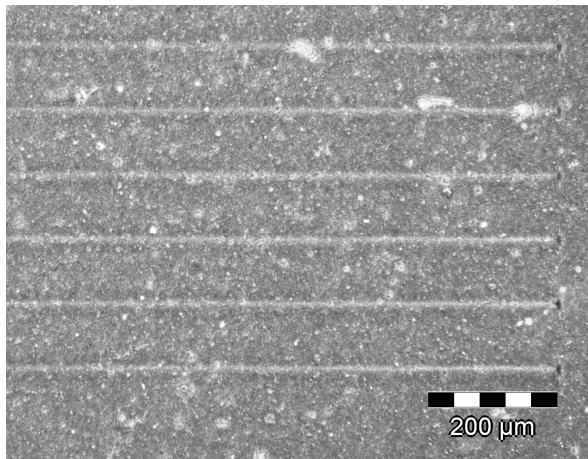


**Figure 36: Phase contrast image of a film of P1b after irradiation with a Ti:sapphire femtosecond laser ( $\lambda = 610$  nm) with different pulse powers. For laser powers between 800 and 900  $\mu\text{W}$  clearly resolved lines are discernible, indicating an increase in refractive index.**

In Figure 36 a phase contrast image of a film of P1b after the laser irradiation at 610 nm with pulse powers of 800, 820, 840, 860, 880 and 900  $\mu\text{W}$  are shown. Irradiation with these pulse powers resulted in clearly resolved lines. The phase contrast mode of the microscope allows distinguishing between areas with different refractive indices. Thus, the lines are indicating an increase of the refractive index. For higher laser power, illumination led to destruction of the material (not shown in the figure), whereas lower power didn't have any visible effect to the polymer.

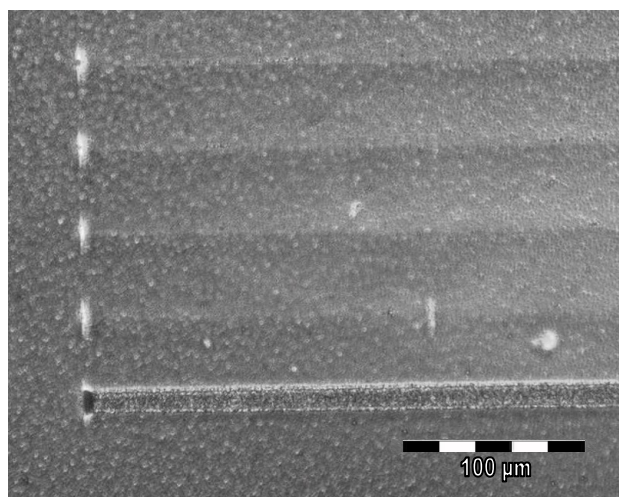


**Figure 37: Phase contrast images of a film of P2b after irradiation with a Ti:sapphire femtosecond laser ( $\lambda = 800$  nm) with different pulse powers. For laser powers between 175 and 300  $\mu$ W lines are discernible.**

In Figure 37 a phase contrast image of a film of P2b after the laser irradiation at 800 nm with pulse powers of 175, 200, 225, 250 and 300  $\mu$ W are shown. Irradiation with pulse powers up to 250  $\mu$ W (top 4 lines) resulted in lines that are lighter than the surrounding material. Although this colour difference, indicating a higher refractive index, is clearly visible, the boundary between illuminated and non illuminated areas is indistinctive. The bottom line is written with a pulse power of 300  $\mu$ W where a destroyed line was produced due to laser ablation, as observed in the microscopic image. For lower powers no waveguides could be generated.

#### **2.4.5 Conclusion**

New polynorbornenes, bearing two different photoreactive aryl ester units, 4-(diphenylamino)phenyl benzoate and 4-(4-(diphenylamino)styryl)phenyl carboxylate, in the side chain were investigated. In this paper the irradiation under one photon and two photon conditions of the polymers are discussed. Photoreactions due to illumination via a mercury medium pressure lamp were followed by FT-IR. Out of these results a photodecarboxylation (extrusion of  $\text{CO}_2$ ) is proposed as the main reaction occurring in these polymers. Ellipsometry showed that the refractive index of the polymers increased significantly as a result of the photoreaction. Experiments aiming at two-photon patterning of these polymers using a Ti:sapphire laser (610 and 800 nm) succeeded to write 3D waveguides. The waveguide structures were revealed by phase contrast microscopy. The large increase in the refractive index and the possibility to create 3D patterns under two-photon conditions makes these polymers good candidates for optical applications such as holographic recording and fabrication of optical elements, e.g. waveguides.

## 2.4.6 References

- [1] Miranda MA, Galindo F. "Photo-Fries reaction and related processes". In: Horspool WM, editor. "CRC handbook of organic photochemistry and photobiology". 2nd ed. Boca Raton: RC Press; **2004** [chapter 42].
- [2] S. Lochbrunner, M. Zissler, J. Piel, E. Riedle, A. Spiegel, T. Bach, *J. Chem. Phys.* 120, **2004**, 11634.
- [3] T. Höfler, T. Grießer, X. Gstrein, G. Trimmel, G. Jakopic, W. Kern, *Polymer* 48, **2007**, 1930.
- [4] T. Höfler, et al., *Mater. Chem. Phys.* , **2009**, doi:10.1016/j.matchemphys.2009.08.065
- [5] T. Grießer, T. Höfler, S. Temmel, W. Kern, G. Trimmel, *Chem. Mater.* 19, **2007**, 3011.
- [6] J. C. Anderson, C. B. Reese, *Proc. Chem. Soc.* **1960**, 217.
- [7] S. Lochbrunner, M. Zissler, J. Piel, E. Riedle, A. Spiegel, T. Bach, *J. Chem. Phys.*, 120, **2004**, 11634.
- [8] R. A. Finnegan, D. Knudsen, *Tetrahedron Lett.* 9, **1968**, 3429.
- [9] Härtner S., Kim H.-C., Hampp N., *J. Photochem. Photobiol. A: Chem.* 187, 2007, 242-246
- [10] Dobrizhev M., Makarov N.S., Rebane A., Wolleb H., Spahni H., *Journal of Luminescence* 128 (2), **2008**, 217-222
- [11] Sekkat Z., Ishitobi H., Kawata S., *Optics Communications* 222, **2003**, 269–276
- [12] Corredor C, Belfield K., Bondar M, Przhonska O., Hernandez F., Kachkovsky O., *Journal of Photochemistry and Photobiology A: Chemistry* 184, **2006**, 177–183
- [13] T. Höfler, T. Grießer, M. Gruber, G. Jakopic, G. Trimmel, W. Kern, *Macromol. Chem. Phys.* 209, **2008**, 488–498.
- [14] T. Höfler, T. Grießer, X. Gstrein, G. Trimmel, G. Jakopic, W. Kern, *Polymer* 48, **2007**, 1930.
- [15] T. Grießer, J.-C. Kuhlmann, M. Wieser, W. Kern, G. Trimmel, *Macromolecules* **2009** 42 (3), 725-731
- [16] T. Grießer, T. Rath, H. Stecher, R. Saf, W. Kern, G. Trimmel, *Monatshette für Chemie* 138, **2007**, 4, 269 - 276
- [17] C. Slugovc, *Macromol. Rapid Commun.* 25, **2004**, 1283–1297
- [18] Lamberts J.J.M., Neckers D.C., *Z Naturforsch*, 39b, **1984**, 474-484
- [19] Behl M., Hattemer E., Brehmer M., Zentel R., *Macromol. Chem. Phys.*, 203 (3), **2002**, 503-510
- [20] Yao Q., Kinney E. P., Yang Z., *J. Org. Chem.* **2003**, 68, 7528-7531
- [21] Burtscher D., Lexer C., Mereiter K., Winde R., Karch R., Slugovc C., *J. Polym. Sci. Part A: Polym. Chem.* 46, **2008**, 4630-4635
- [22] Socrates G., [Infrared Characteristic Group Frequencies, 2nd edition], John Wiley & Sons, Chichester, **1998**

## 2.5 Conclusion of part A and outlook

In this part, the synthesis and characterization of the following 8 polymeric systems, bearing reactive aryl ester groups in the side chain, are described:

**P1:** Poly[acrylic acid 4-(N,N-diphenylamino)phenyl ester]

**P2:** Poly[4-vinylbenzoic acid naphthalene-1-yl ester]

**P3:** Poly [4-vinylbenzoic acid 4-(N,N-diphenylamino)phenyl ester - co- styrene]

**P4:** Poly-4-(4-(N,N-diphenylamino)styryl)phenyl bicyclo[2.2.1]hept-5-ene-2-carboxylate-co-bicyclo[2.2.1]hept-5-ene-2,3-dicarboxylic acid dimethyl ester

**P5:** Poly-4-(4-(N,N-diphenylamino)styryl)phenyl bicyclo[2.2.1]hept-5-ene-2-carboxylate-co-5,6-Bis(propoxymethyl)bicyclo[2.2.1]hept-2-ene

**P6:** Poly-4-((4-(N,N-diphenylamino)phenoxy)carbonyl)benzyl bicyclo[2.2.1]hept-5-ene-2-carboxylate-co-bicyclo[2.2.1]hept-5-ene-2,3-dicarboxylic acid dimethyl ester

**P7:** Poly-4-((4-(N,N-diphenylamino)phenoxy)carbonyl)benzyl bicyclo[2.2.1]hept-5-ene-2-carboxylate-co-5,6-bis(propoxymethyl)bicyclo[2.2.1]hept-2-ene

**P8:** Hydride terminated methylhydrosiloxane – phenylmethylsiloxane-methyl 4-((4-(diphenylamino)phenoxy)carbonyl)phenethyl siloxane copolymer crosslinked with vinyl terminated diphenylsiloxane - dimethylsiloxane copolymer and hydride terminated methylhydrosiloxane – phenylmethylsiloxane copolymer



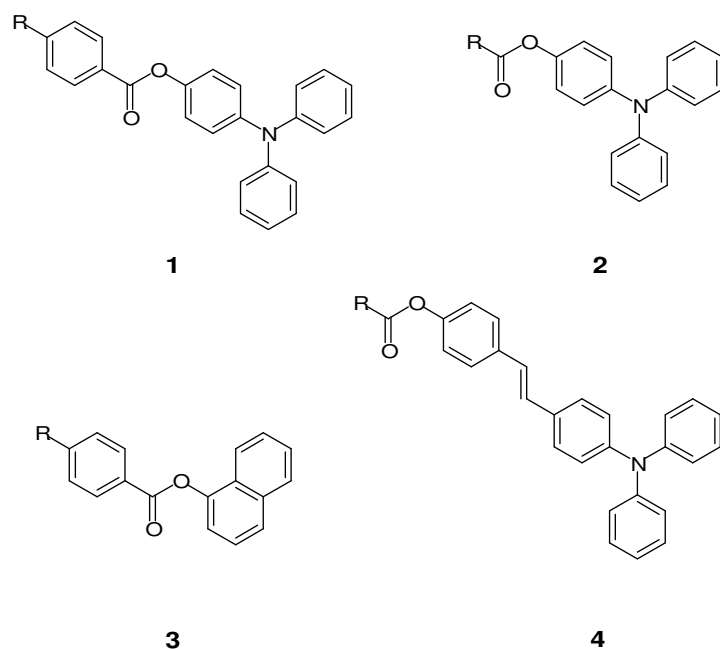


Figure 38: photoreactive aryl ester units in P1 – P8

Table 4: polymer backbone and photoreactive aryl ester units in P1 –P8

Polymer	Ester	Polymer backbone
P1	2	Polyacrylate
P2	3	Polystyrene
P3	1	Polystyrene
P4	4	Polynorbornene
P5	4	Polynorbornene
P6	1	Polynorbornene
P7	1	Polynorbornene
P8	1	Polysiloxane

Four different polymeric backbones and four different reactive esters (Figure 38) are used as described in Table 4. The photoreactions of thin polymer films illuminated with a mercury medium pressure lamp were investigated via FT-IR and UV/VIS spectroscopy. Quantitative calculations from the FT-IR absorbance spectra showed a conversion of the aryl ester groups up to 90 %, which varied depending on the ester and the type of polymer. The strong carbonyl stretching vibration of the ester group was used for these evaluations. As photoproducts, two different species were considered, the photo-Fries product and the decarboxylation product. The photo-Fries product, which is easy to identify due to the strong ketone and hydroxyl vibration of the formed hydroxyketone, was found only in very low amounts below 10 %. The case is more complicated for the decarboxylation product, since the formed hydrocarbon has no new functional group and shows therefore no new signals in the FT-IR spectra. Thus, estimations on the yield of this reaction cannot be given, but we propose that this reaction is the main photoreaction occurring in the polymers **P1 –P8**.

The goal of this work was to achieve refractive index changes upon irradiation, which was measured by ellipsometric spectroscopy. Photoreactions within the polymer change the molecular structure and consequently its refractive index. It is shown that the conversion of the ester upon irradiation results in an increase of this optical property for different esters and polymers. The ester group **1**, showing the highest conversion of the ester, was incorporated in three different polymeric systems: a polystyrene matrix, a polynorbornene matrix and a polysiloxane matrix. It is shown that the kind of polymer influences the yield of photoreaction and the refractive index change. The photoreaction of ester unit **2** and its refractive index change show a strong dependence on the irradiation wavelength and turned therefore out to be inappropriate for the use with TPA. The highest absolute difference of the refractive index was produced by illumination of **3** with a polyvinyl backbone and amounts to +0.07. It has to be considered that every vinyl unit in the polymer contained a reactive ester group. The best relative result was  $\Delta n = +0.016$ , obtained with **1** covalently bonded to a polysiloxane with only 10 wt % reactive ester in the polymer. Similar changes were obtained for **4** in the polynorbornene matrix.

For 3 D pattern irradiations with a femtosecond pulsed Ti: Sapphire laser were carried out. Thicker films up to 80 microns were cast onto glass or  $\text{CaF}_2$  substrates and waveguides were inscribed in the depth of the polymer layer. The results were observed via a phase contrast mode of a microscope that depicts different refractive indices in light/dark contrasts. Polymers **P1**, **P5** and **P7** showed unsatisfying results, which means that illumination only caused material ablation instead of an increase in refractive indices. Lower laser powers didn't cause any reaction in the material. **P2** showed good results, but only where the beam waist of the focused laser was in the range of about 1  $\mu\text{m}$ . For higher beam waists (up to 20  $\mu\text{m}$ ) the photoreaction didn't occur in the polymer. In contrast, **P4** showed the ability to be patterned by the laser irradiation at higher beam waists, but the inscribed waveguides were not defined to the surrounding polymer. Good results could be obtained for **P3**, **P6** and **P8** for various average laser powers. The structured waveguides had a diameter between 10 and 20  $\mu\text{m}$ . These three polymers contained the photoreactive ester **1**, which leads to the assumption that this ester shows the highest TPA cross section. It is also shown that the kind of polymer used as matrix has a deep impact on the quality of the structured area and the waveguides, respectively, as comparison of these three polymers indicates. This fact correlates with the studies under irradiation with the mercury medium pressure lamp, discussed above. Studies concerning the photoreaction under TPA conditions were carried out with a film of P3 on  $\text{CaF}_2$ , where a field was structured and analysed by FT-IR microscopy. The conversion of ester is estimated to be 40 % in the structured area.

Furthermore the TPA photoreaction is assumed to be the same reaction as for one photon conditions, the photodecarboxylation.

In summary, it can be concluded that 8 new polymers have been synthesised and their photoreactions have been investigated. All of the reactions show an increase of the refractive index upon irradiation with a mercury lamp, which makes them interesting for applications in waveguide technology. 3 of them show also good results when irradiated with a laser under two photon conditions, enabling 3 D structuring of the refractive index in only one step. This allows the employments of these materials for holography, optical data storage and new approaches towards waveguide fabrication.

Future work on this topic presents the development of new ester units in different polymers. The cross section of TPA is dependent on the chemical structure, as shown by Marder et al. Therefore, the TPA photoreaction of aryl esters can be improved by varying the absorbing unit. Another improvement of the shown systems could possibly be done by improving the matrix concerning the impurities, the polymerisation and the process of coating the polymer. For applications in waveguide technology, light extraction tests and cut-back measurements can be applied to detect the optical loss.

### **3 Part B: UV and VUV Assisted Patterned Surface Modification of PS and LDPE in a Reactive Gas Atmosphere**

#### **3.1 Introduction to Part B**

Whilst in part A of this work the modulation of optical properties of UV reactive polymers was investigated, part B is devoted to the use of photochemical reactions to achieve specific surface properties. In previous works, reactive gases, such as sulphur dioxide, cyanogen bromide, phosphorous tribromide and hydrazine have been employed to confer hydrophilic and chemical reactive functionalities onto polymer surfaces in the presence of UV light.<sup>[1,2,3,4]</sup> A major drawback of these reagents is their high toxicity, corrosive properties as well as their unpleasant odour. Only recently organosilanes such as trimethylsilane (TMS) and ethyldimethylsilane (EDMS) have been explored for their reactions at the surfaces of polybutadiene and polystyrene in the presence of UV light.<sup>[5]</sup> A major finding of these investigations was that this type of surface modification achieves hydrophobic as well as protective properties on polymer surfaces. Organosilanes are non-toxic and practically odourless, however they are inflammable.

The goal of part B of this thesis is the photochemical modification of polymers such as polystyrene (PS) and low density polyethylene (LDPE) in the presence of organosilanes. Therefore, the polymer surfaces are irradiated in the presence of trimethylsilane (TMS) and a TMS/O<sub>2</sub> mixture. Different light sources and different pattern techniques are applied. A chemical modification of the polymer surfaces with organo-silyl and SiO<sub>x</sub> containing groups is aimed at. The focus was set on the combination of TMS and oxygen as reactive gases. To the best of our knowledge such a photochemical approach has not been investigated before.

Surface analysis is carried out by means of X-ray induced photoelectron spectroscopy (XPS), FT-IR spectroscopy and scanning electron microscopy (SEM). For the photochemically created pattern light microscopy, FT-IR microscopy, SEM coupled with energy dispersive X-ray spectroscopy (EDX) and profile measurements are carried out to describe and characterise the produced structure.

In chapter 3.2 experiments with a Xe<sup>\*</sup>-lamp with an emission wavelength of 172 nm are described. The photochemical modification of the surface of LDPE is investigated. A contact mask technique is described to produce chemical surface patterns. Chapter 3.3 deals with irradiation of polystyrene films with a KrF excimer laser (248 nm). PS is expected to be modified in the presence of a TMS/O<sub>2</sub> mixture under UV irradiation. A projection system

coupled with the excimer laser is used to transfer the mask pattern onto the polymer surface (demagnification). This approach combines the principles of projection lithography with surface functionalization.

[1] Buchgraber C., Ebel M. F., Svagera R., Schröttner H., Kern W., *Macromol. Chem. Phys.* 208 (11) **2007**, 1159–1167

[2] Meyer U., Köstler S., Ribitsch V., Kern W., *Macromol. Chem. Phys.* 206 (2) **2005**, 210–217

[3] Meyer U., Ebel M. F., Svagera R., Kern W., *Macromolecular Rapid Communication* 20 (10) **1999**, 515–520

[4] Kern W., Eur. Pat. Appl. (2001), EP 1072635, A1 20010131

[5] Spanring J., Buchgraber C., Ebel M. F., Svagera R., Kern W., *Macromol. Chem. Phys.* 206, **2005**, 2248–2256

## 3.2 Modification of Polyethylene by VUV Irradiation in the Presence of Trimethylsilane and Oxygen

### 3.2.1 Summary

The photoassisted modification of low-density polyethylene (LDPE) by vacuum UV (VUV) irradiation in a reactive gas atmosphere was investigated. Irradiation experiments were carried out with a xenon excimer lamp (172 nm VUV) in the presence of a trimethylsilane / oxygen mixture. The modified LDPE surface was investigated by spectroscopic techniques (FT-IR, XPS), contact angle measurements and electron microscopy. This VUV process leads to the attachment of alkylsilyl and Si-O units (organosilicate groups) to LDPE as evidenced by FTIR and XPS data. Optimum results were obtained at a ratio trimethylsilane/oxygen = 1/1. Contact angle measurements showed that low-energy surfaces are obtained after few minutes of irradiation at a radiant intensity of  $1.7 \text{ mW cm}^{-2}$ . After prolonged irradiation, the thickness of the modified polyethylene layer is approximately 700 nm. Using a TEM grid as contact mask, a patterned surface modification was achieved. Surface modifications of this type may be of interest to obtain protective and barrier layers on polyolefines.

### 3.2.2 Introduction

Commodity polymers such as polyolefines play a predominant role in the world of polymers. With appropriate modification methods it is possible to adjust the properties of polymeric materials depending on the designed application. A prominent example is the surface modification of polymers which leaves the bulk properties of the materials unchanged but allows to adjust surface properties such as polarity, wettability and chemical reactivity. Surface modification techniques such as chemical etching, plasma discharge and corona treatments have been studied thoroughly.<sup>[1,2]</sup> Over the past years, UV based techniques have been developed, among them photoassisted grafting and UV irradiation in the presence of reactive gases.<sup>[3-5]</sup> While mercury lamps are most frequently applied in photoassisted reactions, irradiations with short wavelength UV light (vacuum UV; VUV) can be performed with excimer lasers (e.g.  $\text{F}_2$  157 nm and ArF 193 nm) and with excimer lamps (e.g. 126, 172 and 222 nm).<sup>[6,7]</sup> Examples for surface reactions induced by excimer lamps are the surface modification of fluorocarbon polymers by irradiation in ammonia or hydrazine atmosphere,<sup>[8]</sup> the change of surface wettability by irradiation of polymers in the presence of atmospheric

oxygen<sup>[9]</sup> and the photoassisted conversion of polysiloxanes to silicon oxide surface layers.<sup>[10]</sup> Only recently, the VUV photooxidation of organosilane precursors to extremely thin silicon oxide layers on polymer surfaces has been reported.<sup>[11,12]</sup>

In previous contributions we have demonstrated the surface modification of *cis*-1,4-polybutadiene and polystyrene by UV irradiation in the presence of gaseous trialkylsilanes such as trimethylsilane (TMS) and ethyldimethylsilane (EDMS).<sup>[13,14]</sup> Trialkylsilanes provide advantages when applied as a reactive gas in such processes. They are easy to handle, odourless, and non-toxic. For trialkylsilanes such as trimethylsilane (TMS) the homolytic cleavage of the R<sub>3</sub>Si-H bond is the predominant photoreaction.<sup>[15]</sup> For the Si-H bond in trimethylsilane the bond dissociation energy (BDE) amounts to 378 kJ mol<sup>-1</sup> <sup>[16]</sup> which compares to the BDE of hydrocarbons. The BDE of the Si-H bond is especially low for *tris*(trimethylsilyl)silane (BDE = 330 kJ mol<sup>-1</sup>) which therefore is an excellent hydrogen donor.<sup>[17]</sup> When polybutadiene is used as target polymer,<sup>[13]</sup> the C=C double bonds participate in free radical reactions and thus facilitate light induced surface reactions with reagents such as trimethylsilane. In a similar fashion, the CH groups in the benzylic  $\alpha$ -position of polystyrene are highly reactive and photoassisted surface modifications proceed rapidly.<sup>[14]</sup> As a result of these surface modifications, the free surface energy of polybutadiene and polystyrene turn to very low values.<sup>[13,14]</sup>

In the present investigation we wished to see if also polyethylene, which is a far less reactive target than polybutadiene and polystyrene, can be surface-modified with trialkylsilanes. Low-density polyethylene (LDPE) was UV irradiated in the presence of trimethylsilane and oxygen. The experiments were carried out with a xenon excimer lamp emitting at  $\lambda = 172$  nm. In the following, investigations on the photoreaction and the characterisation of the modified LDPE surfaces are described. Surface analyses were carried out with Fourier-transform infrared spectroscopy (FT-IR), X-ray photoelectron spectroscopy (XPS) and scanning electron microscopy (SEM). The aim of the present investigation was to create organosilicate layers on polyethylene. Surface modifications of this type may be of interest to obtain protective and barrier layers on polyolefines. Compared to plasma-driven processes<sup>[18]</sup>, photo-assisted reactions can be used in surface patterning strategies based upon photolithographic techniques.

### 3.2.3 Experimental Part

#### 3.2.3.1 Materials

Trimethylsilane (TMS) was received from ABCR (Karlsruhe, Germany) in the form of a liquefied gas. Oxygen (99,999% purity) was obtained from Air Liquide. Low-density polyethylene foils (LDPE; food grade) with 35  $\mu\text{m}$  thickness were obtained from a commercial supplier (Melitta, Austria). Specimens were prepared by punching circular discs with 30 mm in diameter. Prior to modification, the samples were extracted with an acetone/water mixture in an ultra sonic bath (20 °C; three times 15 min each) to remove any additives and processing aids. The sample foils were dried *in vacuo* at 40 °C, and then subjected to modification.

#### 3.2.3.2 Characterisation Methods

Infrared spectra were taken with a Perkin Elmer Spectrum One instrument. FTIR spectra were recorded in either in transmission or by attenuated total reflection (ATR). For standard ATR spectra, a single reflection unit (Harrick split pea) with a hemispheric silicon crystal was used. FTIR microscopy was run with a Perkin Elmer Autoimage system. The aperture was set to 20  $\mu\text{m}$  x 20  $\mu\text{m}$ .

For X-ray photoelectron Spectroscopy (XPS) measurements the polymer foils were placed on metal substrates. XPS spectra were taken with a Kratos XSAM 800 spectrometer (twin anode Mg/Al X-ray tube). Mg  $K\alpha$  radiation was used as excitation source. The angle between the X-rays and the normal to the sample surface was 54°. The analyzer was located along the normal to the sample surface. The depth of XPS analysis was in the range of a 1-3 nanometers. C 1s, O 1s and Si 2p photoelectron peaks were evaluated. The binding energy of C 1s photoelectrons was defined to 285.0 eV (reference line). Shifts of O 1s and Si 2p photoelectrons were calculated with reference to the C 1s signal. The surface composition in atom-% was calculated by a quantitative XPS analysis algorithm based on fundamental parameters.<sup>[19]</sup> In these calculations, hydrogen is omitted.

For scanning electron microscopy (SEM) the polyethylene specimens were sputter coated with graphite (thickness 25 nm). A microtome was used to prepare cross sections. SEM measurements were taken with a Leo Gemini DSM 986 equipped with a field emission gun and an EDX Voyager 3105A Noran detector. Optical micrographs were taken in transmission with an Olympus BX 60 microscope equipped with a phase contrast objective.



Surface roughness  $R_{\text{rms}}$  (average root mean square) was determined from atomic force microscopy.<sup>[20]</sup> AFM measurements were conducted with a Digital Instruments Nanoscope IIIa atomic force microscope (silicon nitride tip; tapping mode).

Contact angles  $\theta$  (sessile drop) were determined with a Krüss DSA 100 drop shape analysis system. Contact angles of water (deionized, resistivity approx. 18 M $\Omega$ ) and diiodomethane (99%, GC) were determined on unmodified and modified polymer surfaces. Data for  $\theta$  were averaged over eight individual measurements. For calculation of the surface tension (surface energy) values we referred to Ström's calculated surface tension values for H<sub>2</sub>O (72.8 mJ m<sup>-2</sup>) and CH<sub>2</sub>I<sub>2</sub> (50.8 mJ m<sup>-2</sup>).<sup>[21]</sup> For the calculation of the surface tension  $\gamma$  and its components  $\gamma^D$  (dispersive component) and  $\gamma^P$  (polar component) the method of Owens and Wendt was applied.<sup>[22]</sup>

### 3.2.3.3 VUV Irradiation Experiments

The irradiation process was performed with a xenon excimer lamp (Heraeus Noblelight) with an emission wavelength of 172 nm. The excimer lamp was mounted in a nitrogen flushed housing. The whole equipment (excimer lamp and reaction chamber) was operated in a glove box under nitrogen atmosphere. This was important to exclude any oxygen in the light path between the lamp housing and the reaction chamber since oxygen strongly absorbs at 172 nm and would reduce the radiant intensity at the sample surface. The radiant intensity was 1.7 mW cm<sup>-2</sup> as measured with a calibrated sensor (Gentec). The VUV intensity was measured at the same position (relative to the excimer lamp) where the LDPE foils were placed during the irradiation experiments. The sample foils were mounted in a reaction chamber (Graseby Specac) equipped with CaF<sub>2</sub> windows (transparent both for VUV and infrared radiation). The foil samples were in close proximity to the front CaF<sub>2</sub> window (approx. 100  $\mu\text{m}$  distance) to avoid losses in radiant intensity due to light absorption by gaseous TMS and oxygen. Then the chamber was evacuated and subsequently filled with the desired reactive gases (TMS and oxygen). The partial pressures were controlled by a manometer and adjusted to make up to 10<sup>5</sup> Pa (1 bar). All illumination experiments were carried out immediately after filling the reaction chamber. After illumination, the chamber was evacuated and flushed with nitrogen. For patterning, honeycomb copper grids (600 mesh; available from Ted Pella, Inc., Redding, U.S.A.) were used as contact masks.

## 3.2.4 Results and Discussion

### 3.2.4.1 General Aspects

The 172 nm emission of the xenon excimer lamp provides high energy (696 kJ per mol photons) to the illuminated target. It is therefore expected that bond cleavage occurs both in the used gases (trimethylsilane and oxygen) as well as in the polymer.

Polyethylene absorbs in the VUV range due to  $\sigma - \sigma^*$  transitions of C-H and C-C bonds. For LDPE, which is a branched polyolefin, C-H bond fission is most probable at tertiary carbons (BDE of tertiary C-H: 384 kJ mol<sup>-1</sup>) but occurs also at secondary carbons (BDE of secondary C-H: 397 kJ mol<sup>-1</sup>).<sup>[16]</sup> The photon energy at 172 nm is high enough to lead to dissociations of the C-C bonds in the polymer as well (BDE = 355 kJ mol<sup>-1</sup>).<sup>[23]</sup> Since the absorbance of polyethylene at 172 nm is very low, bond cleavage will be limited when this wavelength is applied. However, with VUV wavelengths < 160 nm free radicals at polyethylene surfaces are generated readily which can further react with a variety of gaseous compounds.<sup>[24-26]</sup>

Vacuum UV (VUV) absorption spectra of trimethylsilane (TMS) have been reported in the literature. UV absorption of TMS peaks at three wavelengths in the VUV range (115, 140, and 165 nm).<sup>[27,28]</sup> For TMS, an absorption coefficient of  $3.8 \pm 0.5 \text{ L mol}^{-1} \text{ cm}^{-1}$  has been reported at the wavelength  $\lambda = 172 \text{ nm}$ .<sup>[29]</sup> Investigations on the mercury sensitized photolysis of trimethylsilane showed that fragmentation into trimethylsilyl and hydrogen radicals (BDE = 378 kJ mol<sup>-1</sup>) proceeds, which then yields H<sub>2</sub> and (CH<sub>3</sub>)<sub>6</sub>Si<sub>2</sub> as reaction products.<sup>[15]</sup> When UV irradiation of TMS was carried out with an ArF excimer laser ( $\lambda = 193 \text{ nm}$ ), also CH<sub>4</sub> and (CH<sub>3</sub>)<sub>4</sub>Si were detected by FTIR.<sup>[30]</sup> From this it can be concluded that Si-H scission is the predominant photolytic reaction for TMS, while Si-C fragmentation occurs to a lesser extent.

It is well known that oxygen readily produces ozone under UV radiation with wavelengths < 240 nm. Ozone can dissociate to a singlet O<sub>2</sub> (<sup>1</sup>Δg) and an oxygen biradical O (<sup>1</sup>D) <sup>[31]</sup> which leads to further radical reactions. It is therefore expected, that both reactive gases will generate radicals under VUV illumination at 172 nm, while the polyethylene target is less reactive at this wavelength.

#### VUV Irradiation of LDPE under Trimethylsilane/Oxygen atmosphere

LDPE foils of 35 microns thickness were employed in the experiments. Initial experiments with VUV illumination of LDPE under pure TMS atmosphere showed that silicon was only scarcely incorporated into the polymer surface, even after prolonged irradiation. This was evidenced by FTIR spectra which lacked the signals typical of trialkylsilyl groups. This result is a distinct contrast to polybutadiene and polystyrene which can be modified easily with neat

TMS under UV irradiation. This result can be explained by the low absorbance of polyethylene at 172 nm:<sup>[26]</sup> surface modification *via* recombination of macroradicals with silyl radicals does not proceed efficiently under these conditions. However, VUV surface modification of LDPE proceeded rapidly when feeding both TMS and oxygen into the reactive gas atmosphere. Three series of experiments were run: 20 kPa TMS / 80 kPa oxygen, 50 kPa TMS / 50 kPa oxygen and 80 kPa TMS / 20 kPa oxygen. Both FTIR and XPS spectra of modified LDPE samples indicated that a gas composition of 50 kPa TMS and 50 kPa oxygen lead to the most efficient surface modification. These results will be discussed in more detail.

### 3.2.4.2 Spectroscopic Measurements

XPS spectra were recorded to obtain information on the chemical composition of the surfaces. Generally, the depth of XPS analysis amounts to a few nm. Figure 39 displays the Si2p signal recorded for pristine LDPE (trace A) and for samples of LDPE irradiated under different gas atmospheres (traces B, C, and D). The ratio TMS/O<sub>2</sub> was varied from (B) 20 kPa/80 kPa to (C) 50 kPa/50 kPa and to (D) 80 kPa/20 kPa. It is seen that the surface of pristine LDPE contains only traces of silicon (residual impurities). The content of Si increases upon VUV irradiation in TMS/O<sub>2</sub> atmosphere. Keeping the duration of VUV illumination constant (300 s at a radiant intensity of 1.7 mW cm<sup>-2</sup>), surface modification is most efficient at a gas composition TMS/O<sub>2</sub> = 50 kPa/50 kPa. The position of the Si2p signal is found at 102.6 eV (with respect to the C1s signal fixed at 285 eV). Comparing with the XPS data obtained for alkylsilyl groups attached to polybutadiene and polystyrene (Si2p signal at 102.8 eV and 102.5 eV, respectively <sup>[13,14]</sup>) this would point to alkylsilyl groups (CH<sub>3</sub>)<sub>3</sub>Si-alkyl, but also silicon attached to oxygen displays XPS signals in this spectral region. For amorphous silicon dioxide (SiO<sub>2</sub>) the Si2p signal is located at 103.6 eV.<sup>[11]</sup> Consequently, the observed Si2p signal at 102.6 eV is probably a superposition of signals which stem from Si atoms bound to carbon and Si atoms bound to oxygen.

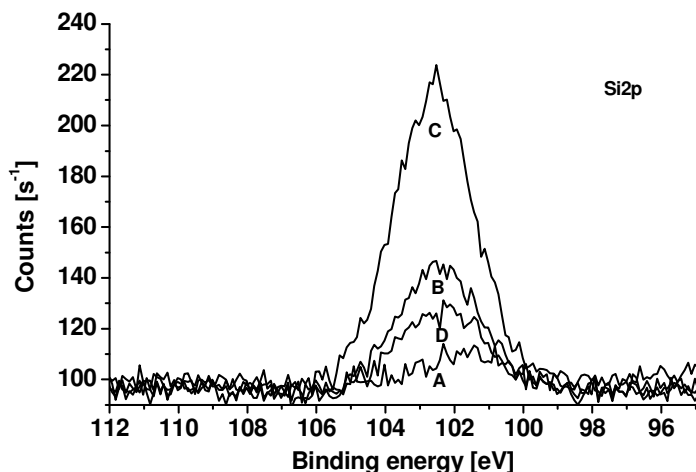


Figure 39: Detailed XPS spectra of polyethylene (LDPE) surfaces. The spectral range typical of the Si2p signal is shown for pristine polyethylene (A) and for polyethylene modified by VUV irradiation under TMS/O<sub>2</sub> atmosphere. (B) 20 kPa/80 kPa; (C) 50 kPa/50 kPa; and (D) 80 kPa/20 kPa. All illuminations were carried out for 300 s at a radiant intensity of 1.7 mW cm<sup>-2</sup> at  $\lambda = 172$  nm.

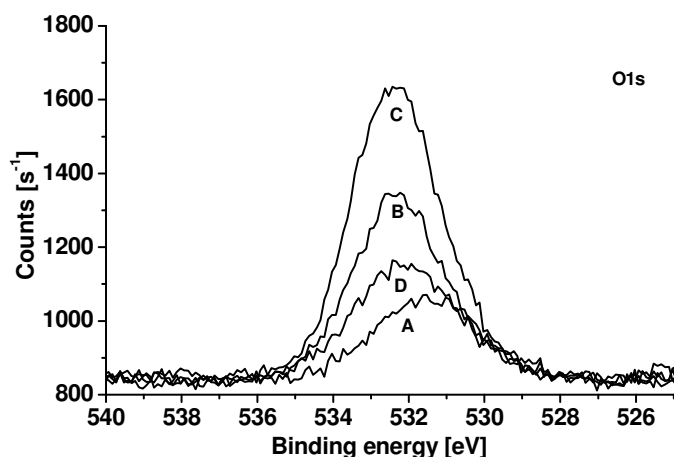


Figure 40: Detailed XPS spectra of polyethylene (LDPE) surfaces. The spectral range typical of the O1s signal is shown for pristine polyethylene (A) and for polyethylene modified by VUV irradiation under TMS/O<sub>2</sub> atmosphere. (B) 20 kPa/80 kPa; (C) 50 kPa/50 kPa; and (D) 80 kPa/20 kPa. All illuminations were carried out for 300 s at a radiant intensity of 1.7 mW cm<sup>-2</sup> at  $\lambda = 172$  nm.

Detailed XPS spectra of the O1s signal are given in Figure 40. While pristine LDPE contained small amounts of oxygen (signal at 531.6 eV), the VUV modification in the presence of TMS and oxygen leads to the evolution of a peak at 532.3 eV. The position of this O1s signal is typical of Si-O groups as reported for SiO<sub>2</sub>.<sup>[32]</sup> Regarding the intensity of the O1s signal in dependence of the gas composition, the same trend is found as for the intensity of the Si2p signal: at a gas composition TMS/O<sub>2</sub> = 50 kPa/50 kPa the highest amount of oxygen is incorporated into the surface. For this sample, XPS data were quantified and data on the surface composition (in atom-%) were derived, see Table 5. To examine the influence of the duration of illumination, XPS spectra were also recorded for a LDPE sample

which was irradiated for 2700 s under TMS/O<sub>2</sub> (50 kPa/50 kPa), see Table 5. In this case, the position of the Si2p signal shifted to 103.7 eV.

**Table 5. Composition of LDPE surfaces<sup>1)</sup>**

Sample	C	O	Si
	atom %	atom %	atom %
Pristine LDPE	97.0	2.6	0.4
Modified LDPE <sup>2)</sup>	89.2	8.0	2.8
Modified LDPE <sup>3)</sup>	83.6	11.6	4.8

<sup>1)</sup> Hydrogen is omitted in this calculation

<sup>2)</sup> 300 s of 172 nm irradiation under TMS / O<sub>2</sub> (50 kPa / 50 kPa)

<sup>3)</sup> 2700 s of 172 nm irradiation under TMS / O<sub>2</sub> (50 kPa / 50 kPa)

These XPS data on VUV modified LDPE show that a surface layer containing Si and O (atomic ratio approx. 1:2) is created. The surface still contains a large amount of carbon (>80 at.-%). For both irradiation times (300 and 2700 s, respectively) a similar composition of the surface is found. These results indicate that the surface layer consists of polyethylene modified with groups that contain oxygen and silicon (organosilicates). If the surface layer were a polymerization product of silane and oxygen, the content of carbon would be far lower. At the same time it can be excluded that the VUV irradiation of LDPE in the presence of TMS/O<sub>2</sub> generates a SiO<sub>2</sub> layer at the surface.

To obtain additional information on the modified LDPE surface, ATR-FTIR spectra were taken of LDPE samples irradiated under TMS/O<sub>2</sub> atmosphere (50 kPa/50 kPa). Spectra were recorded (A) prior to and after VUV irradiation for different periods of time (B, 15 min; C, 30 min; and D, 45 min). Figure 41 displays ATR-FTIR spectra in the spectral region 2300 – 500 cm<sup>-1</sup>. With the ATR equipment used (Si ATR crystal), the penetration depth of IR radiation is in the range of 1 μm. In the FTIR spectrum of the non-irradiated LDPE sample signals at 1472 cm<sup>-1</sup> (-CH<sub>2</sub>- deformation vib.) and at 719 cm<sup>-1</sup> (rocking vib. of alkylene chains) are detectable, see spectrum A in Figure 41. For the VUV irradiated samples a modification of the polymer surface is detectable already after 15 minutes, and IR signals at 2110 (weak), 1718 (weak), 1261 (strong), 1054 (broad, strong), 906, 842 and 799 cm<sup>-1</sup> evolve. *Table 2* gives the assignment of these bands according to the literature.<sup>[33]</sup>

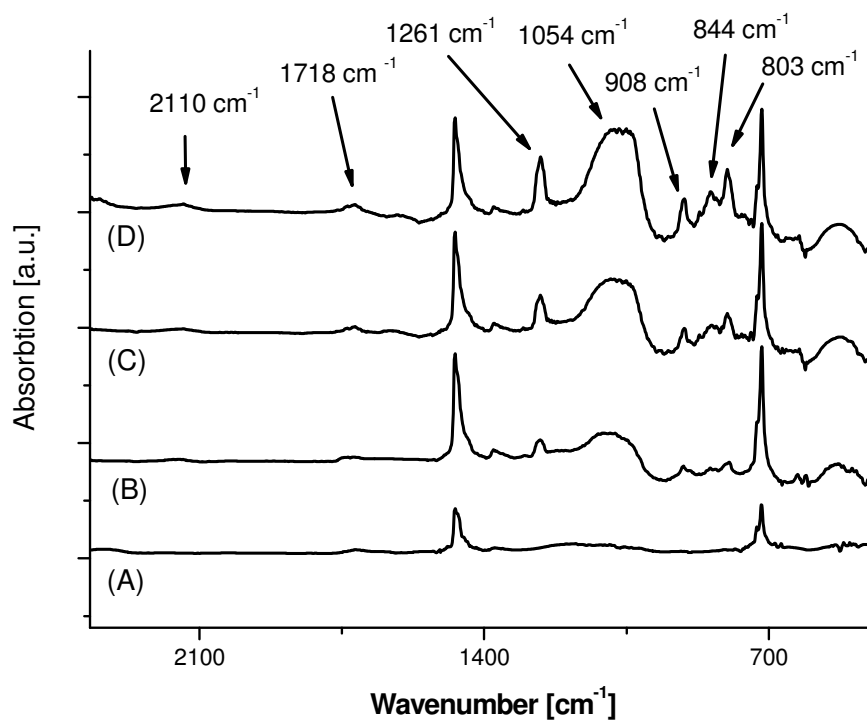


**Figure 41:** ATR-FTIR spectra of polyethylene (LDPE) surfaces. The spectra refer to pristine polyethylene (A) and for polyethylene modified by VUV irradiation under TMS/O<sub>2</sub> atmosphere (50 kPa/50 kPa). (B) 15 min, (C) 30 min and (D) 45 min of irradiation (radiant intensity: 1.7 mW cm<sup>-2</sup>).

**Table 6:** New IR signals in LDPE after VUV modification in the presence of trimethylsilane and oxygen (50 kPa/50 kPa).

IR signal (in cm <sup>-1</sup> )	Assignment according to ref. <sup>[33]</sup>	Comment
2110	valence vib. of Si-H	
1718	valence vib. of C=O (aldehyde)	oxidation of polyethylene
1261	sym. deformation vib. of CH <sub>3</sub> in Si(CH <sub>3</sub> ) <sub>n</sub> units	
1054	valence vib. of Si-O	
908	deformation vib. of Si-H	
844	Si-C rocking vib. of Si(CH <sub>3</sub> ) <sub>3</sub>	
803	valence vib. Of Si-C	

The infrared data show that the surface layer contains Si-O groups (as indicated by the broad intense signal at 1054 cm<sup>-1</sup>) as well as Si(CH<sub>3</sub>)<sub>n</sub> groups, which are revealed by the

strong band at  $1261\text{ cm}^{-1}$  and the signal at  $844\text{ cm}^{-1}$ . Interestingly, also Si-H units are present as indicated by the signals at  $1210$  and  $908\text{ cm}^{-1}$ . The presence of Si-H groups has also been found for polystyrene after UV modification with trimethylsilane.<sup>[14]</sup> This indicates that trimethylsilane also yields radicals  $\bullet\text{SiH}(\text{CH}_3)_2$  upon VUV irradiation, which are then incorporated in the surface layer to give free Si-H units. The concentration of organosilicon groups at the surface of LDPE increases upon prolonged VUV irradiation. It is important to note that the polyethylene band at  $719\text{ cm}^{-1}$  (rocking vib. of alkylene chains) is not affected in the course of the reaction. Also these FTIR data suggest that the LDPE surface is not covered by a  $\text{SiO}_x$  layer, but that the polyethylene itself is modified by the photoreaction.

Clearly, it is almost impossible to describe the structure of the surface layer in detail. Nevertheless, in Figure 42 a possible reaction sequence based on radical reactions is depicted. We wish to point out that this is *not* considered as a proven reaction mechanism, but should rather provide *examples of reaction steps* in the photoassisted modification reaction. It is reasonable to assume the formation of polyolefin macroradicals (1), which can occur by direct VUV photolysis of C-C bonds or by reaction with oxygen (peroxide intermediates are possible). The preferred photolysis reaction of TMS is the homolytic cleavage of the Si-H bond which yields trimethylsilyl radicals (2). A recombination with macroradicals would give a silyl substituted polyethylene chain, which may be further oxidized by singlet oxygen ( $\text{O}_2\ ^1\Delta_g$ ) and an oxygen biradical ( $\text{O}\ ^1\text{D}$ ) (3). An exemplary structure of modified polyethylene containing -Si-O-Si- units is then represented in line (4).

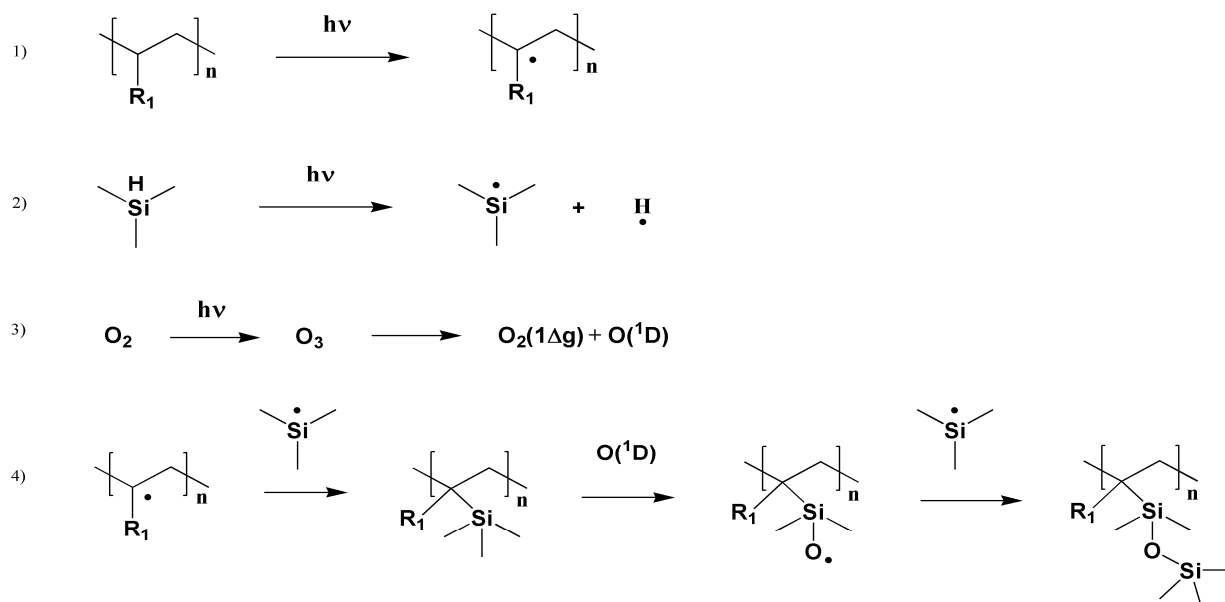


**Figure 42: A possible reaction sequence for the VUV assisted surface modification of polyolefines in the presence of trimethylsilane and oxygen. Examples of reaction steps in the modification reaction based on radical intermediates are depicted.**

### 3.2.4.3 Scanning Electron Microscopy, AFM and Contact Angle Measurements

In an additional experiment the thickness of the modified surface layer of LDPE was investigated by scanning electron microscopy (SEM). A sample was irradiated for 30 min under TMS / O<sub>2</sub> atmosphere (50 kPa / 50 kPa), then a cross section was prepared with a microtome. The SEM image in Figure 43 shows the cross section of the modified LDPE sample consisting of zone (1) and (2), while zone 3 represents the top surface of the prepared specimen. The lower zone (1) (dark) is non-modified polyethylene, and zone (2) (bright; between the white bars) is the modified surface layer containing silicon. The thickness of the modified layer (2) amounts to approx. 700 nm (with variations in thickness).

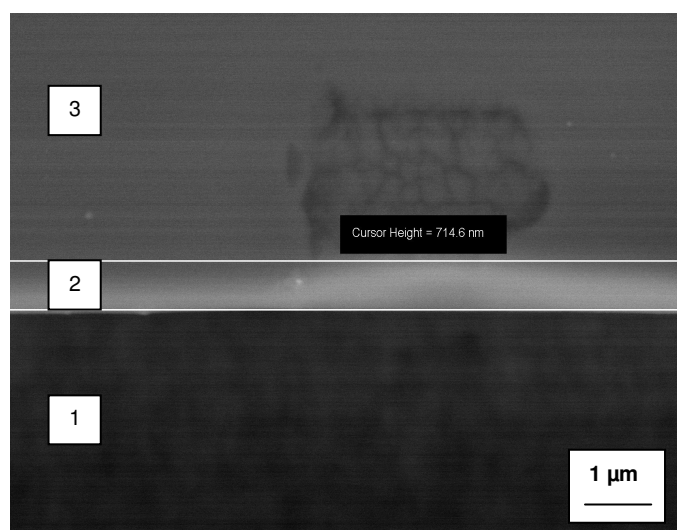


**Figure 43: SEM image of a cross section of surface modified polyethylene. The sample was irradiated for 30 min under TMS / O<sub>2</sub> atmosphere (50 kPa / 50 kPa), The silicon rich surface layer (2) can be clearly distinguished from non-modified bulk material (1). While zones (1) and (2) represent the cross section, zone (3) is the top surface of the prepared specimen.**

From AFM measurements the surface roughness  $R_{\text{rms}}$  was calculated.<sup>[20]</sup> Both for the pristine LDPE surface and for the VUV irradiated sample a roughness  $R_{\text{rms}} \sim 70$  was found. The process does not lead to significant changes in surface morphology.

Contact angle measurements on LDPE showed that the wetting angle  $\Theta$  of water (sessile drop) decreased slightly from  $\Theta = 102.0^\circ$  (pristine LDPE) to  $\Theta = 97.1^\circ$  after 45 min of irradiation under TMS / O<sub>2</sub> atmosphere (50 kPa / 50 kPa). At the same time, the contact angle of CH<sub>2</sub>I<sub>2</sub> increased from  $\Theta = 56.1^\circ$  (pristine LDPE) to  $63.3^\circ$ . From these data, the overall surface tension  $\gamma$  and its polar and dispersive components ( $\gamma^P$  and  $\gamma^D$ ) were calculated by the Owens-Wendt method. For non-modified LDPE a value  $\gamma = 30.7 \text{ mJ m}^{-2}$  was obtained



(polar component  $\gamma^P = 0.2 \text{ mJ m}^{-2}$ ; dispersive component  $\gamma^D = 30.5 \text{ mJ m}^{-2}$ ). These data are in good agreement with literature data.[22] After 45 min of VUV treatment, for the modified LDPE a surface tension  $\gamma = 27.8 \text{ mJ m}^{-2}$  was found (polar component  $\gamma^P = 1.2 \text{ mJ m}^{-2}$ ; dispersive component  $\gamma^D = 26.6 \text{ mJ m}^{-2}$ ). The surface tension  $\gamma$  of polyethylene mainly consists of the dispersive component  $\gamma^D$ , while the polar component  $\gamma^P$  of the surface energy is comparably small. After VUV treatment of polyethylene with trimethylsilane/oxygen the dispersive component  $\gamma^D$  decreases significantly and causes a drop of the overall surface tension  $\gamma$ . Summing up, the modification process results in a low-energy surface with increased oleophobic properties. Figure 44 displays the changes in the overall surface tension  $\gamma$  as a function of the irradiation time.

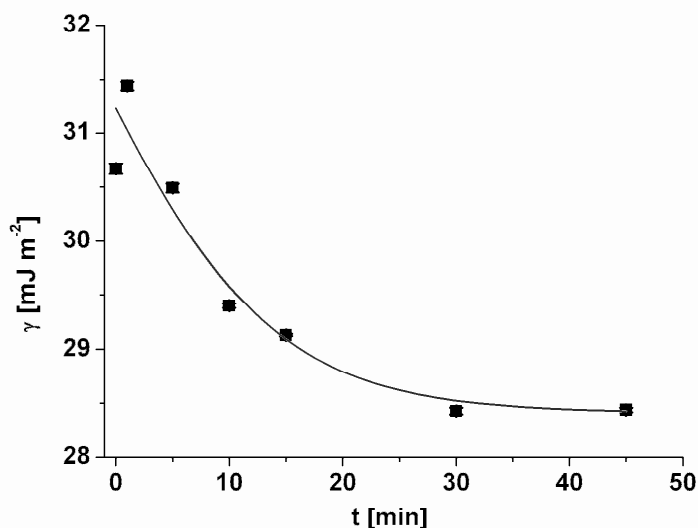


**Figure 44: Surface tension  $\gamma$  of polyethylene after UV modification with trimethylsilane/oxygen (TMS/O<sub>2</sub> = 50 kPa/50 kPa) for different periods of time. Values of  $\gamma$  were calculated from H<sub>2</sub>O and CH<sub>2</sub>I<sub>2</sub> contact angles (error bars are also indicated)**

### 3.2.4.4 Surface Patterning

Finally, a patterned surface modification of polyethylene was carried out. A honeycomb copper grid (mesh 600) was placed on the 35  $\mu\text{m}$  LDPE foil, then the sample was VUV irradiated in TMS / O<sub>2</sub> atmosphere (50 kPa / 50 kPa) for 30 min. Figure 45 displays an optical micrograph (phase contrast) of the LDPE foil after VUV patterning. It can be seen that the honeycomb grid structure, which was applied as a contact mask, is reproduced well. To probe the composition of the polymer sample in the shaded areas (bars) and in the illuminated areas (hexagonal fields), transmission FTIR microscopy was applied (aperture set to 20  $\mu\text{m}$  x 20  $\mu\text{m}$ ). The FTIR spectra taken at the position of the bars represented neat

LDPE, while the FTIR spectra recorded within the hexagonal fields featured the typical Si-O signal. The spectra on the right side of Figure 45 represents the difference of these two FTIR spectra (spectral range 2500 to 700  $\text{cm}^{-1}$ ). The characteristic Si-O signal at approx. 1040  $\text{cm}^{-1}$  can be discerned unambiguously, and also the  $\text{Si}(\text{CH}_3)_n$  band around 1260  $\text{cm}^{-1}$  is detectable. These results show that the VUV modification of LDPE with TMS /  $\text{O}_2$  as reactive gas can be carried out with contact masks to create patterns on the micrometer scale.

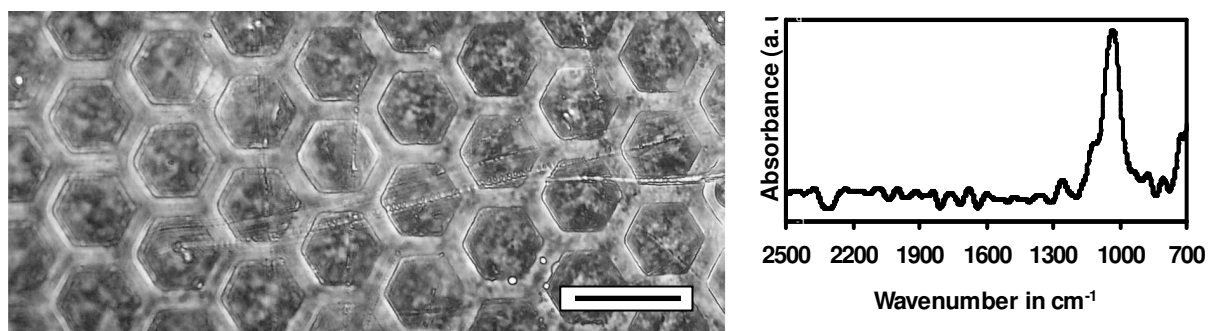


**Figure 45:** Optical micrograph (phase contrast) of a LDPE surface after patterned surface modification with trimethylsilane/oxygen using a honeycomb grid (mesh 600). The hexagonal pattern is well reproduced. The spectra on the right side shows the differential spectrum calculated from FTIR spectra recorded at the position of the bar and inside the hexagons. The signal at approx 1040  $\text{cm}^{-1}$  proves the presence of Si-O units inside the hexagonal mesh. The scale bar represents 50  $\mu\text{m}$

### 3.2.5 Conclusion

It has been demonstrated that LDPE can be modified by VUV irradiation in the presence of trimethylsilane and oxygen (optimum ratio  $\text{TMS}/\text{O}_2 = 1/1$ ). This modification leads to the introduction of organosilicate, trimethylsilyl, and also Si-H units onto the LDPE surface, but not to the formation of a silicon oxide ( $\text{SiO}_x$ ) layer. After 30 min of 172 nm irradiation with 1.7  $\text{mW cm}^{-2}$ , a modified surface layer of approx. 700 nm thickness is obtained. Surface sensitive techniques such as XPS and contact angle measurements show significant changes in the properties of the surface after a few minutes of illumination. A patterned surface modification on the  $\mu\text{m}$  scale can be achieved when contact masks are applied.

### 3.2.6 References

- [1] C.-M. Chan, ‘‘Polymer surface modification and characterization’’, Carl Hanser Verlag, Munich 1994.
- [2] C.-M. Chan, T.-M. Ko, H. Hiraoka, *Surf. Sci Rep.* **1996**, *24*, 1.
- [3] I. Mathieson, R. H. Bradley, *Intern. J. Adhesion Adhesives*, **1996**, *16*, 29.
- [4] N. Chanunpanich, A. Ulman, Y. M. Stzhemechny, S. A. Schwarz, A. Janke, H. G. Braun, T. Kratzmüller, *Langmuir* **1999**, *15*, 2089.
- [5] T. Kavc, W. Kern, M. F. Ebel, R. Svagera, P. Pölt, *Chem. Mater.* **2000**, *12*, 1053.
- [6] Z.-Y. Zhang, I. W. Boyd, H. Esrom, *Surf. Interf. Anal.* **1996**, *24*, 718.
- [7] U. Kogelschatz, H. Esrom, Z.-Y. Zhang, I. W. Boyd, *Appl. Surf. Sci.* **2000**, *168*, 29.
- [8] J. Heitz, H. Niino, A. Yabe, *Jpn. J. Appl. Phys.* **1996**, *35*, 4410.
- [9] A. Hozumi A., H. Inagai, T. Kameyama, *J. Colloid Interface Sci.* **2004**, *278*, 383.
- [10] V.-M. Graubner, R. Jordan, O. Nuyken, B. Schnyder, T. Lippert, R. Kötz, A. Wokaun, *Macromolecules* **2004**, *37*, 5936.
- [11] A. Hozumi, H. Inagai, Y. Yokogawa, T. Kameyama, *Thin Solid Films* **2003**, *437*, 89.
- [12] A. Hozumi, T. Masuda, H. Sugimura, T. Kameyama, *Langmuir* **2003**, *19*, 7573.
- [13] J. Spanring, C. Buchgraber, M.F. Ebel, R. Svagera, W. Kern, *Macromol. Chem. Phys.* **2005**, *206*, 2248.
- [14] J. Spanring, C. Buchgraber, M.F. Ebel, R. Svagera, W. Kern, *Polymer* **2006**, *47*, 156.
- [15] M.A. Nay, G.N.C. Woodall, O.P. Strausz, H.E. Gunning, *J. Am. Chem. Soc.* **1965**, *87*, 179.
- [16] R. Walsh, *Acc. Chem. Res.* **1981**, *14*, 246.
- [17] C. Chatgililoglu, *Chem. Rev.* **1995**, *95*,1229.
- [18] M. Morra, E. Occhiello, F. Garbassi, *J. Appl. Polym. Sci.* **1993**, *48*, 1331
- [19] W. Hanke, H. Ebel, M.F. Ebel, A. Jablonski, K. Hirokawa, *J. Electron. Spectrosc. Relat. Phenom.* **1986**, *40*, 241.
- [20] Command Reference Manual, version 4.10, Digital Instruments Inc., 1995.
- [21] G. Ström, M. Frederiksson, P. Stenius. *J. Colloid Interf. Sci.* **1987**, *119*, 352.
- [22] D. K. Owens, R.C. Wendt, *J. Appl. Polym. Sci.* **1969**, *13*, 1741.
- [23] J.F. Rabek, ‘‘Photodegradation of Polymers, Physical Characteristics and Applications, Springer, Berlin, 1996
- [24] F.-E. Truica-Marasescu, M. R. Wertheimer, *Macromol. Chem. Phys.* **2005**, *206*, 744.
- [25] F.-E. Truica-Marasescu, S. Guimond, M.R. Wertheimer, *Nucl. Instr. Meth. Phys. Res. B* **2003**, *208*, 294.
- [26] F. Truica-Marasescu, M.R. Wertheimer, *J. Appl. Polym. Sci.* **2004**, *91*, 3886.

- [27] A.G. Alexander, O.P. Strausz, *Chem. Phys. Lett.* **1972**, *13*, 608.
- [28] Y. Harada, J.N. Murrell, H.H. Sheena, *Chem. Phys. Lett.* **1968**, *1*, 595.
- [29] M. Ahmed, P. Potzinger, H.G. Wagner, *J. Photochem. Photobiol. A* **1995**, *86*, 33.
- [30] A. Watanabe, K. Osato, S. Ninomiya, M. Mukaida, T. Tsunoda, Y. Imai, *Thin Solid Films* **1996**, *274*, 70.
- [31] A.M. Brown, M.T. Maurette, E. Oliveros, "*Photochemical Technology*", p. 346-347, Wiley, Chichester 1991.
- [32] C.D. Wagner, W.M. Riggs, L.E. Davis, J.F. Moulder, G.E. Muilenberg. "*Handbook of X-ray Photoelectron Spectroscopy*". Physical Electronics Division, Appandix B. Eden Prairie: Perkin Elmer Corporation, 1979.
- [33] G. Socrates, "*Infrared characteristic group frequencies*", John Wiley & Sons, Chichester 1998.

## 3.3 Patterened Surface Modification of Polystyrene by UV Irradiation in the Presence of Trimethylsilane

### 3.3.1 Summary

A new surface modification method for polystyrene by laser irradiation was investigated. Polymer films were irradiated with a KrF excimer laser at 248 nm coupled with a UV projection system. During illumination, the polymer surface was in contact with a reactive gaseous atmosphere consisting of trimethylsilane and oxygen. A mask projection system was used for the process, and surface patterns with feature sizes of 40 and 500 micrometers, respectively, were obtained after UV irradiation. The modified polymer surface was analysed by light microscopy, infrared-microscopy, profile measurements, scanning electron microscopy (SEM) equipped with an energy dispersive X-ray spectroscope (EDX) as well as X-ray photoelectron spectroscopy (XPS). The profile of the generated surface pattern showed shallow indents with a depth between 50 and 90 nm. In the illuminated areas organosilicate groups are attached to the surface, as has been evidenced by XPS and EDX. Projection lithography coupled with reactive gas atmosphere is an interesting method to generate patterned surfaces containing specific functional groups in a one-step process.

### 3.3.2 Introduction

Control of the surface properties of technical polymers plays an important role with regard to their wettability, adhesion and coating. Surface modification can be done by plasma surface modification<sup>[1]</sup>, chemical etching<sup>[2]</sup>, chemical vapour deposition<sup>[3]</sup> and UV techniques. By UV irradiation of polymer surfaces in the presence of reactive gases such as oxygen, halogens or sulphur dioxide, specific functional groups can be attached to the surface.<sup>[4,5,6]</sup>

Polystyrene (PS) is one of the most important polymers for industrial applications and is also used for biomedical<sup>[7]</sup> and optical<sup>[8]</sup> materials. Using UV assisted techniques, the surface properties of PS have for example been modified by photooxidation with 172 nm, resulting in improved wettability,<sup>[9]</sup> and by the controlled adsorption of proteins and cells on polystyrene surfaces modified by laser irradiation<sup>[10]</sup>.

In previous contributions we have investigated the surface modification of various polymers, among them polyethylene, cis-1,4-polybutadiene and polystyrene, by UV (and vacuum UV) irradiation in the presence of gaseous trialkylsilanes.<sup>[11,12,13]</sup> Trialkylsilanes such

as trimethylsilane (TMS) have many advantages when employed as reactive gases in surface processes as they are odourless and non-toxic.

The silicon-hydrogen bond dissociation energy (BDE) in alkylsilanes amounts to 378 kJ/mol.<sup>[14,15]</sup> This value is in the same region as the BDE of C-H units in hydrocarbons. For trialkylsilanes such as TMS the homolytic cleavage of the silicon-hydrogen bond is the predominant photoreaction.<sup>[16]</sup>

As shown in previous contributions, the surface modification of polystyrene in the presence of ethyldimethylsilane or trimethylsilane (TMS) proceeded rapidly when a 193 nm ArF excimer laser or an unfiltered medium pressure Hg lamp was used for irradiation. In these cases, the incorporation of organosilyl groups onto the surface was found, with the benzylic  $\alpha$ -position in polystyrene expected to have the highest reactivity in free radical processes.<sup>[13]</sup> Silyl radicals can also react with the aromatic units to give substitution products as described by Chatgililoglu.<sup>[15]</sup> It has also been demonstrated that the 172 nm irradiation of polyethylene surfaces in the presence of a gaseous mixture of TMS and oxygen resulted in surface layer containing organo-silyl and Si-O (organosilicate) groups.<sup>[11]</sup>

In this contribution we investigated the patterned surface modification of PS by projection lithography in the presence of trimethylsilane and oxygen. For the surface modification, an excimer laser (KrF, 248 nm) was coupled with an optical projection system to create photo-patterns at the polymer surface. Surface characterisation was done by means of optical, FT-IR and scanning electron microscopy (SEM), profile measurements and by X-ray photoelectron spectroscopy (XPS). It is shown that functional patterns can be created at the PS surface by this technique.

### **3.3.3 Experimental Part**

#### **3.3.3.1 Materials**

Trimethylsilane (TMS) was received from A.B.C.R. (Germany) in form of a liquefied gas. TMS was filtered with an oxygen absorber (Air Liquide) for irradiation under pure TMS atmosphere. Oxygen (99.999%) was obtained from Air Liquide. Polystyrene with  $M_w = 560.000 \text{ g mol}^{-1}$  was received from Polymer Standards Service (Mainz, Germany). The polymer was reprecipitated several times prior to use. Polystyrene films of approx. 0.5  $\mu\text{m}$  film thickness were prepared by spin casting a 2.0 wt.-% solution of PS in toluene onto  $\text{CaF}_2$  discs.

### 3.3.3.2 Characterisation methods

Optical micrographs were taken with an Olympus Microscope. Micro FT-IR spectra were measured with a Perkin Elmer Autoimage system coupled with a Perkin Elmer Spectrum One FT-IR spectrometer (all spectra recorded in transmission). XPS: All measurements were performed in an ultrahigh vacuum (UHV) chamber (SPECS) at a pressure of  $1 \times 10^{-10}$  mbar and the samples were introduced via a fast entry load-lock. XPS experiments were carried out using  $MgK\alpha$  radiation (1253.6 eV) and a hemispherical analyzer (Phoibos100) and with an energy resolution of 1.2 eV. All spectra were acquired in normal emission. All spectra reported here have been adjusted to yield constant binding energy for the C 1s line at 285 eV. SEM: For scanning electron microscopy (SEM) the patterned polymer films were sputter coated with graphite (thickness 25 nm). SEM measurements were done with a Leo Gemini DSM 986 equipped with a field emission gun and an EDX Voyager 3105A Noran detector. Surface profiles were recorded with a stylus instrument (Dektak 150 from Veeco Instruments).

### 3.3.3.3 Irradiation Experiments

Laser irradiation experiments were carried out with a 248 nm KrF excimer laser (Lambda Physik LPX 100) at 5 Hz repetition rate (pulse duration 20 ns). The primary pulse energy (before entering the projection system) was approx. 25 mJ per pulse per  $cm^2$ . The beam of the excimer laser was coupled into a mask projection system (Light Bench from OPTEC, Belgium), see Scheme 1 for the optical setup. The laser beam was then passed through a beam attenuator and a chromium/quartz mask. The image of the mask was demagnified by a lens system and projected onto the surface of the polystyrene film. The demagnification was varied between a factor of 4 and 16, with a demagnification by 10 resulting in the highest resolution according to the manufacturers specifications. The polystyrene film (cast onto a transparent  $CaF_2$  substrate) was placed in a reaction chamber equipped with a  $CaF_2$  window, a gas inlet and a gas outlet. During laser processing, the reflected beam was guided through an optical system to a CCD camera, which records the irradiation pattern and allows for the observation on a monitor. Additionally, a visible light illumination system facilitates the optical inspection of the modified polymer surface. The chamber was purged for 20 min with pure  $N_2$  (99.999%, from Air Liquide) prior to the photoreaction. The gas mixture for the patterning experiment was continuously passed through the reaction chamber for at least 5 min before

the start of the irradiation and during the irradiation process. After the irradiation, the chamber was again flushed with nitrogen for 5 min, before the sample was withdrawn from the reaction chamber.

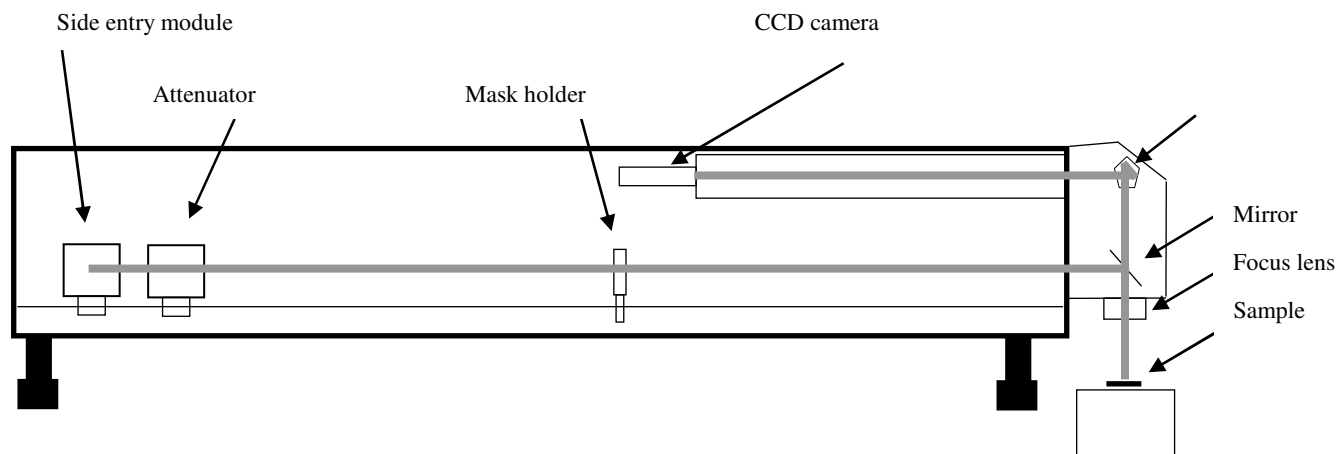


Figure 46: Optical projection system (OPTEC, Belgium) coupled to a 248 nm KrF excimer laser.

### 3.3.4 Results and Discussion

In these experiments we wished to see if the UV-induced surface modification of polystyrene with organosilicate groups can be achieved in a patterned way. Thin polystyrene (PS) films (approx 0.5  $\mu\text{m}$  film in thickness on  $\text{CaF}_2$  substrates) were illuminated with pulsed UV light in a reaction chamber containing a defined gas mixture made up of trimethylsilane (TMS) and oxygen. Trimethylsilane absorbs in the VUV range (up to 220 nm), and molecular oxygen absorbs up to 240 nm. From this it comes clear that the 248 nm radiation is absorbed only by the aromatic units in polystyrene, but not by the components of the reactive gas mixture (TMS,  $\text{O}_2$ ) which is in contact with the polymer surface.

The irradiation set-up consisted of a 248 nm KrF excimer laser coupled with a mask projection system that allows the lithographic patterning of surfaces and thin films. Using a demagnification of the UV laser beam by a factor between 5 and 10, square patterns with 30  $\mu\text{m}$  x 30  $\mu\text{m}$  up to 500  $\mu\text{m}$  x 500  $\mu\text{m}$  feature size were projected onto the PS surface. The modified samples were investigated by optical and spectroscopic techniques (e.g. infrared microscopy) and by profilometry.

To obtain a photoassisted surface modification irradiations were carried out under neat TMS and a gas mixture containing TMS and  $\text{O}_2$  (volume ratio 1:1). As reference, irradiation was also conducted under neat oxygen. Thus, illuminated and non illuminated areas of the polystyrene films on  $\text{CaF}_2$  were analysed for three different reactive gases: pure



oxygen, pure TMS and  $\text{TMS/O}_2 = 1/1$ . In all cases, the desired pattern was created at the PS surface as detected by the monitor of the projection system and by optical microscopy. In Figure 47, a microscopic image of a square pattern on the PS surface is shown (irradiation under TMS atmosphere). The 10 fold demagnification of the projection system allowed replication with high resolution. Squares with a dimension of  $40\ \mu\text{m} \times 40\ \mu\text{m}$  became visible after irradiation of the sample with the KrF laser beam. To obtain larger features, either a lower demagnification or a different mask was used. For qualitative surface analysis (e.g. by FT-IR microscopy, XPS and EDX) fields with a dimension of about  $500\ \mu\text{m} \times 500\ \mu\text{m}$  were illuminated on the PS surface, see Figure 48). Profile measurements were conducted to investigate the profile of the irradiated surface.

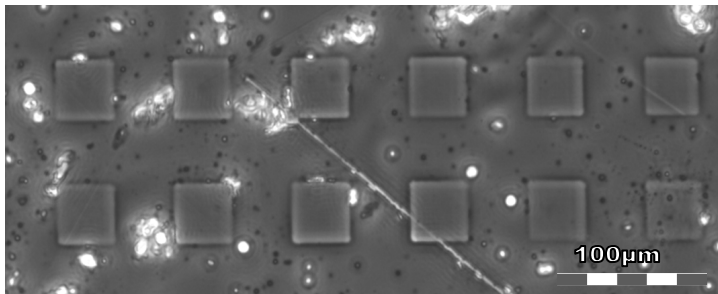


**Figure 47: micrograph of a PS surface after lithographic patterning under TMS atmosphere. In this case, a square pattern has been projected onto the surface. The squares, which correspond to the irradiated areas, are  $40\ \mu\text{m}$  by  $40\ \mu\text{m}$  in size.**

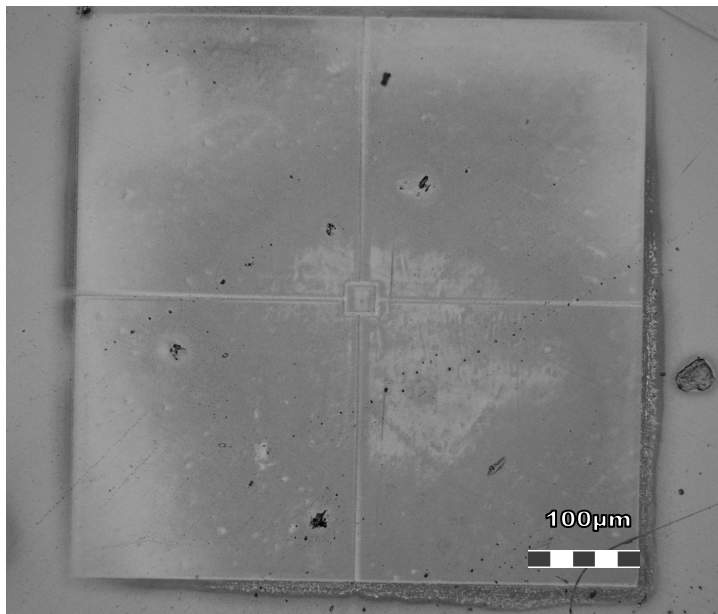


**Figure 48: microscopic image of a PS surface irradiated under  $\text{TMS/O}_2$  atmosphere. In this case, a mask pattern consisting of four squares ( $250\ \mu\text{m} \times 250\ \mu\text{m}$ ) separated by thin lines has been projected onto the polymer surface.**

### 3.3.4.1 Irradiation of PS under neat oxygen

Under the given irradiation conditions, laser ablation occurred when the 248 nm irradiation was conducted under neat oxygen. This became evident from the complete disappearance of the FTIR signals in the illuminated areas of the PS film as evidenced by infrared microscopy. Controlled laser ablation of polymers has been investigated intensively before. For high energy laser radiation ( $\lambda < 340$  nm) the predominant mechanism of laser ablation is proposed to be the photochemical decomposition of the initially formed electronically excited states. This holds true for polymers which absorb at the irradiation wavelength.<sup>[17]</sup> A laser fluence of 200 mJ/cm<sup>2</sup> is reported as ablation threshold for polystyrene at an irradiation wavelength of 248 nm. At this wavelength, the absorption coefficient is 0.5  $\mu\text{m}^{-1}$ .<sup>[18]</sup>

Figure 49 shows micro FT-IR spectra of PS irradiated under neat oxygen. The microscope aperture was 100 x 100  $\mu\text{m}$ . The non-irradiated areas of this sample (solid line) show characteristic polystyrene peaks at 3026, 2923, 1601, 1493 and 1453  $\text{cm}^{-1}$ . The irradiated areas (dotted line) don't show any signal of the original polymer. This proves that in case of illumination under oxygen material ablation proceeds.

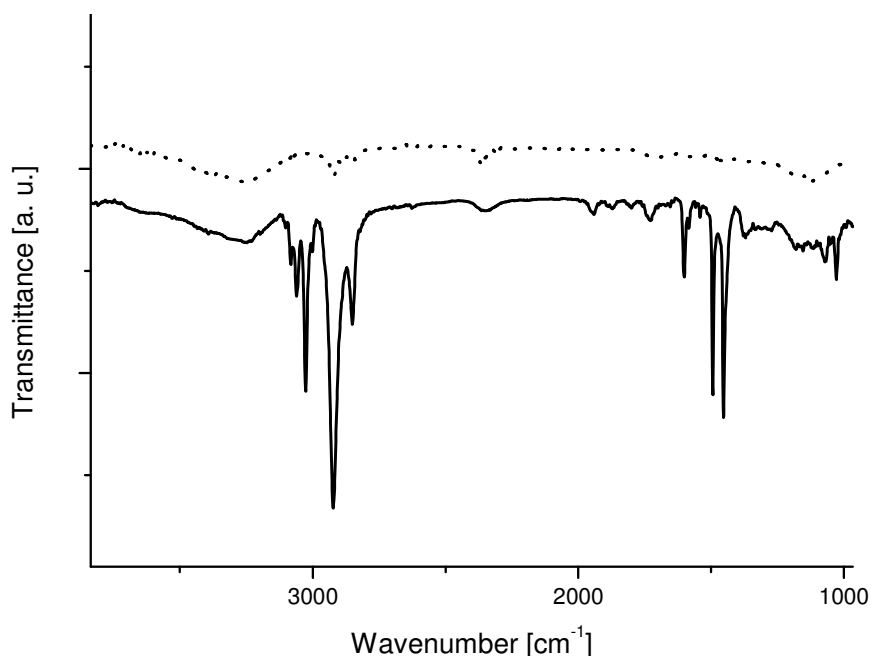


Figure 49: micro FT-IR spectra of PS non irradiated (solid line) and irradiated under O<sub>2</sub> atmosphere (dotted line); microscope aperture 100 x 100  $\mu\text{m}$

In a similar experiment, polystyrene was irradiated under pure TMS atmosphere. Also in this case, laser ablation was observed, and with FTIR spectroscopy a similar situation as described in Figure 49 was found.

### 3.3.4.2 Irradiation of PS under TMS/O<sub>2</sub>

#### FT-IR microscopy

As discussed in chapter 3.3.4.1, both under oxygen atmosphere and under pure TMS atmosphere laser ablation of PS proceeds. In contrast to this, laser ablation does not proceed when the irradiation is conducted under TMS/O<sub>2</sub> atmosphere. The FTIR spectra in Figure 50 do not show differences between irradiated (dotted lines) and non-irradiated areas (solid lines) of the polystyrene film. On the one hand, no signals typical of Si-O units evolve, and on the other hand no considerable decrease of the hydrocarbon peaks is observed. Since the pattern is clearly visible by optical microscopy, the irradiation may cause changes in the material that cannot be followed via FT-IR microscopy. At the same time it is possible, that a photochemical modification proceeds only at the very surface, so that no changes are detectable in the transmission FTIR spectra.

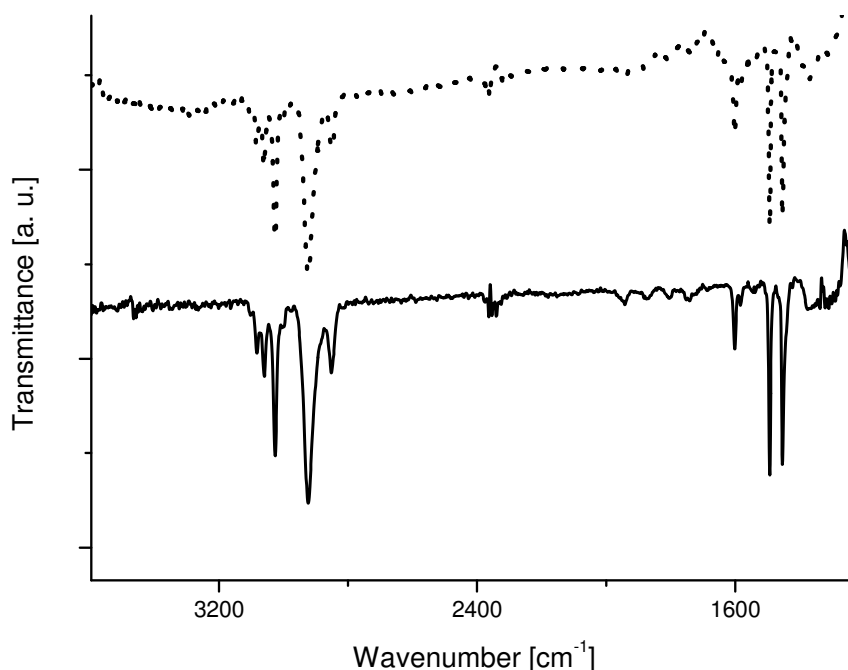
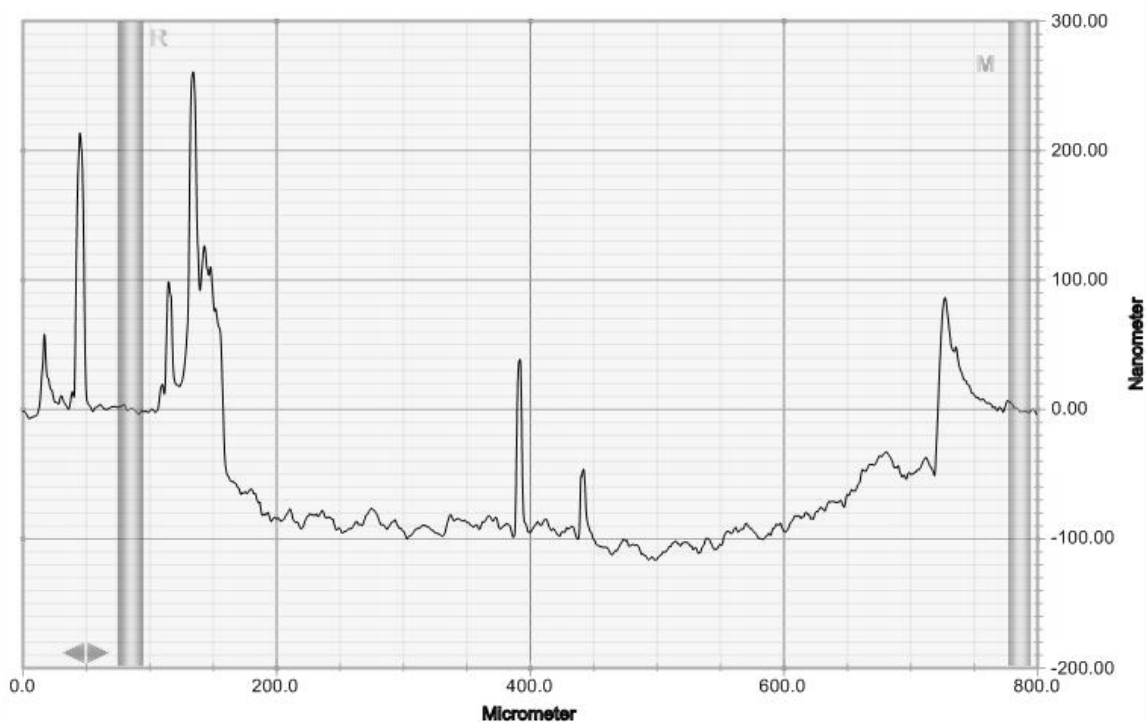


Figure 50: FT-IR spectra of a PS film, non irradiated (lower graph) and irradiated under TMS/O<sub>2</sub> atmosphere (upper graph); microscope aperture 40 x 40  $\mu\text{m}$

## Profile measurements



**Figure 51: Profile of a PS film irradiated under TMS/O<sub>2</sub> atmosphere**

To obtain information on topographical changes at the PS surface during laser illumination, profile measurements were carried out at the intersection between irradiated and non irradiated areas. In Figure 51 the profile of a PS surface irradiated under TMS/O<sub>2</sub> atmosphere is shown. The profile refers to the micrograph shown in Figure 48. The height level of non-irradiated zones (left and right side of the graph) significantly differs from the height level of the irradiated area (starting at the position  $x = 150 \mu\text{m}$ ) by about 100 nm. At the position  $x = 390 \mu\text{m}$  the intersection of two neighboured squares is clearly visible, where the intensity of the laser light was zero. The results of these measurements lead to the assumption, that only moderate laser ablation occurs when polystyrene is irradiated under TMS/O<sub>2</sub> atmosphere. It has to be considered, that in both experiments (oxygen atmosphere and TMS/O<sub>2</sub> atmosphere, resp.) comparable laser fluences were employed. The presence of TMS at the surface of the polymer seems to protect the polymer from the ablation reaction.

## XPS measurements

To analyse the chemical composition of the modified polystyrene surface, XPS measurements were conducted. These spectra allow quantifying the elements contained in the depth of a few nanometers of the polystyrene surface. Figure 52 shows the Si2p signal of non-irradiated polystyrene (lower graph) and of polystyrene irradiated under TMS/O<sub>2</sub> atmosphere (upper graph). The analysis of the untreated PS showed a silicon content of 2.4 at-% and a ratio oxygen : silicon = 2,3 : 1. For samples illuminated in TMS/O<sub>2</sub> atmosphere, the amount of silicon was measured to be 5.1 at-% with an ratio oxygen : silicon = 1,7:1. This indicates that the silicon content was more than doubled, whilst the oxygen amount increased less than that of silicon. The binding energy of 102.4 eV, where the si2p peak is located in the corresponding XPS spectra (with respect to the C1s signal fixed at 285 eV), indicate alkylsilyl groups<sup>[13]</sup>. Silicon attached to oxygen also peaks in this region, but is not in accordance with the ratio found between the two species. Therefore, the Si2p peak at 102.4 eV may be a superposition of SiC and SiO peaks.

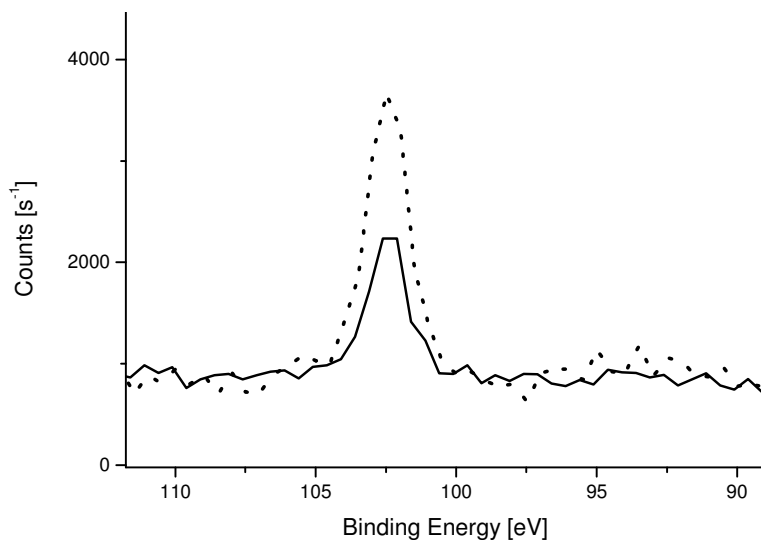


**Figure 52: Detail XPS spectra of PS prior to (solid line) and after 248 nm irradiation under TMS/O<sub>2</sub> atmosphere (dotted line).**

**Table 7: Composition of PS surfaces<sup>1)</sup>**

Sample	C	O	Si
	atom %	atom %	atom %
Pristine PS	92.2	5.4	2.4
Modified PS	86.3	8.6	5.1

<sup>1)</sup> Hydrogen is omitted in this calculation

## SEM-EDX measurements

To support the attachment of organosilicate groups onto the polymer surface, SEM-EDX measurements were performed. This method provides the possibility to obtain energy dispersive X-ray spectra measured at certain positions in a SEM micrograph. The depth of this analysis amounts to a few  $\mu\text{m}$ , depending on the material of the sample. A comparison of the spectra recorded at illuminated and non-illuminated positions of the PS film is provided in Figure 53.

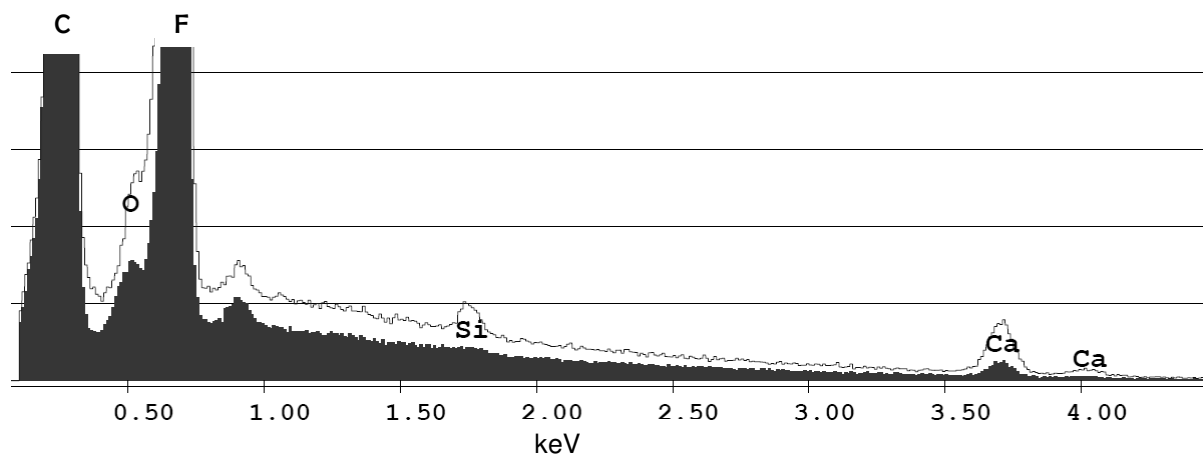


**Figure 53: EDX spectra of non-irradiated PS (dark filled spectrum, bottom) and irradiated PS (solid line)**

In the EDX spectra of the non irradiated area, the elements carbon (C), oxygen (O), fluorine (F) and calcium (Ca) were found. The signals of Ca and F stem from the substrate, a  $\text{CaF}_2$  disc. The signals of C and O stem from the polymer (and its surface) and are in good agreement with the data of the XPS measurements. The spectrum of the irradiated area (Figure 53 solid line on top) shows the same signals as the unirradiated polystyrene but - in

addition – the signal of Si. Thus the EDX spectra provide a further proof of a chemically modified polystyrene surface containing organosilicate groups. The proposed mechanism of this surface modification is depicted in the following.

### Proposed Mechanism

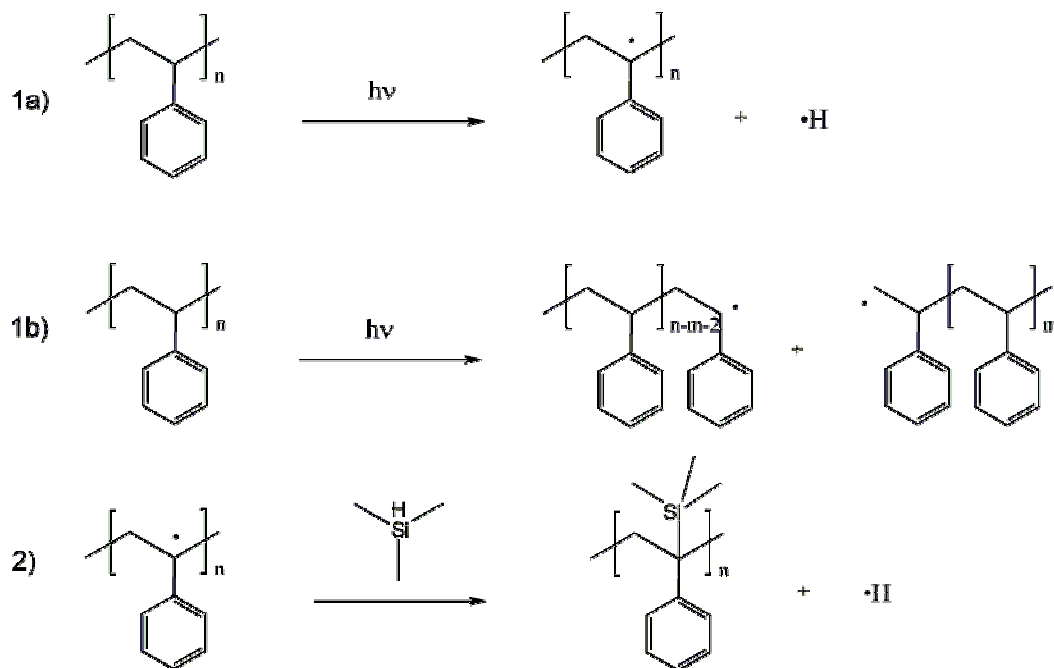


**Figure 54: proposed reaction sequences for the photoreaction of PS under TMS/O<sub>2</sub> atmosphere**

It is clear that the complex radical mechanism of the photoreactions occurring in the upper surface layer of the polymer cannot be described exactly. In Figure 54 *possible* initiation mechanism and propagation reactions are shown to provide examples for the photoreaction. 1a and b present initiation steps of photodegradation, generating reactive polymer alkyl radicals. In 1a the hydrogen atom abstraction of a polymer is shown, whilst in 1b two radical fragments of the original polymer chain are formed. All radicals can react with the trimethylsilane leading to a stable and inactive reaction product.

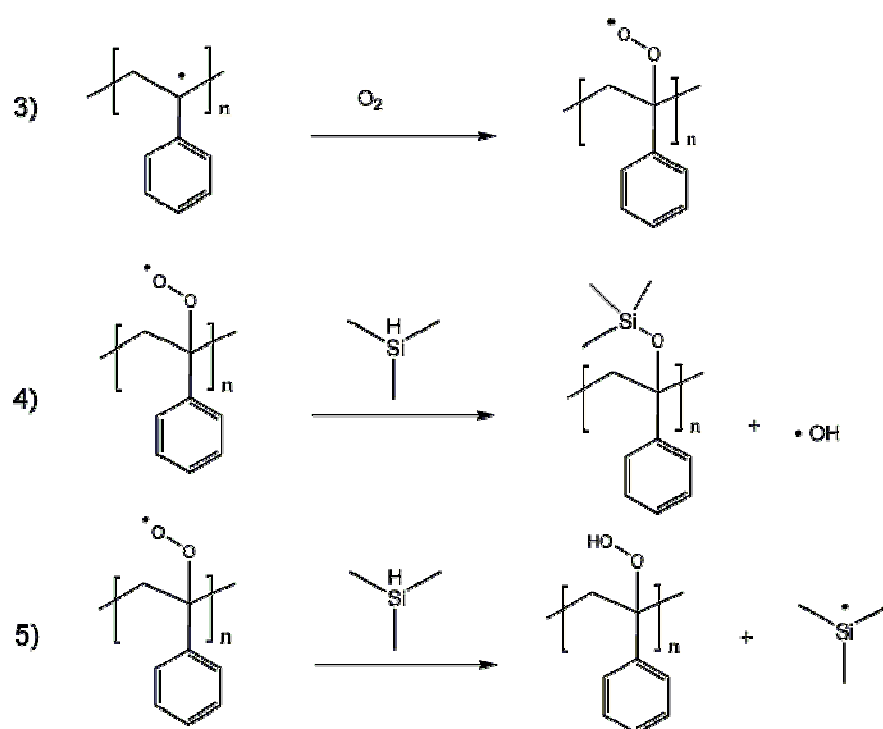


**Figure 55: Reactions of polymer photo-oxidative degradation**

Oxygen plays a key role in free radical processes since numerous highly reactive oxygen containing radicals can be formed. As an example, the formation of a polymer peroxy radical is shown in Figure 55 -3. This radical can further react, e.g. with the reactive trimethylsilane, available in the gas atmosphere as presented in 4. Another possibility is the formation of new radicals by hydrogen abstraction (5). As mentioned before, these reactions present only a part of the processes occurring in the polymer surfaces. Obviously, the radicals formed can react further in different reactions, e.g. chain propagation, crosslinking or bimolecular recombination also called termination.<sup>[19]</sup> From the results of the surface analysis (XPS, EDX) it is concluded that R-Si-O units (R = alkyl), which may be termed as “organosilicates”, are formed in this photoassisted process.



### 3.3.5 Conclusion

We investigated a new process for surface modification in a reactive gas atmosphere, where a polystyrene surface was patterned by a pulsed KrF excimer laser (248 nm) coupled with a lithographic projection system. Investigations by means of FT-IR microscopy showed that illumination in oxygen atmosphere (and in pure TMS atmosphere) results in strong material ablation, whilst the irradiation under a mixture of *TMS and O<sub>2</sub>* only leads to slight material ablation under comparable laser fluence. X-ray photoelectron spectroscopy (XPS) and energy dispersive X-ray spectroscopy (EDX) support the assumption of attaching silicon containing groups onto the polystyrene surface: after irradiation in TMS/O<sub>2</sub> atmosphere, the polystyrene samples displayed a significant increase in the content of silicon and oxygen at the surface. Measurements with a stylus instrument showed shallow features with a depth of approximately 100 nm at surfaces irradiated under TMS/O<sub>2</sub>. Summing up, patterned irradiation of polystyrene with a 248 nm KrF laser under TMS/O<sub>2</sub> atmosphere results in (a) surface modification of the polystyrene with organosilicate units and (2) very slight laser ablation at the same time.

### 3.3.6 References

- [1] Wang X., McCord M.G., *J. Appl. Polym. Sci.* 104, **2007**, 3614.
- [2] Guruvenket S., Rao G. M., Komath M., Raichur A. M., *Applied Surface Science* 236, **2004**, 278–284
- [3] Feddes B., Wolke J.G.C., Weinhold W.P., Vredenberg A.M., Jansen J.A., *J. Adhes. Sci. Technol.* 18, **2004**, 655
- [4] Mathieson I., Bradley R. H., *Intern. J. Adhesion Adhesives* 16, **1996**, 29.
- [5] Chanunpanich N., Ulman A., Stzhemechny Y. M., Schwarz S. A., Janke A., Braun H. G., Kratzmüller T., *Langmuir* 15, **1999**, 2089
- [6] Kavc T., Kern W., Ebel M. F., Svagera R., Pölt P., *Chem.Mater.* **2000**, 12, 1053
- [7] Huhtala A., Pohjonen T., Salminen L., Salminen A., Kaarniranta K., Uusitalo H., *J. Biomed. Mater. Res. A* 83A, **2007**, 407
- [8] Mendonca C.R., Misoguti L., Andrade A.A., Yamaki S.B., Dias V.D., Atvars T.D.Z., Oliveira O.N., *Opt. Mater.* 30, **2007**, 216
- [9] Gotoh K., Kikuchi S., *Colloid Polym. Sci.* 283, **2005**, 1356
- [10] Pfleging W., Torge M., Bruns M., Trouillet V., Welle A., Wilson S., *Applied Surface Science* 255, **2009**, 5453–5457
- [11] Daschiel U., Spanring J., Ebel M. F., Svagera R., Schröttner H., Kern W. *Macromol. Chem. Phys.* 209, **2008**, 1232–1239
- [12] Spanring J., Buchgraber C., Ebel M. F., Svagera R., Kern W., *Polymer* 47, **2006**, 156
- [13] Spanring J., Buchgraber C., Ebel M. F., Svagera R., Kern W., *Macromol. Chem. Phys.* 206, **2005**, 2248–2256
- [14] Walsh R., *Acc. Chem. Res.* 14, **1981**, 246
- [15] Chatgililoglu C., *Chem. Rev.* 95, **1995**, 1229
- [16] Nay M. A., Woodall G. N. C., Strausz O. P., Gunning H. E., *JACS.* 87, **1965**, 179
- [17] Rabek J. F., “*Photodegradation of Polymers*”, Springer, **1996**, 146-157
- [18] Pfleging W., Bruns M. , Welle A., Wilson S., *Applied Surface Science* 253, **2007**, 9177
- [19] Rabek J. F., “*Photodegradation of Polymers*”, Springer, **1996**, 59-80

### 3.4 Conclusion of Part B and outlook

In this part of the thesis, investigations towards the surface modification of commodity polymers, more precisely low density polyethylene (LDPE) and polystyrene (PS) are reported. UV and VUV assisted methods were developed to obtain a surface modification of the polymers in a reactive gas atmosphere. Two different light sources have been used: a xenon excimer lamp (172 nm) and a KrF excimer laser (248 nm) coupled with a projection system. The reactive gas atmosphere consists of a mixture of trimethylsilane (TMS), a non toxic, odourless gas, and oxygen.

With respect to the occurring photoreactions, two different situations have been investigated: irradiation at 172 nm provides high energy photons which lie in the energy level of the absorbance of TMS and oxygen. The absorption of LDPE is rather low at this energy. For irradiations at 248 nm the opposite situation is present. The energy of the photons is in the absorbance range of the phenyl rings in PS, whilst both oxygen and TMS do not absorb at 248 nm.

Both polymers were analyzed via XPS, FT-IR and SEM prior to and after irradiation. XPS measurements showed for both polymers the attachment of silicon-containing groups onto the surface as a result of the irradiation under TMS/O<sub>2</sub>.

**Table 8: Comparison of the composition of the polymer surfaces obtained by XPS<sup>1)</sup>**

Sample	C atom %	O atom %	Si atom %	Irradiation under TMS/O <sub>2</sub>
Pristine LDPE	97.0	2.6	0.4	-
Modified LDPE	83.6	11.6	4.8	172 nm
Pristine PS	92.2	5.4	2.4	-
Modified PS	86.3	8.6	5.1	248 nm

<sup>1)</sup> Hydrogen is omitted in this calculation

The results of the XPS measurements are listed in Table 8. Irradiation leads to a change of the silicon and oxygen content in the surface for both polymers. While irradiation of LDPE at 172 nm leads to a ratio silicon / oxygen = 5 at.-% / 12 at.-%; irradiation of PS results in a ratio

silicon / oxygen = 5 atom% / 9 atom %. In both cases, we propose a superposition of Si-O and Si-C groups in the surface.

The ATR FT-IR spectra of the modified LDPE show that the surface layer contains Si-O groups (as indicated by a broad intense signal at  $1054\text{ cm}^{-1}$ ) as well as  $\text{Si}(\text{CH}_3)_n$  groups, which are revealed by the strong band at  $1261\text{ cm}^{-1}$  and the signal at  $844\text{ cm}^{-1}$ . Interestingly, also Si-H units are present as indicated by the signals at  $1210$  and  $908\text{ cm}^{-1}$ . For the patterned modification of PS, FT-IR microscopy showed no additional signals. Therefore, the information on the kind of silicon groups generated was not available for this modification.

SEM measurements showed a layer thickness of about 0.7 microns for the modified LDPE layer, observed at a cross section of an irradiated polymer film. XRD spectra of an illuminated area of PS showed another proof of the incorporation of silicon upon irradiation, since no silicon was detected at non irradiated PS.

For LDPE, patterning was created by a contact mask method using a TEM grid as mask. Honeycomb structures in the range of 50 microns were observed in the light microscope. FT-IR microscopy showed silicon signals at irradiated areas (hexagonal fields), while fields where the mask hindered the modification (bars) no signals have been found. In the case of the irradiation of PS, a projection system was used for all illuminations, using different masks and different demagnifications. Square features between  $30\text{ }\mu\text{m} \times 30\text{ }\mu\text{m}$  and  $500\text{ }\mu\text{m} \times 500\text{ }\mu\text{m}$  were obtained. To scan the height of the modified areas profile measurements were conducted. The irradiated fields turned out to be shallow indents with a depth of approx. 100 nm (slight laser ablation).

Summing up, the patterns generated via photochemical modification of polymer surfaces in reactive gas atmospheres ( $\text{TMS}/\text{O}_2$ ) showed that the illumination leads to an incorporation of silicon onto the polymer surface. Therefore, these techniques could be applied to create e.g. protective layers on PS and LDPE.

Further investigations could be done using other reactive gases, such as sulphur dioxide to create photochemically patterned surfaces. Furthermore, other polymers such as polybutadiene (expected to be more reactive) could be modified and thus protected with the developed techniques.



## 4 General Summary

In this work different approaches to create photochemical pattern are described. In the first part (part A) the two photon induced change of the refractive index of polymers bearing aromatic aryl ester units was studied. Therefore, different polymers were synthesised containing different aromatic ester units. Varying synthetic methods have been reported: free radical polymerisation, ring opening metathesis polymerisation (ROMP) and the crosslinking of chemically modified polysiloxane chains via hydrosilylation reaction. In a first step, FT-IR studies of irradiation experiments with a mercury pressure lamp showed that the occurring photoreaction in the polymers seems to be the photodecarboxylation as the main reaction, accompanied by the photo-Fries rearrangement for the used polymers. Ellipsometric measurements showed high refractive index changes up to +0.07, indicating the enormous molecular change of the aromatic ester unit within the polymer. Two photon experiments were carried out to investigate the refractive index pattern for advanced applications, as 3D optical memories or waveguide technology. In three polymers waveguides could be inscribed, showing high contrast in the phase contrast microscopic images.

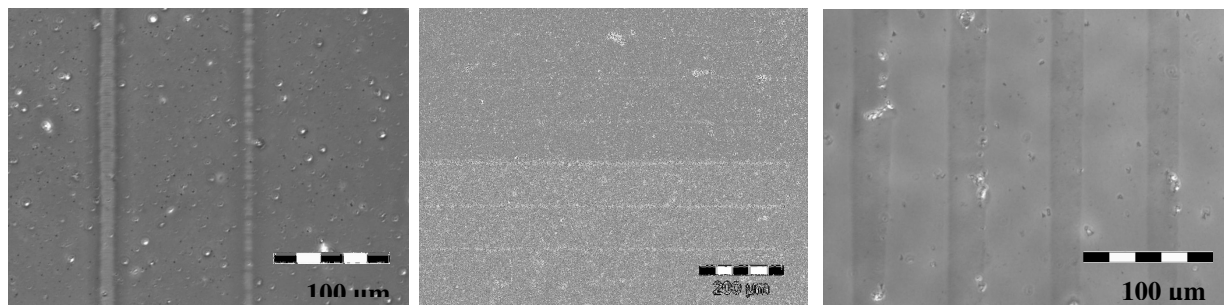


**Figure 56: Comparison of waveguide structures of 3 different polymers in microscopic images measured in phase contrast mode**

In Figure 56 the comparison of the laser inscribed waveguide structures in three different polymers, all bearing the 4-(N,N-diphenylamino)phenyl benzoate as reactive chromophore is shown (left: polystyrene derivative, middle: polynorbornene derivative, right: modified polysiloxane).

In the second part (part B) surface modification of LDPE and PS was performed. Oxygen mixed with trimethylsilane, an odourless, non toxic gas, was used as a reactive gas atmosphere in irradiation experiments. Two different illumination sources, a Xe excimer lamp (172 nm) for LDPE and a KrF excimer laser (248 nm) coupled with a projection system for PS were used. XPS measurements showed for the modified LDPE and PS surfaces an increase in the silicon content after irradiation. Furthermore, FT-IR measurements of the

irradiated LDPE foils showed the incorporation of organosilyl groups and  $\text{SiO}_x$ -units into the surface. SEM pictures of a cross section of a LDPE foil depicted a modified layer of about  $0.7 \mu\text{m}$ . Both polymers were photochemically structured, as evidenced by light microscopy (cf. Figure 57).

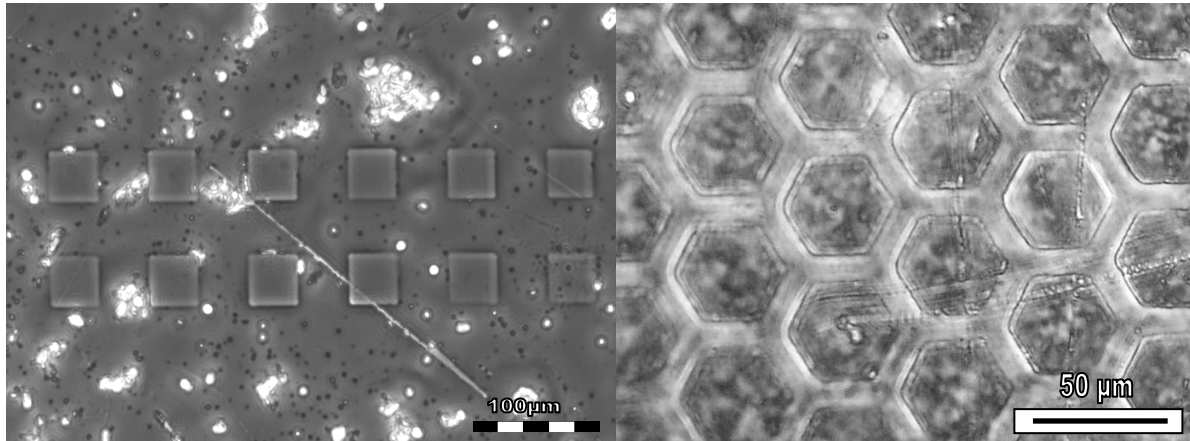


**Figure 57: Microscopic images of modified PS (left) and modified LDPE (right)**

For LDPE, a contact mask technique using a TEM grid as a mask was performed. PS was structured with a projection system, resulting in a demagnified pattern of a quartz/chromium mask on the polymer surface. This pattern was further investigated by profile measurements, showing shallow indents with a depth of approximately 100 nm. EDX spectra showed the incorporation of silicon in the illuminated areas when compared to the non-illuminated areas of the same sample. Both methods for the patterned modulation of the surface properties are of potential interest for the generation of anti-adhesive and protective layers on polymers.

## **5 Appendix 1**

### **Curriculum Vitae**

Ute Daschiel

Born in Linz on the 15<sup>th</sup> of October 1981

Ute.Daschiel@gmx.at

### **Education**

Ph.D., Technical Sciences, October 2006 - January 2010

Institute of Chemical Technology of Materials (Technical University of Graz) and Institute of Chemistry of Polymeric Materials (University of Leoben)

Diploma Thesis: "UV reactive polymers with tunable refractive index", July 2006

Institute of Chemical Technology of Organic Materials (TU Graz)

Matura, 2000

BRG Landwiedstraße, Linz



## 6 Appendix 2: List of publications

### Publications

Daschiel U., Führer R., Bauer T., Jakopic G., Satzinger V., Schmidt V., Kern W., „Index pattern of photoreactive polymers“, Proc. SPIE, Vol. 7413, **2009**, 74130V; doi:10.1117/12.828335

U. Daschiel, J. Spanring, M. F. Ebel, R. Svagera, H. Schröttner, W. Kern, „*Surface Modification of Polyethylene by VUV Irradiation in the Presence of Trimethylsilane and Oxygen*“, Macromol. Chem. Phys. 209, **2008**, 1232-1239

U. Daschiel, T. Höfler, W. Kern, G. Jakopic, V. Schmidt, „*Selected polymers containing aromatic ester units: synthesis, photoreactions and refractive index modulation*“, Macromol. Chem. Phys. 208, **2007**, 1190-1201

### Presentations

U. Daschiel, T. Höfler, G. Jakopic, S. Temmel, W. Kern, „*Photo-Fries rearrangements in functional polymers*“, 1<sup>st</sup> European Chemistry Congress, **2006**, Budapest (H)

### Posters

Daschiel U., Spanring J., Ebel M. F., Svagera R., Schröttner H., Track A. M., Riess G., Kern W., „*Photoassisted surface modification in the presence of trimethylsilane*“, EPF European Polymer Congress, **2009**, Graz (A)

Daschiel U., Führer R., Bauer T., Jakopic G., Satzinger V., Schmidt V., Kern W. „*Index pattern of photoreactive polymers*“, SPIE Optics and Photonics, **2009**, San Diego (USA)

Daschiel U., Schmidt V., Jakopic G., Satzinger V., Riess G., Kern W.: „*Photoreactive Polymers with Tunable Refractive Index*“, poster at MRS Spring Meeting, **2008**, San Francisco (USA)

Daschiel U., Spanring J., Ebel M. F., Svagera R., Schroettner H., Riess G., Kern W.: „*Photoassisted surface modification of PE by VUV irradiation in the presence of trimethylsilane*“, Poster at Austrian & Slovenian Polymer Meeting (ASPM 08), **2008**, Graz (A)

Daschiel U., Bauer T., Jakopic G., Schmidt V., Satzinger V., Riess G., Kern W.: „*Index Patterning of Photoreactive Polymers*“, poster at e-MRS, **2008**, Strasbourg (F)

Daschiel U., Hoefler T., Jakopic G., Kern W.: „*UV reactive polymers with tunable refractive index*“, EPF European Polymer Congress, **2007**, Portoroz (SLO)

Daschiel U., Spanring J., Ebel M. F., Svagera R., Kern W.: „*Photochemical Modification of Polymer Surfaces: Investigations with FT-IR Spectroscopy and other Techniques*“, poster at European symposium on Polymer Spectroscopy” (ESOPS 17), **2007**, Seggauberg (A)

Daschiel U., Höfler T., Jakopic G., Temmel S., Griebner T., Trimmel G., Kern W.: „*Photo-Fries rearrangements in polymers: Index patterning and Surface modification*“, 1st European Chemistry Congress, **2006**, Budapest (H)

## Work as co-author

Führer R., Daschiel U., Bauer T., Jakopic G., Satzinger V., Schmidt V., Kern W.: „UV reactive flexible polynorbornenes with modifiable refractive index“, poster at EPF European Polymer Congress, **2009**, Graz (A)

Kern W., Hoefler T., Daschiel U., Hernandez-Sosa G., Resel R., Simbrunner C., Sitter H., Trimmel G.: „Reactive Patterns and optical Structures in Polymer Layers by UV induced Rearrangements of Aryl Ester Groups“, poster at e-MRS, **2008**, Strasbourg (F)

Hoefler T., Griesser T., Daschiel U., Trimmel G., Kern W., Temmel S., Jakopic G.: “Polymers and ultrathin surface layers containing UV reactive aryl esters: photoinduced modulation of optical properties and chemical reactivity”, poster at e-MRS **2007**, Strasbourg (F)

Griesser T., Hoefler T., Trimmel G., Kern W., Jakopic G., Temmel S., Daschiel U.: „Photoreactions in aromatic esters: modulation of optical properties and chemical reactivity in polymers and ultrathin surface layers“, poster at EUROMAT **2007**, Nürnberg (D)

Daschiel U., Höfler T., Jakopic G., Kappaun S., Temmel S., Kern W.: “Photo-Fries rearrangements for UV assisted polymer surface modification”, lecture by W. Kern at E-MRS Spring Meeting **2006**, Nice (F)

## Additional publications (manuscripts under preparation)

Daschiel U., Bauer T., Jakopic G., Satzinger V., Schmidt V., Kern W., “Refractive index and waveguide patterning of polynorbornene copolymers bearing 4-(N,N-diphenylamino)phenyl benzoate units”, to be submitted to Macromol. Chem. Phys.

Daschiel U., Jakopic G., Satzinger V., Schmidt V., Kern W. “Photoreactive styrene and silicone polymers bearing 4-(N,N-diphenylamino)phenyl benzoate units: one-photon and two-photon reactions”, to be submitted to Polymer

Daschiel U., Track A.M., Wagner J., Pichler H., Kern W. “Patterened Surface Modification of Polystyrene by UV Irradiation in the Presence of Trimethylsilane” to be submitted to Thin Solid Films